A Hydrologic Calibration of the SWAT Model in Kranji Catchment, Singapore

by

Laurie Kellndorfer

S. B. Environmental Engineering
Massachusetts Institute of Technology, 2011

Submitted to the Department of Civil and Environmental Engineering
in Partial Fulfillment of the Requirements for the Degree of

MASTER OF ENGINEERING
IN CIVIL AND ENVIRONMENTAL ENGINEERING
at the

MASSACHUSETTS INSTITUTE OF TECHNOLOGY

June 2012

Signature of Author _____
Laurie Kellndorfer
Department of Civil and Environmental Engineering
May 11, 2012

Certified by _____
Peter Shanahan
Senior Lecturer of Civil and Environmental Engineering
Thesis Supervisor

Accepted by _____
Heidi M. Nepf
Chair, Departmental Committee for Graduate Students

A Hydrologic Calibration of the SWAT Model in Kranji Catchment, Singapore

By

Laurie Kellndorfer

S. B. Environmental Engineering
Massachusetts Institute of Technology, 2011

Submitted to the Department of Civil and Environmental Engineering on May 11, 2012 in Partial Fulfillment of the Requirements for the Degree of Master of Engineering in Civil and Environmental Engineering

Abstract

The Public Utilities Board (PUB) of Singapore wishes to expand recreational activities in Singapore's surface waters through the Active, Beautiful, and Clean Waters Program (ABC Waters). One area of concern with ABC Waters is microbial pollution. Pathogens pose an immediate and substantial risk to human health when humans come into contact with contaminated water. In order to open surface waters for public recreation, PUB must insure that these waterways are free of pathogens. The Massachusetts Institute of Technology in the United States and Nanyang Technological University in Singapore are working together on several water quality research projects related to ABC Waters.

A surface runoff model for Kranji Catchment, located in northwest Singapore, was created in the Soil and Water Assessment Tool (SWAT) by Granger (2010) and improved by Bossis (2011). The model incorporates hydrology, land use, weather, soil, and slope to calculate surface flows and water quality constituents. The model was originally created to be a prediction tool for bacteria concentrations in outflows throughout the Kranji Catchment. Earlier versions of the model, however, grossly underpredict flows.

In an effort to improve the accuracy of the SWAT model, the surface hydrology was calibrated to flows measured at five stream gauge stations in Kranji Catchment. Precipitation within the SWAT model was changed to equal a rainfall record at one of the stream gauge stations. A sensitivity analysis was also conducted for surface flows. Surface flows were most sensitive to changes in six input parameters, and two of these parameters were changed in the final, calibrated model. The soil evaporation compensation factor (ESCO) was increased, and the curve number for moisture condition II (CN2) was decreased. These three changes in the model greatly improved the way the SWAT model predicts surface outflows, and with these changes, surface outflows predicted by the model match measured values very closely at all five stream gauge stations.

While hydrologic calibration greatly improved surface flow calculations in the SWAT model, predictions of bacteria concentrations did not improve. The SWAT model still requires further calibration work to bring bacteria concentrations closer to measured values.

Thesis Supervisor: Peter Shanahan
Title: Senior Lecturer of Civil and Environmental Engineering

Acknowledgements

I would like to extend my deepest thanks to my thesis advisor, Dr. Peter Shanahan, for his unending encouragement, thoughtful advice, and constant feedback throughout this project.

To my project team members Suejung Shin, Kathyayani Shobhna Kondepudi , and Janhvi Doshi for great adventures in Singapore, Malaysia, and Indonesia, late nights of project work, and long days in the field and in the lab.

To project members at Nanyang Technological University in Singapore: Eveline Ekklesia for her hard work, unbelievable attention to detail, and wonderful hospitality; Syed Alwi Bin Hussien Alkaff for his support in the field, construction of the Sterivex-o-matic, and good sense of humor; and Professor Lloyd Chua for his advice on this project and for helping me access stream gauge data.

To the M. Eng Class of 2012 for making long days in Building 1 pass by quickly.

To Ryan Bossis and Erika Granger for their previous work with the SWAT model.

To my parents, Jim and Betsy Kellndorfer, and my sisters Jamie, Lisa, and Julie Kellndorfer for their constant love and support. I would not have been able to make it through this year without your words of encouragement, meals filled with laughter, or the laptop I borrowed.

To close friends in Cambridge, New Hampshire, Indiana, Washington DC, New York, and California for celebrating my triumphs and commiserating my defeats.

Table of Contents

List of Figures

List of Tables

1. Introduction

This thesis describes the process of manual calibration of the hydrology for a model constructed with the Soil and Water Assessment Tool (SWAT). This particular SWAT model was constructed by Granger (2010) and improved by Bossis (2011) for a watershed in northwest Singapore called Kranji Catchment (Figure 1). SWAT uses hydrology, weather, land use, soil, and land-surface slope to calculate surface flows and concentrations of water quality constituents from Kranji Catchment into Kranji Reservoir. The overall goal of this project is to use the SWAT model to accurately predict bacterial loading into Kranji Reservoir. Past versions of the model have been problematic because bacteria concentrations differ from field measurements by as much as three orders of magnitude. Past versions of the model have also underestimated surface flows throughout Kranji Catchment. The work presented in this thesis aims to bring model-predicted bacteria concentrations closer to measured values by improving the way the model predicts surface hydrology.

Figure 1 - Kranji Reservoir is located in northwest Singapore (Asia Online 2011).

This thesis is divided into chapters that walk through the process of manual calibration. Chapter 2 provides a context for this project and contains background information on water resource management in Singapore, Singapore's water use history, current water usage in Singapore, and the geology of the island. Chapter 3 introduces the SWAT software, describes the SWAT model that was made for Kranji Catchment, and provides an overview of model calibration. Chapter 4 provides a methodology for the manual calibration and describes changing precipitation within SWAT, running a sensitivity analysis, and iteratively making changes to model input parameters. Chapter 5 summarizes the results of the changes made to the model inputs. The results are discussed in Chapter 6, where a final, calibrated model is described and compared to a set of calibration criteria. Finally, Chapter 7 concludes by evaluating whether the changes to the model's hydrology affected the model's bacteria predictions. Recommendations for future calibration work are also made in this final chapter.

2. Background Information

This chapter was co-written by Suejung Shin, Kathyayani Shob Kondepudi, and Janhvi Doshi.

2.1. Active, Beautiful, and Clean Waters Program

The Singapore Public Utilities Board (PUB) wishes to expand recreational activities within Singapore's reservoirs. Singapore has limited land area for recreation, and making use of selected waterways and waterbodies is an integral part of PUB's plan to meet public recreational needs. Singapore has been working to enhance the accessibility, usability, and aesthetics of green spaces and parks, especially near waterways and drainage (Soon et al. 2009). The PUB wishes to open more of Singapore's surface waters to recreational activities, under the Active, Beautiful, and Clean Waters Program (ABC Waters). The goals of the ABC Waters program are to bring the people of Singapore closer to their water resources by providing new recreational space and developing a feeling of ownership and value. The program aims to develop surface waters into aesthetic parks, estates, and developments. This plan will minimize pollution in the waterways by incorporating aquatic plants, retention ponds, fountains, and recirculation to remove nutrients and improve water quality (PUB 2011a). One of the greatest areas of concern with this plan is microbial pollution.

Disease-causing pathogens pose the greatest immediate threat to human health in polluted surface waters. Humans can come into contact with waterborne pathogens through drinking water supply and through recreation in contaminated surface waters. Infection in humans can be caused by ingestion of, contact with, or inhalation of contaminated water (Hurston 2007). While the exact total number of waterborne pathogens is unknown, it is estimated that over 1,000 viral and bacterial agents in surface waters can make humans sick. Diseases from waterborne pathogens can range from mild to life-threatening forms of gastroenteritis, hepatitis, skin and wound infections, conjunctivitis, respiratory infection, and other general infections (Moe 2007). In order to open surface waterways and reservoirs for recreation, PUB must minimize pathogenic pollution in surface waters and keep the public safe.

Testing surface water for all disease-causing agents is time consuming, costly, and nearly impossible. Fecal indicators are used to assess the microbiological quality of surface waters and are used as a proxy for risk of pathogenic infection. Fecal indicators are typically nonpathogenic organisms, viruses, and compounds that can accurately represent the concentration of human fecal matter in a sample of water. Fecal indicators must exist in high concentrations in waste water and sanitary sludge and must not be produced or degrade naturally in the environment in order to be representative of contamination from human waste (National Research Council 2004). The most commonly used indicator organisms are total and fecal coliform, *E. coli*, fecal streptococci, and enterococci (Toranzos 2007). Maximum Contaminant Levels (MCLs) of these indicators are determined and regulated for recreation in surface waters and in drinking water.

2.2. Singapore's Water History

Water use and water resources have been of great concern to Singapore throughout its history. After over a century under British rule and Japanese occupation during World War II, Singapore and Malaysia became one independent nation in1963 (Evans and Scrivers 2008). Singapore separated from Malaysia two years later and became its own independent nation in 1965. Although Singapore had gained political independence, Singapore had no adequate source of fresh drinking water for its citizens. Singapore has been dependent on Malaysia for freshwater for its entire history as an independent country and still depends on Malaysia for a large portion of its municipal water supply today.

To date, Singapore and Malaysia have signed four water agreements— one each in 1927, 1961, 1962, and 1990 (Chew 2009). Two of these agreements have already expired, but the 1962 Johor River Water Agreement and a 1990 agreement between PUB and the Johor State Government, allow Singapore to use freshwater from Malaysia until 2061. While Singapore has access to Malaysian freshwater for almost 50 more years, the government of Singapore is constantly working towards water independence. Imported water from Malaysia is Singapore's largest single source of freshwater (PUB 2011b), but the price of water from Malaysia has been steadily increasing. Singapore wishes to separate itself from this source of water to avoid future price increases and political conflict.

2.3. Innovative Water Resource Management

With a dense population inhabiting a small island, Singapore is forced to be innovative with its water management practices. The PUB attributes its success in water management to the separation of storm water and wastewater, incorporation of technological developments, and strict regulation and legislation. About 20 percent of Singapore's water supply comes from rainfall, about 40 percent is imported from Malaysia, about 30 percent comes from reclaimed wastewater, and about 10 percent comes from desalination (PUB 2011b).

Singapore keeps its stormwater and wastewater streams completely separate. Stormwater is collected in a network of drains, rivers, canals, ponds, and reservoirs. All collected water, even from urban catchments, is collected and treated for drinking water. Singapore aims for sustainable stormwater management practices and has been using Best Management Practices (BMPs) to treat stormwater before it enters rivers and reservoirs. Many BMPs in Singapore include bioretention and vegetated swales, bioretentive basins, rain gardens, sedimentation basins, constructed wetlands, and cleansing biotopes (PUB 2011).

Singapore also has the largest desalination capacity in Southeast Asia. Currently, Singapore treats 30 million gallons per day (MGD) sea water for drinking water. By 2060, PUB hopes to expand this capacity to meet 30 percent of Singapore's drinking water supply (PUB 2011b).

All sewage and wastewater is collected and treated. Wastewater is reclaimed after secondary treatment, dual-membrane filtration, and ultraviolet treatment technologies through the NEWater program. NEWater reclaimed wastewater is of drinking water quality but is mostly used for industrial and commercial water supply. Its purity is higher than most tap water, making it ideal for industries such as semiconductor manufacturing requiring ultrapure water (Tortajada 2006). Currently there are four NEWater plants in Singapore that contribute to approximately 30 percent of Singapore's water needs. PUB plans to expand NEWater to 50 percent of Singapore's water needs by 2050 (PUB 2011b).

2.4. Population Growth and Water Use in Singapore

Singapore is highly urbanized, with an ever growing population living on a 700-km^2 island (CIA 2011). Despite Singapore's increasing population (Figure 2), per-capita water consumption has decreased due to successful demand management practices (Figure 3). Singapore has implemented a progressive water tariff structure, a water-conservation tax, and a water-borne fee that all encourage reductions in water consumption. The tariff charges 117 cents per m^3 for 1-20 m^3 of water used per month, with progressively higher rates for 20-40 m^3 used and above 40 m^3 used. The water conservation tax charges 30 percent for consumption of 40 m^3 and under, and 45 percent for consumption above 40 m^3. The water-borne fee charges 30 percent for all consumption blocks (Tortajada 2006). These charges and taxes are much higher than the original tariffs and fees implemented prior to 1997 and are believed to be the cause of the decline in per capita water use.

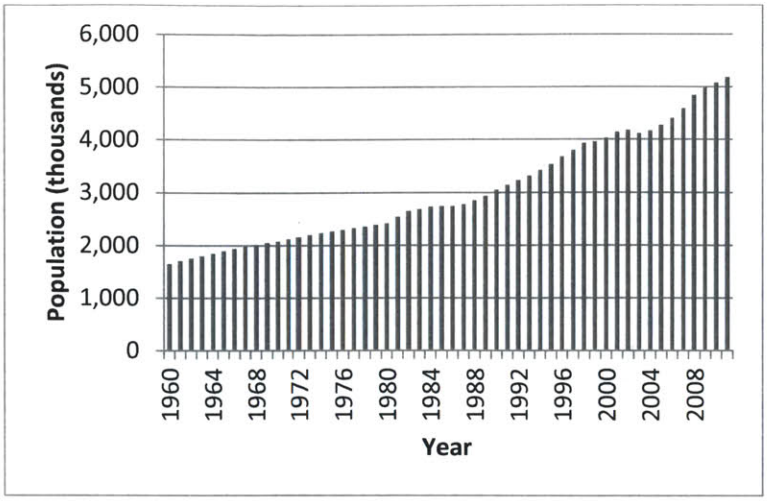

Figure 2 - Singapore population growth over time (Singapore Department of Statistics 2011).

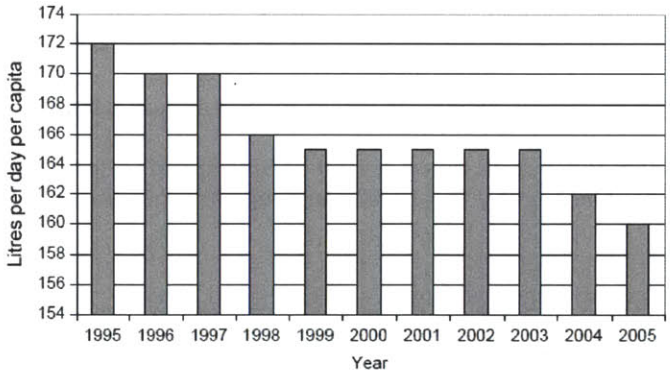

Figure 3 - Per-capita domestic water consumption (Tortajada 2006).

2.5. Overview of the Geology and Soils of Singapore

Singapore's geology and soils have a large impact on hydrologic processes, including above-ground and below-ground transport of water and contaminants. This section contains a brief introduction to the island's geology and soil types and properties.

The solid rock foundation below Singapore is generally divided into four main series (Sharma et al. 1999): igneous rocks called Bukit Timah granite and Gombak norite, sedimentary rocks called the Jurong Formation, quaternary deposits called Old Alluvium, and recent alluvium and marine clay called the Kallang Formation. The geologic map below includes these four rock types, along with two others that make up a small part of the island (Figure 4).

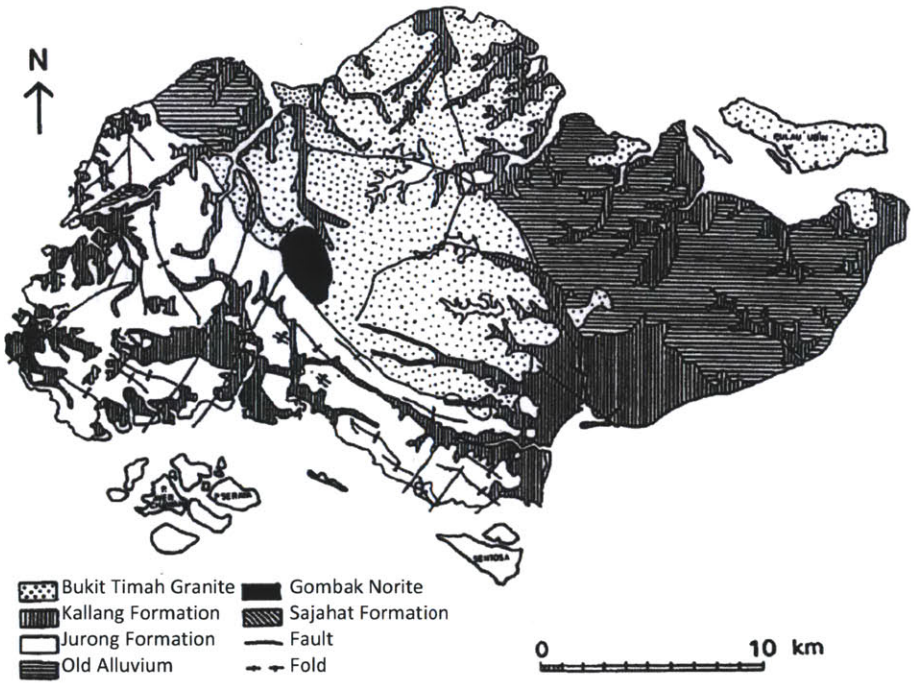

Figure 4 - Geologic rock types found in Singapore (Sharma et al. 1999). Originally published by Public Works Department, Singapore in 1974.

The soils found in Singapore are largely a function of the island's geology. In equatorial regions, soil formation is a primary result of the gradual weathering of the bedrock (Rahman 1991). Singapore's tropical climate and warm, humid weather induce heavy weathering, and thus the categorization of soil types of Singapore is commonly based on its underlying geology.

A third of the island of Singapore rests on the Bukit Timah granite foundation comprised of igneous rocks. This granite weathers extensively. The regolith—or layer of weathered soil covering the solid rock—ranges from a few meters to far above 30 m thick in many areas (Rahman 1991). The faults in the granite rock are nearly vertical, and Sharma et al. (1999) report that the faults that are water-bearing and water-conducting are in isolated areas. They report granite rock permeability values of 10^{-9} to 10^{-7} m/s, which means groundwater will flow only in fractured zones and faults. They also report a granite residual that is completely weathered and soil permeability values on the order of 10^{-5} m/s. The Bukit Timah soil is sandy silty clay, and its properties vary significantly according to the degree of weathering the soil has undergone. The clay fraction of the soil decreases dramatically with depth while the silt and sand fractions generally increase with depth. Bukit Timah granite underlies much of the area around Kranji Reservoir, though the Kallang marine clay underlies the former estuary that was impounded to form Kranji Reservoir.

The Jurong Formation directly underlies the southwestern tip of the area around the Kranji Reservoir. It is made up of a number of sedimentary rock types that vary both vertically and laterally, all with a gradation of weathering that ranges from fine-grained mudstone to coarse conglomerates. The weathering and soil formation of sedimentary rocks is generally less advanced than that of igneous rocks, in part because igneous rocks are generally older and possibly also because they may have been in different topographical and geological conditions (Rahman 1991). Nevertheless, due to Singapore's climate the Jurong Formation

has undergone heavy weathering. Residual soil depths range from a few meters to 50 m. The Jurong Formation is folded intensely and the faults are aligned with or perpendicular to its folds which are northwest-southeast (Sharma et al. 1999). Published values of permeability of the residual soil on the Jurong formation range from 10^{-9} to 10^{-6} m/s, a thousand-fold range. The residual soils are mostly composed of interbedded layers of clayey silt and sandy clay. The soil over the Jurong foundation is again, as expected, highly variable in space because of the wide variety of parent rocks, the high frequency of faults, and the thin bedding.

Old Alluvium underlies a large part of the island, particularly the eastern section. Some of the area west of the Kranji Reservoir is also over Old Alluvium. The deposits are made up of alluvial gravels, sands, and thin silts (Thomas 1991). The horizontal permeability of the residual soils is estimated between 3×10^{-8} to 2×10^{-7} m/s depending on the depth (Sharma et al. 1999). Sharma et al. wrote that there was not enough data to determine the vertical conductivity but estimated that it is one fifth to one half of the horizontal permeability. Interestingly, the Old Alluvium is economically very significant to Singapore; it is the source of much of the sand used for the island's construction.

The Kallang Formation underlies much of the area directly around the Kranji Reservoir. It is a recent deposit (~120,000 years old) with marine clay and peaty soils as its most distinctive components (Sharma et al. 1999). The vertical permeability is estimated to be in the range of 10^{-10} to 10^{-9} m/s, and the horizontal permeability in the range of 10^{-10} to 10^{-8} m/s. The horizontal and vertical permeability both decrease with depth, primarily due to the drop in the void ratio.

The space limitations of the island coupled with the drive for infrastructure development has meant that soil studies rarely impact the decision to develop a plot of land. If the original soil is deemed unsuitable, the project is built all the same on modified, additionally supported, or replaced soil (Rahman 1991). The island's geology makes the extraction of groundwater unfeasible (Rahman 1993), though Pitts (1985) reported that in the low-lying areas of the island the groundwater table is only 1.5 m below the ground surface. Because of the lack of general interest in the soils of Singapore, there are only a handful of cited soil studies. Most of these studies look at the impact of soils on construction rather than the hydrogeology. However, since the 1980s there have been several studies aimed at classifying soils around the island and estimating values of permeability including Ives (1977), Chia (1991), and Rahman (1991, 1993). Given the highly varied geology, these studies report that the soil is extremely heterogeneous and the reported hydraulic conductivity range is over multiple orders of magnitude. The hydraulic conductivity of a highly productive aquifer can range from 10^{-4} m/s for gravels and sands to as much as 1 m/s for gravels. In comparison, the hydraulic conductivity values of the soils of Singapore are extremely low and, as a result, groundwater is not regarded as part of the island's resources. Table 1 summarizes the values of permeability for the major soil types found in Singapore.

Table 1 - Major soil types and their permeabilities.

Residual Soil Series	Residual Soil Permeability [m/s]
Bikat Timah Granite	10^{-5}
Jurong Formation	10^{-9} to 10^{-6}
Old Alluvium	10^{-8} to 10^{-7}
Kallang Formation	10^{-10} to 10^{-8}

3. SWAT Background

To assist the PUB in the ABC Waters program, a watershed runoff model of Kranji Catchment was created in using the Soil and Water Assessment Tool (SWAT) (Neitisch et al., 2002). This chapter provides an introduction to SWAT software and the SWAT model for Kranji Catchment.

3.1. SWAT software

The Soil and Water Assessment Tool (SWAT) is a modeling software used in conjunction with ESRI ArcGIS software that models the impact of human development on a watershed. SWAT has a graphical user interface that can be installed as an add-on in ArcMap and incorporates spatially varying weather, hydrology, soil, land-surface slope, plant growth, and land-use data for a watershed. The SWAT model uses those watershed properties to quantify water, sediment, nutrient, bacterial, and chemical runoff (UC Davis 2008) . Weather data includes precipitation, maximum and minimum temperatures, solar radiation, evapotranspiration, relative humidity, and wind speed (Winchell et al. 2007). Hydrology inputs include surface runoff, return flow, pond and reservoir storage, percolation, and groundwater flow. SWAT is a continuous model with a daily time step and is organized on a watershed scale. SWAT divides a watershed into subbasins and divides each subbasin into hydrologic response units (HRUs). Each HRU within a SWAT model is a microwatershed that has homogenous land-use, soil type, and land slope.

3.2. Granger 2010 Model

A SWAT model of the Kranji Catchment was first created by Granger (2010) (Figure 5). Her model quantified bacterial loading of total coliform and *E. coli* into Kranji Reservoir. Granger used ArcGIS to delineate the watershed modeled by SWAT. Areal distribution of land-use came from the PUB of Singapore. Soil types and properties came from a combination of Ives (1977), Chia (1991), and Granger's own work (Granger 2010). Land-surface slope was derived by ArcGIS software from a Digital Elevation Model (DEM). Weather data for the SWAT model was generated by SWAT from statistical analysis of meteorological measurements in Kranji Catchment by NTU (2008). While this model was essentially a "first draft" of a SWAT model for Kranji Catchment, it was able to predict the presence/absence of bacteria within each subbasin fairly well compared to field measurements (Granger 2010). However, the model consistently overestimated the bacterial concentrations within individual subbasins. This model was a useful first attempt at modeling bacterial loading into Kranji Reservoir, but it required major changes to make it more accurate.

3.3. Bossis 2011 Model

3.3.1. Improvements from 2010 Model

The second generation of the SWAT model for Kranji Catchment was built by Bossis (2011). He updated Granger's 2010 model by making changes to the hydrology and land use used by the model. The model was run with and without point sources of bacterial pollution. While the 2011 SWAT model contains more detailed information about Kranji Catchment, the model underestimates flow and bacterial loading throughout the watershed.

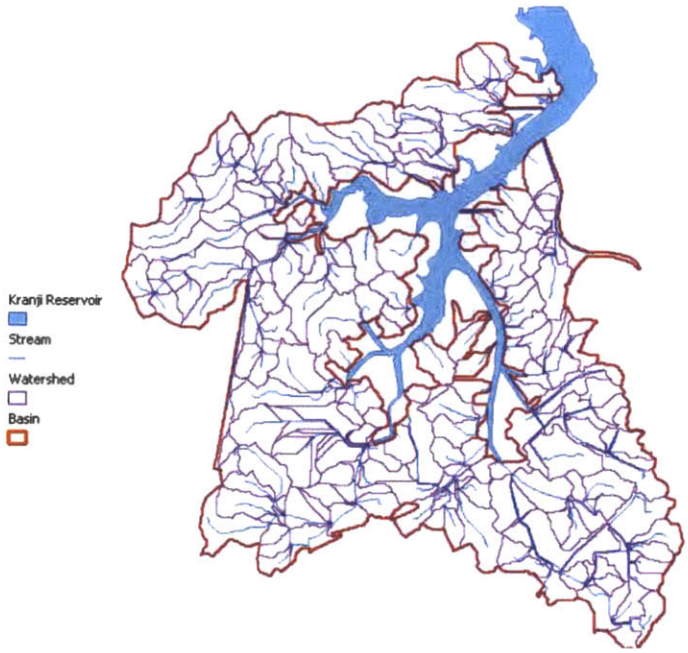

Figure 5 - Boundaries of 2010 SWAT model of Kranji Catchment (Granger 2010).

Bossis expanded the boundaries of the Kranji Catchment within the model to include the entire Kranji Reservoir and the reservoir shoreline. The boundary expansion allowed areas draining directly into the reservoir via overland flow to be included in the model (Bossis 2011). Previously, only streamflow into the reservoir was included and areas directly draining into the reservoir were omitted (shown as white area adjoining the reservoir in Figure 5). Many agricultural regions with high potential for bacterial runoff are drained by overland flow directly into the reservoir. By including the reservoir and its shoreline in the model, Bossis ensured that the Kranji Catchment was modeled as one basin with a single outlet at the outlet of Kranji Reservoir. Previously, all streams entering the reservoir were defined as basin outlets in the SWAT model.

Bossis also updated the stream network within the model. He included a large portion of land in the east of the basin called Kranji Catchment 7 (KC7). Previously, this land was not included in the model, leaving a large portion of the basin out of SWAT's calculations (Bossis 2011). When including KC7, Bossis used PUB plans to create a network of canal drainage that was later verified with field inspections. To keep an active stream network with a single outlet, Kranji Reservoir is modeled as one very long, deep, and wide slow-moving stream within the model. A map of the full boundaries of the 2011 model can be seen in Figure 6.

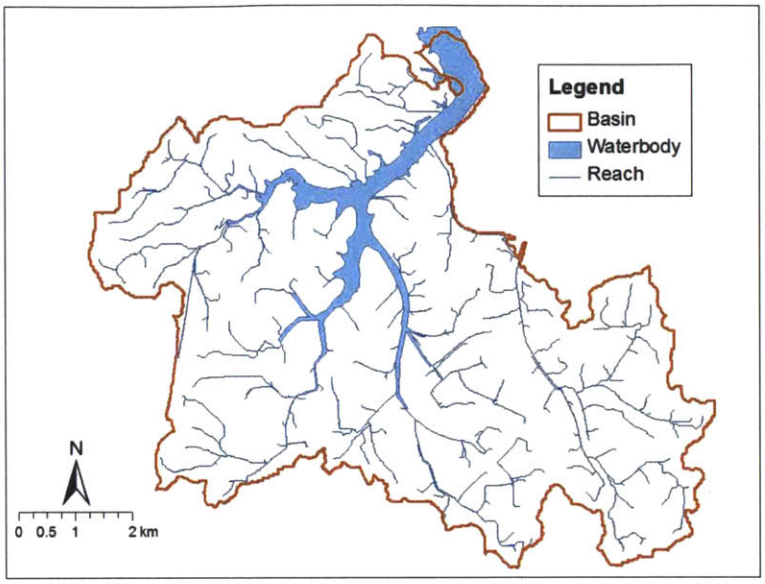

Figure 6 - Boundaries of 2011 SWAT model of Kranji Catchment with one single outlet.

While the Granger model (2010) used land use for Singapore published by PUB, Bossis worked to reclassify some land-use terms and to make export coefficients for individual land-use types more accurate by measuring bacteria concentrations in the field (Bossis 2011). He quantified bacterial runoff for several low-density residential neighborhoods within the catchment and updated agricultural land use to reflect agricultural practices in Singapore. Agricultural land use was reclassified to include chicken farms, tree farms, fish farms, nurseries, leafy row crops, and brush. Bacterial loading coefficients for these areas were calculated from field bacteria measurements and updated within the SWAT model.

3.3.2. Results

Bossis (2011) compared bacterial concentrations from the 2011 SWAT model with bacterial concentrations measured in 35 different subbasins within Kranji Catchment. The model underestimates bacterial concentrations for total coliform and *E. coli* by 1 to 3 orders of magnitude. Results of the model are compared with bacterial concentrations measured in the field in Figure 7 and Figure 8. Overall, the model predicts a similar trend to measurements, but grossly underpredicts bacterial concentrations.

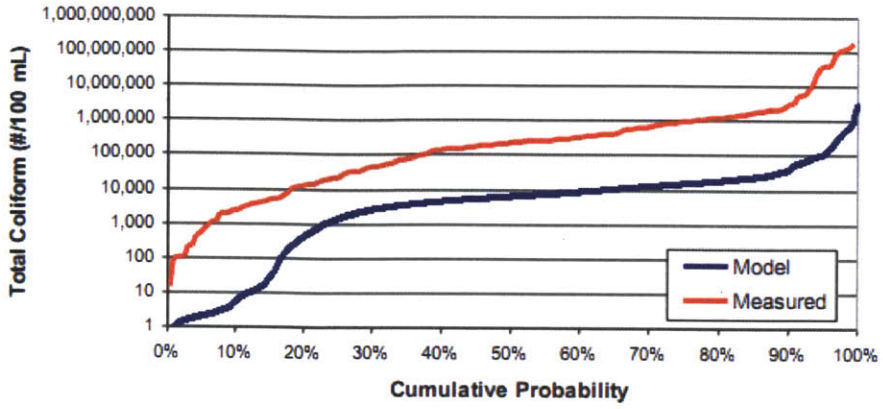

Figure 7 - Cumulative density of total coliform predicted by the 2011 SWAT model (Bossis 2011).

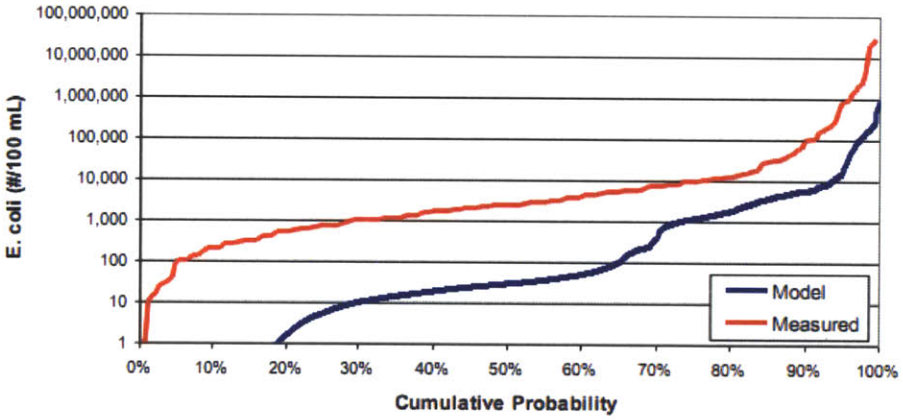

Figure 8 - Cumulative density of *E. coli* predicted by the 2011 SWAT model (Bossis 2011).

The low predicted bacteria counts can partially be explained by an underprediction of output of the model. The SWAT model output reports a daily volumetric flow for each subbasin, but the vast majority of flow entries in the output are reported as 0 cms, or no flow. A lack of flow in stream reaches within SWAT indicate that sources of water in the catchment are being underrepresented or that losses of water are being overrepresented in the model (Bossis 2011). This volume of water that is missing from SWAT outputs would contain bacteria in the actual catchment. Since the water is missing from the model, any bacteria that it would contain are also missing from the model. The lack of flow for many days throughout the SWAT simulation does not make sense given the heavy rainfall in Singapore and indicates that there is a problem with the way the model predicts flows within Kranji Catchment.

The bacteria concentrations may also be underestimated by SWAT due to errors in bacterial fate and transport within the model. In the model, only residential and agricultural areas contribute to bacterial loading (Bossis 2011). The model was set up this way assuming that these sources would be much more significant than industrial or commercial sources, but other land-use types may be contributing to bacteria counts in Kranji Reservoir. The bacterial concentrations also depend on other inputs to the SWAT model

including bacterial loading rates, point sources, and estimates of bacteria decay rates. If these inputs are incorrect, the model predictions and outputs will be incorrect as well.

3.3.3. Remaining Problems

The 2011 SWAT model for Kranji Catchment requires improved calibration. The model correctly predicts trends in bacteria population density, but grossly underestimates flow and bacterial loading (Bossis 2011). The model needs to be calibrated to existing field measurements of flow and bacterial loading in order to more accurately quantify total coliform and *E. coli* in individual subbasins.

3.4. Overview of Model Calibration

Without model calibration, a model may not accurately predict environmental conditions. Model calibration is the process of changing model input parameters in an attempt to match model outputs to field measurements (MDEQ 2011). Calibration is an iterative process that requires changing input parameters, running the model, checking the results, comparing outputs to field conditions or measurements, and deciding whether or not a model run meets calibration criteria. If the results of a model run do not meet the calibration criteria, model inputs should be changed again, starting a second iteration of calibration. The calibration criteria should be predetermined before calibration is conducted and should provide a range of acceptable values near measured values. When iterations of the calibration fall within the range of calibration criteria, a model has been successfully calibrated.

Environmental and hydrologic models can be calibrated to either steady-state or transient conditions. In a steady-state solution, the model output of interest—coliform or *E. coli* concentrations in the SWAT model—has reached a point where it does not vary with time. In a transient solution, the modeled parameter does change with time and the range of variation within the model over time can be adjusted with calibration (MDEQ 2011).

Depending on the type of model, some field conditions that may be compared with model results during calibration include surface flows, hydraulic head data and gradients, groundwater flow direction, water mass balance, contaminant concentrations, transport rates, and degradation rates (MDEQ 2011). No universally applicable goodness-of-fit criteria can be used to evaluate the success of a model calibration. A modeler needs to use discretion in evaluating and comparing maps, tables, and plots generated by both the model results and field data. A general rule of thumb is that the difference between the model results and field data should be less than 10 percent of the natural variability in the data set (MDEQ 2011).

The theory behind model calibration in SWAT is very similar to any other model's calibration. Input parameters to SWAT are modified, the model is run, and outputs are compared to measured field values (Neitsch et al. 2002). Iterations of calibration are then repeated until output values meet calibration criteria. Some of the most common calibration difficulties in SWAT are determining the proper land-use parameters and export coefficients, the location of gauging and water quality monitoring stations in the field compared to subbasin outlets in the model, and the completeness and availability of monitoring data. In SWAT, calibration can be done either manually or with auto-calibration (Winchell et al. 2007). Both processes are described below.

3.4.1. Manual Calibration: Hydrology

The first step in a manual calibration of SWAT is calibrating the hydrology (Neitsch et al. 2002). This step is prioritized in calibration methods because hydrologic flows are independent of chemical, biological, and physical transport in the model, but transport is highly dependent on the hydrology. Calibration should start with the most upstream monitoring station, and model results at upstream stations should be calibrated before moving downstream. In addition, if field measurements are available in large

data sets, a calibration should start with annual data and then be fine-tuned with monthly or daily data in order to first capture annual trends and then capture seasonal and storm variability.

In a hydrologic calibration, a mass balance for water must be maintained at all times. A model calibration can be solved iteratively by calibrating stream flow, calibrating subsurface flow, and repeating those two steps until model results meet the calibration criteria (Neitsch et al. 2002). In a manual calibration, input parameters in SWAT must be adjusted manually, and the parameters and degree to which they are changed is left to the discretion of the modeler. All input parameters to SWAT must remain reasonable for given environmental conditions. The parameters that can be adjusted in a hydrologic calibration in SWAT include the curve number, soil water capacity, soil evaporation compensation factor, groundwater recharge coefficient, threshold depth of water in the shallow aquifer, channel hydraulic conductivities, and the baseflow recession factor. These parameters are specified in input tables for the SWAT model and can be manually adjusted in Microsoft Access or other database software.

3.4.2. Manual Calibration: Sediment

In a manual calibration of SWAT, sediment is the second model output that must be considered (Neitsch et al. 2002). Sediment transport in the environment is strictly physical. There are no chemical or biological decay, adsorption, or degradation coefficients to consider for sediment, so a calibration of sediment in a SWAT model is a calibration of physical transport only. Like the hydrologic calibration, sediment calibration should start at the most upstream monitoring stations and should move downstream only when the upstream stations are calibrated. Sediment calibration should also start with an annual dataset and then be fine-tuned to monthly and daily datasets which include seasonal and storm variability.

Sediment loading in a catchment comes from individual HRUs and subbasins and from stream degradation and erosion (Neitsch et al. 2002). When calibrating the sediment loading in a SWAT model, both of these sources of sediment must be considered. In order to calibrate the sediment loading from HRUs and subbasins, the HRU slope, crop management factor, slope length factor, crop practice factor, crop residual coefficient, and biomixing efficiency can be adjusted. To calibrate channel degradation and deposition, the linear and exponential sediment routing parameters, the channel erodibility factor, and the channel cover factor can be adjusted. These parameters can be found in the hydrologic, soil, and land-use databases in SWAT input files and can be manually edited in database management software.

3.4.3. Manual Calibration: Bacteria Loading

The bacterial loading for coliform and *E. coli* should be addressed last in a manual calibration (Neitsch et al. 2002). Bacterial loading is highly dependent on physical and chemical characteristics of the catchment and cannot be accurately represented in the model until the flow and physical transport within the model are calibrated. Like the hydrology and sediment calibrations, bacterial calibrations in the model should begin at the most upstream monitoring stations and progressively move downstream in the watershed. Bacterial concentrations should first be calibrated annually and then adjusted to a monthly and daily timescale to account for seasonal and storm variation.

Surface loading from HRUs and subbasins is the source of bacteria within the model (Neitsch et al. 2002). Chemical and biological processes within the stream network can cause bacteria to grow, degrade, or die off. These factors are accounted for in the manual calibration and include the die-off and growth factors for persistent bacteria adsorbed to soil particles, the die-off and growth factors for less persistent bacteria adsorbed to soils, the die-off and growth factors for persistent bacteria in soil solutions, the die-off and growth factors for less persistent in soil solutions, the bacterial partition coefficient, the concentration of persistent and less persistent bacteria in fertilizer and manure, and daily, monthly, and yearly loading of persistent and less persistent bacteria. These parameters are found in soil and land-use inputs to SWAT and can be edited with database management software.

3.4.4. Auto-Calibration and Uncertainty Analysis

Auto-calibration techniques were introduced to SWAT in SWAT2005 (Veith and Ghebremichael 2009). These techniques simplify the calibration process so that the user can use an auto-calibration toolbox instead of manually changing parameters in SWAT input files. The basic steps in a SWAT auto-calibration are 1) define a simulation model run, 2) select an HRU or subbasin to calibrate using measured data, 3) import a file of measured data, 4) use SWAT to adjust calibration parameters, and 5) iteratively run auto-calibration until model results meet calibration criteria.

One added benefit to SWAT2005's auto-calibration toolkit is that it includes a sensitivity analysis. The sensitivity analysis enables one to examine the overall impact on the model caused by changing one specific input. SWAT's sensitivity analysis combines two statistical sampling techniques called Latin Hypercube and One-Factor-at-a-Time to select parameters within the model and vary them by a user-specified percentage change (Veith and Ghebremichael 2009). At the end of the sensitivity analysis, SWAT outputs a table summarizing the inputs changed in the analysis and the results. The sensitivity analysis allows a user to see which input parameters are most influential within the model and can provide information about which parameters to change in a calibration.

SWAT auto-calibration contains three options for calibration: ParaSol, ParaSol with Uncertainty Analysis, and SUNGLASSES (Veith and Ghebremichael 2009). The ParaSol option focuses on parameter calibration and the SUNGLASSES option focuses on model uncertainty. All necessary data entry and calibration decisions are made in the SWAT auto-calibration and Uncertainty Analysis window and are specified by the user.

In ParaSol, SWAT optimizes values of flexible parameters so that the model meets a certain calibration criterion for a given field data set (Veith and Ghebremichael 2009). The user sets a confidence window for the model results determined by a 90%, 95%, or 97.5% probability and either a chi-squared or Bayesian distribution of model outputs. Maximum and minimum parameter values and the range of model results are provided in the ParaSol output file along with the optimal solution. All inferior solutions can also be found within ParaSol's outputs.

The output of the SUNGLASSES analysis is very similar to ParaSol but it also ranks all simulated runs by a global optimization criterion (GOC) which is similar to an objective function value (Veith and Ghebremichael 2009). The optimal solution will have the lowest GOC. In calibrating a SWAT model, Veith and Ghebremichael (2009) suggest running both the ParaSol and SUNGLASSES analysis and comparing results to find the best calibration of a given model.

4. Manual Hydrologic Calibration Methodology

Despite SWAT's extensive auto-calibration software options, a manual calibration of the hydrology was conducted on the 2011 SWAT model. This calibration method was selected in order to have more control over which parameters were changed and to make sure parameters were not changed beyond reasonable environmental values. This project is also intended to be a learning exercise, and a manual calibration requires a deeper understanding of how a model works than an auto-calibration. The only tool from the SWAT auto-calibration software package used in this project was the sensitivity analysis tool.

4.1. Stream Gauge Stations

In the manual calibration, subbasin discharges from SWAT outputs were compared to volumetric stream flows from five stream gauge stations located throughout Kranji Catchment. The five stream gauges were installed and maintained by NTU during Phase I and II of work for the Water Quality Monitoring, Modeling, and Management for Kranji Catchment/Reservoir System project (NTU 2008). The five stations are located at Bricklands Road (CP1), Choa Chu Kang Walk (CP2), Tengah Air Base (CP4), Sungei Kangkar (CP6), and Sungei Pang Sua (CP7) (Figure 9).

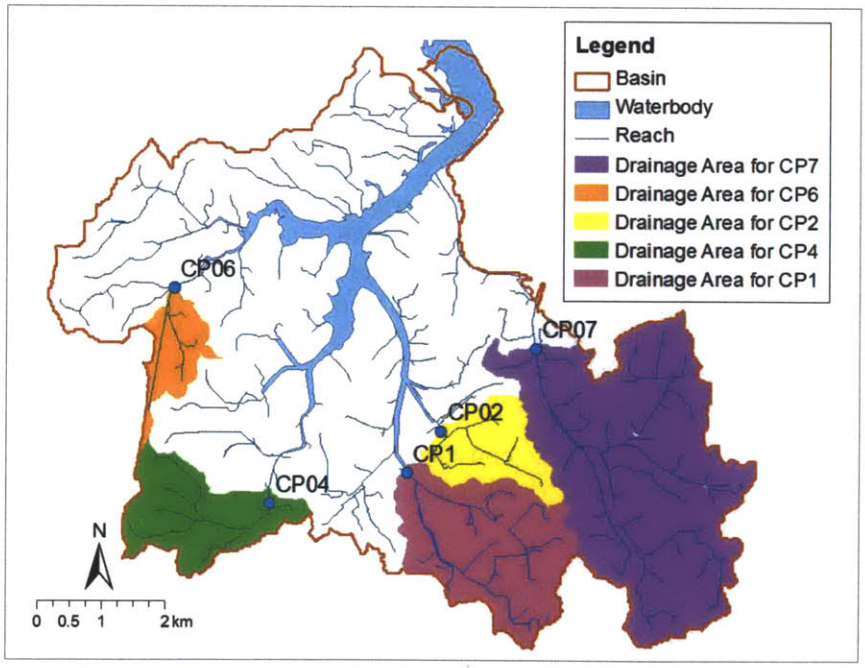

Figure 9 - Locations and drainage areas of five stream gauge stations in Kranji Catchment.

Each stream gauge station drains a different area within Kranji Catchment, each with varying land-use. Land-use types for Kranji Catchment used by the SWAT model are described in detail by Bossis (2011), but for these five drainage areas, land use was defined simply as either urban or non-urban. Urban land-uses include businesses with a public health, safety, and nuisance buffer, commercial, commercial and residential, civic-community institution, industrial, education institution, health and medical care, landed property, light rapid transit, mass rapid transit, place of worship, high-density residential, medium-density residential, low-density residential, roads, transportation facilities, and utilities. Non-urban land uses

include agriculture, brush, cemetery, chicken farm, farm market, fish farm, leafy row crop, nursery, open space, park, reserve site, special use, and tree farms. The percentage of land area with an urban land use was calculated for each subbasin. CP1, CP2, and CP7 have the highest percentage of urban land use in their drainage areas, while CP4 and CP6 have the least. The exact drainage area, percentage of land area with an urban classified land use, and subbasin location for each stream gauge station can be found in Table 2.

Table 2 - Stream gauge names, drainage areas, land uses, and locations. (Color coding corresponds to map colors in Figure 9.)

Station Name	Drainage Area [km^2]	Percent of Drainage Area with an Urban Land Use	Subbasin Location
CP1	5.09	42%	324
CP2	2.02	78%	281
CP4	3.04	7%	352
CP6	1.29	8%	124
CP7	11.7	52%	164

Each gauging station consisted of a combined water level and velocity sensor, tipping bucket rain gauge, auto-sampler, data logger, and modem. Measurements were recorded every 5 minutes by the data logger for periods of time between June, 2005 and August, 2007 (NTU 2008). The volumetric flow for each measurement was calculated by NTU by multiplying the measured stream velocity by the wetted cross-sectional area in the flow channel, which was calculated using the water level measurement. As a part of this project, a daily average flow was calculated for each data collection day by averaging all measurements in 5-minute intervals for the 24-hour period between 00:00 and 23:55. Intervals with a flow calculation of 0 cms were omitted from the daily averages because a base flow should have been seen at each station throughout the measurement period. A calculation of 0 cms is more likely to indicate an equipment malfunction than an actual no-flow period. The daily average flow dataset at each gauge station was used as a baseline to calibrate the modeled subbasin outflows.

4.2. Calibration of Precipitation

Precipitation within a SWAT simulation can consist of either measured rainfall or a simulated forecast generated by SWAT using user-specified weather statistics. Three iterations of precipitation were modeled in SWAT as part of this calibration.

4.2.1. SWAT Simulated Rainfall: Low

The first iteration of precipitation in the SWAT model consisted of a simulated forecast with a low yearly rainfall rate of 1820 $\pm$ 160 mm. Monthly statistics for mean rainfall, standard deviation, and average number of wet days can be found in Table 3. These rainfall statistics were stored in the SWAT input files for Kranji Catchment and were calculated by Granger (2010). These rainfall statistics reflect a year of low rainfall for Kranji Catchment when compared to the long-term yearly average for Singapore of 2340 mm (NEA 2010).

Table 3 - Rainfall statistics for simulated low-level precipitation.

Month	Mean Rainfall [mm]	Standard Deviation [mm]	Average Number of Wet Days
January	155	50	15.5
February	56	9	10.5
March	97	7	11
April	254	17	18.5
May	139	11	19.5
June	190	13	15.5
July	238	15	19.5
August	71	5	13.5
September	95	10	9.5
October	49	7	5
November	109	15	15.5
December	369	39	19

4.2.2. SWAT Simulated Rainfall: High

The second iteration of precipitation in the SWAT model consisted of a simulated forecast with a high yearly rainfall rate of 2990 $\pm$ 280 mm. Monthly statistics for mean rainfall, standard deviation, and average number of wet days can be found in Table 4. These rainfall statistics were estimates loosely derived from a combination of precipitation data collected from rain gauges at each of the five sampling sites. A rainfall measurement was recorded with each stream flow measurement at each stream gauge station. These measurements consisted of intermittent records during a 3-year time period. Average monthly rainfall, standard deviation, and average number of wet days were estimated from this dataset and were meant to represent a year of high rainfall for Kranji Catchment.

Table 4 - Rainfall statistics for simulated high-level precipitation.

Month	Mean Rainfall [mm]	Standard Deviation [mm]	Average Number of Wet Days
January	355	50	15.5
February	100	15	10.5
March	130	15	13
April	500	35	22
May	200	13	19.5
June	190	18	15.5
July	238	18	19.5
August	400	26	19
September	170	13	11
October	225	20	15
November	109	15	15.5
December	369	39	19

4.2.3. Rain Gauge Data from CP1

The last iteration of precipitation in the SWAT model consisted of using a precipitation dataset taken at CP1. This dataset contains a daily rainfall total for each day during the time period January 1, 2005 – October 31, 2007. During the SWAT model simulation, the daily rainfall from this station was used as the daily rainfall in each subbasin in Kranji Catchment. The average annual rainfall throughout this time period was 2640 mm/yr and was taken to be a representative estimate of average rainfall in Singapore.

4.3. Sensitivity Analysis

The only auto-calibration or uncertainty software used in this calibration was the SWAT sensitivity analysis. A sensitivity analysis of subbasin outflow was conducted for subbasins 30 and 420. These two subbasins were selected because they were both in the subset of 35 subbasins used by Bossis (2011) in his multi-basin bacteria comparison. In addition, subbasin 30 consists of mostly non-urban land uses while subbasin 420 consists of mostly urban land uses. Two subbasins with different land use were selected to assess whether sensitivity to calibration parameters varied by land use. In both sensitivity analyses, variation in subbasin outflow was compared to variation in 26 calibration parameters, which relate surface flows to groundwater, evaporation, and precipitation. A full list of parameters assessed and their effect on outflows for both subbasins can be found in Appendix I. Subbasin outflow was most sensitive to the same six parameters in both subbasins (Table 5).

Table 5 - Six most sensitive calibration parameters in subbasins 30 and 420.

Parameter	Name	Description
CN2	Curve number	SCS curve number for moisture condition II; used to calculate maximum soil moisture retention before runoff occurs
ESCO	Soil evaporation compensation factor	Sets depth distribution of soil evaporation; a lower ratio means a lower soil depth at which evaporation can occur
alpha_bf	Baseflow recession factor	Baseflow recession constant; index of groundwater flow response to changes in recharge (low = slow, high = fast)
sol_z	Depth of soil layer	Depth from surface to bottom of soil layer (mm)
sol_awc	Soil available water content	Available water content to plants; sol_awc = Field Capacity – Wilting Point
GWQMN	Minimum depth in shallow aquifer for return flow to occur	Groundwater will flow into stream reach if depth of water in shallow aquifer exceeds this depth

4.4. Parameter Changes

The only calibration parameters adjusted in the manual calibration were the six parameters that resulted in the largest percentage changes in subbasin outflows during the sensitivity analysis. These parameters—CN2, ESCO, alpha_bf, sol_z, sol_awc, and GWQMN—were varied methodically and iteratively in many simulations of the SWAT model. In most of the model simulations, only one parameter was adjusted at a

time, but several model simulations contained a combination of parameter changes. Each time the model was run with updated parameter values, modeled values for subbasin outflows in subbasins 364, 281, 352, 124, and 164 were compared to measured stream flow values at gauge stations CP1, CP2, CP4, CP6, and CP7 respectively. A list of all model simulations run with SWAT can be found in Appendix II. Full results are described in Chapter 5.

5. Results

This chapter describes the results of changes made to the SWAT model during the manual calibration. A full discuss of the changes made in the final model calibration are described in Section 6

5.1. Results of Precipitation Changes

Changes to the precipitation in the SWAT model had a significant impact on subbasin outflows. In this section, the model outputs for subbasin outflow are depicted graphically and compared to measured stream flows at each stream gauge station. Each graph is a flow duration curve, in which ranked discharge is plotted versus exceedance probability. In these graphs, the exceedance probability is defined as the percentage of time that a flow was equaled or exceeded. Exceedance probability was calculated by diving the rank of a flow by the total number of flow entries in a dataset. Flow duration curves were chosen to display the results because model outputs and measurements with varying numbers of data points can easily be compared. All model runs were simulated for the time period of January 1, 2005 – February 5, 2007 and subbasin outflows were reported daily.

All iterations of precipitation change to the SWAT model match measured values better than the 2011 model at all five stream gauge stations (Figure 10). The simulation with low SWAT-simulated rainfall underestimates outflows at model subbasin 324, the same location as gauging station CP1, over all flows. This simulation also underestimates outflows at subbasin 281, the same location as CP2, at subbasin 124, the same location as CP6, and at subbasin 164, the same location as CP7. The model run with low SWAT-simulated rainfall matched peak and mid-range flow values very closely at CP4, but low flow values tail down to values that would be below detection in an actual stream.

The run with high SWAT-simulated rainfall overestimates peak flow at CP1 and CP7, but underestimates outflow for most of the duration curve (Figure 10). This simulation also underestimates outflow at CP2 by as much as 3 orders of magnitude and predicts low flow values that are below detection in a real stream. The high SWAT-simulated rainfall is close to matching measured flows at CP4 and CP6, however. At CP4, this model run overestimates peak flows by a factor of 5, but matches high and low flow values extremely well. The model run matches measured values at CP6 fairly well for high to mid-range flow values, but tails off with low flow values below detection in a real stream.

The model run with the measured rainfall record from CP1 matches peak measured flows at CP1 extremely well (Figure 10). This run matches measured values more closely than all other runs at CP1 and only varies from measured values by about a factor of 2. At CP2, outflows from this model run match peak measured flows at CP2 very closely, and, while the model run underestimates all other flows at CP2, the shape of the flow duration curve at subbasin 281 matches the shape and values of the line of measured flows more closely than other model runs. At CP4, the model run with the measured rainfall record overestimates subbasin outflow for the entire flow duration curve. This model run matches stream flow measured at CP6 very well for peak and high flow values and matches the general shape of the flow duration for measured values, but overestimates flows for lower flow values. At CP7, this model run overestimates the peak outflows at subbasin 164, but underestimates mid-range and low flow values. Overall however, the outflows at CP7 match the shape of measured flow duration curve much better than the other two model runs.

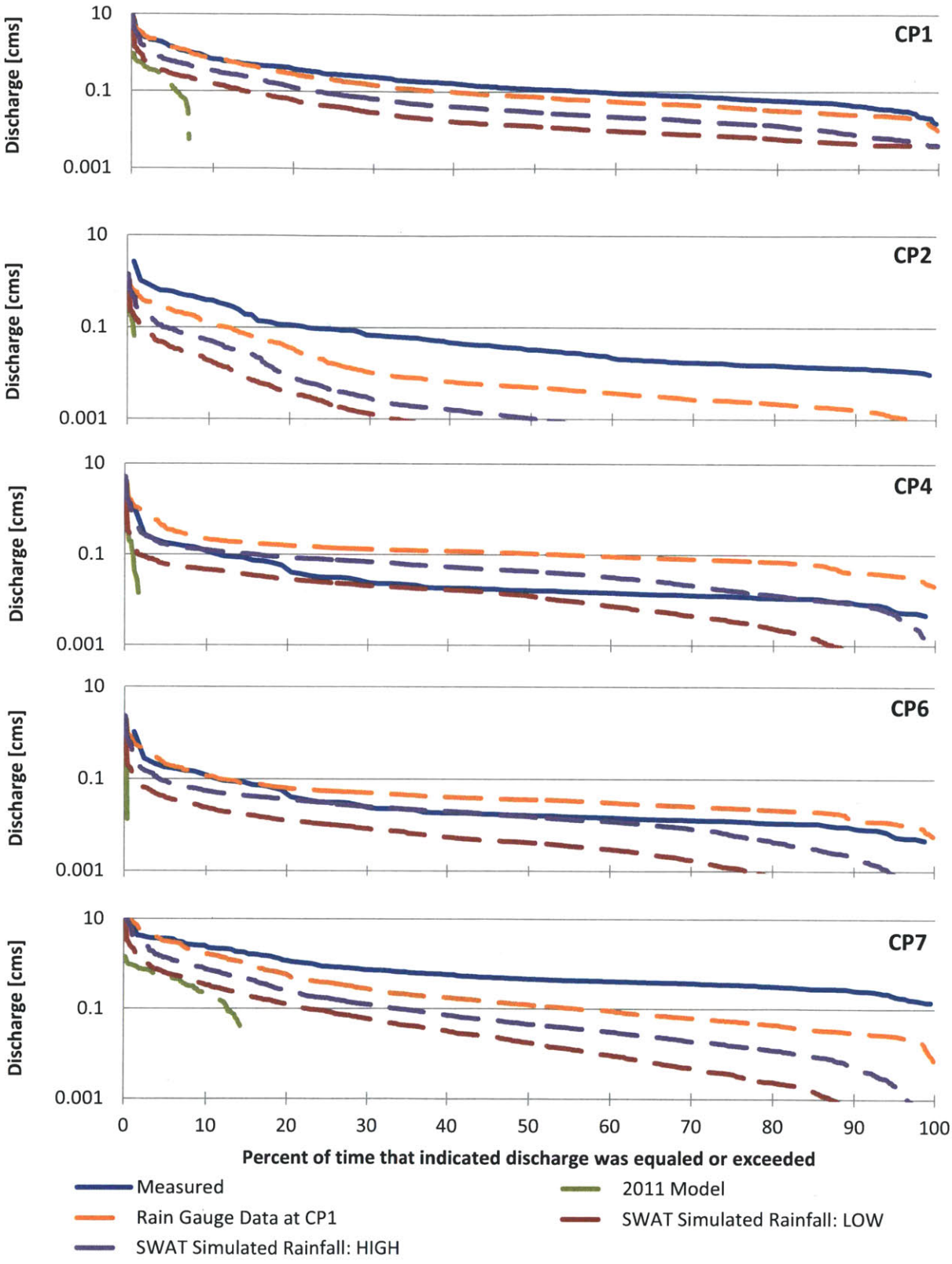

Figure 10 - Flow duration curves comparing changes in precipitation to measurements at CP1, CP2, CP4, CP6, and CP7.

5.2. Parameter Changes

This chapter describes general trends in changing each of the six calibration parameters described in Section 4.4. The model outputs for subbasin outflow are depicted graphically and compared to measured stream flows at each stream gauge station. Each graph is a flow duration curve, where ranked discharge is plotted versus exceedance probability. All model runs were simulated for the time period of January 1, 2005 – February 5, 2007 and subbasin outflows were reported daily. All simulations with parameter changes were run with precipitation equal to rain gauge data from CP1.

5.2.1. Parameter: ESCO

Changing the parameter ESCO, or soil evaporation compensation number, resulted in a slight change in modeled subbasin outflows. ESCO can be any value between 0.0 and 1.0, and its value represents a depth distribution of soil evaporation (Figure 11). Less evaporation will occur at a given soil depth within the model with a higher value of ESCO (Neitsch et al. 2004).

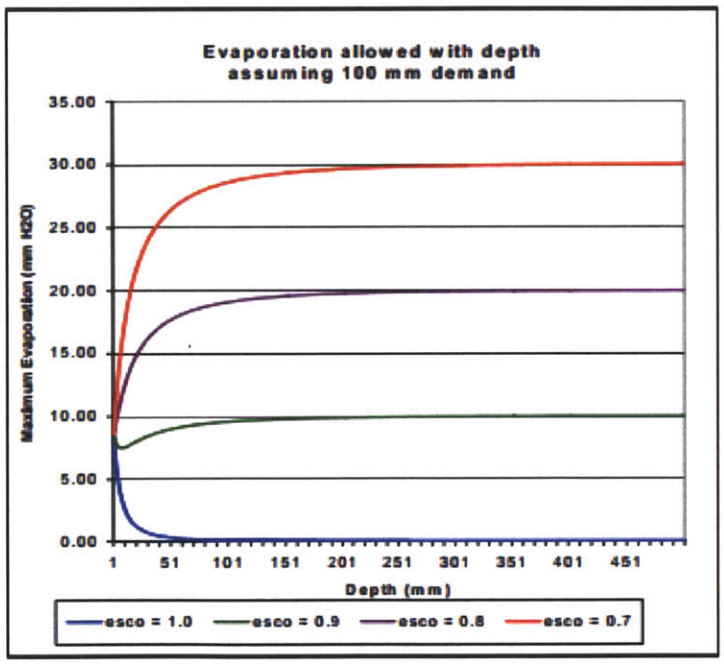

Figure 11 - Depth distributions of soil evaporation with different values of ESCO (Neitsch et al. 2004).

The 2011 model has an ESCO value equal to 0.95. For this thesis, the revised model was run four times, with ESCO = 1.0, 0.95, 0.90, and 0.50 and precipitation equal to the rain gauge data from CP1. The results of the four model runs were very similar when compared to measurements at each of the five stream gauge stations. The results of the model run at CP1 are plotted below (Figure 12), and similar results at CP2, CP4, CP6, and CP7 can be found in Appendix III.

All four model runs match peak flows very well. At lower flow values, a higher ESCO results in slightly higher flow values. At all stream gauge stations, the model run with ESCO = 1.0 has the highest flow

values, while the model run with ESCO = 0.50 has the lowest flow values (Figure 12). The difference in flow values between all four model runs, however, is less than a factor of 2.

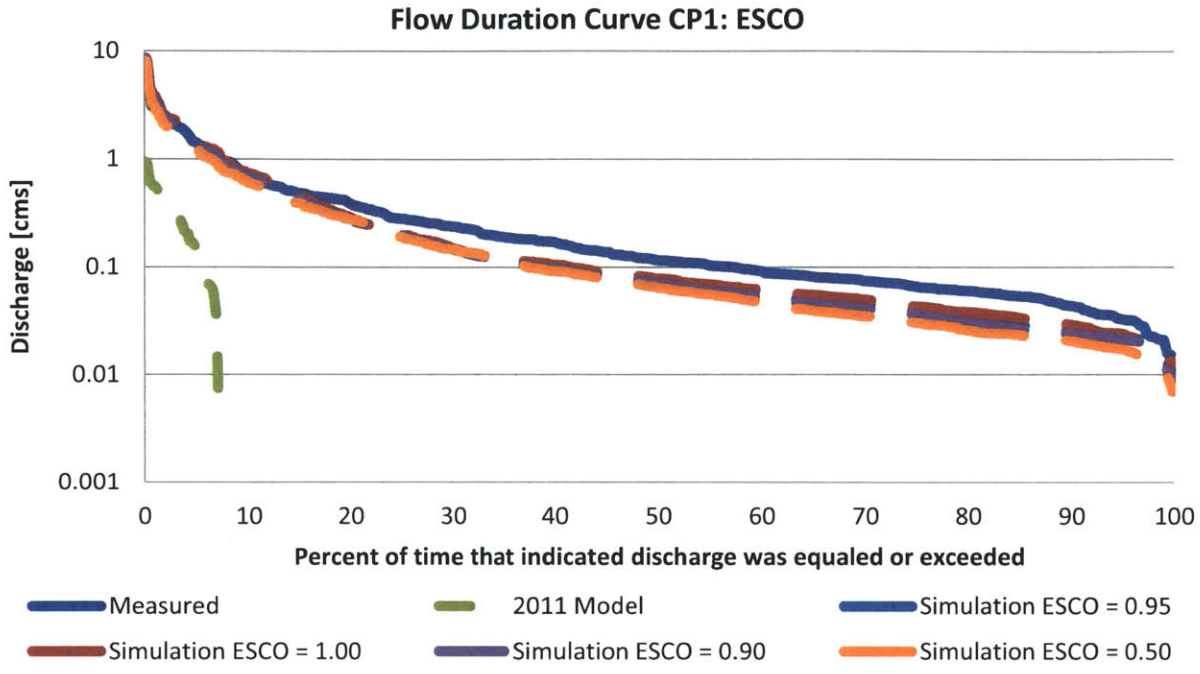

Figure 12 - Flow duration curve comparing changes in ESCO to measurements at CP1.

The best fitting value of ESCO differs at each stream gauge station. In the three drainage areas with high urban land use—CP1, CP6, and CP7—the SWAT model is underpredicting flow, so the highest value of ESCO achieves the closest match to measured values (Figure 12). In the two drainage areas with very low urban land use—CP4 and CP6—the SWAT model is overpredicting flow, so the lowest value of ESCO creates the closest match to measured values (Figure 13).

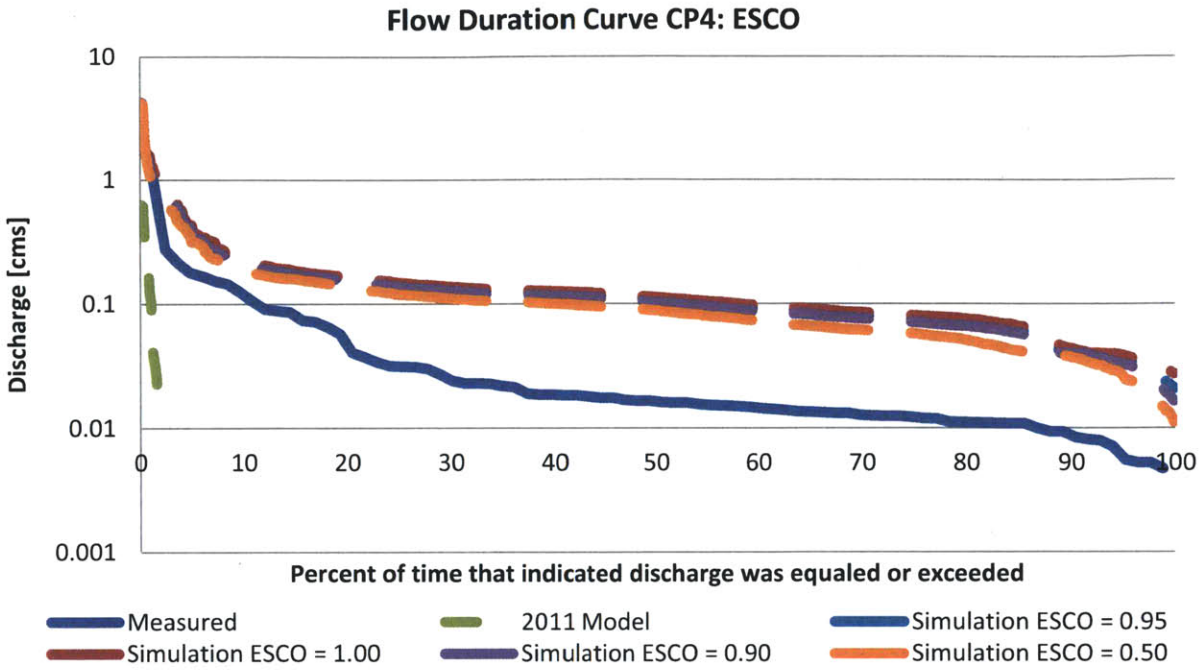

Figure 13 - Flow duration curve comparing changes to ESCO to measured values at CP4.

5.2.2. Parameter: CN2

Variations in CN2 affected low and mid-range flow values for subbasin outflows. CN2 represents the value of the runoff curve number for moisture condition II and varies with each HRU. Curve number depends on a soil's permeability, land-use, and moisture condition. Curve number is inversely proportional to soil water retention, and the higher the curve number, the more surface runoff can be expected from a soil during a rain event. Original values for CN2 in the 2011 model were determined from information about each HRU's soil parameters and land-use.

Curve numbers can range from 30 to 98. Four iterations of changes to CN2 were tested in the SWAT model. Since CN2 varies from HRU to HRU, instead of setting the entire catchment to one value of CN2, stored values of CN2 were increased or decreased by 5 or 10. These changes had a different influence on flows from the urban drainage areas (CP1, CP2, and CP7) and the non-urban drainage areas (CP4 and CP6). A representative flow duration curve of the urban drainage areas can be found in Figure 14. A representative flow duration curve of the non-urban drainage areas can be found in Figure 15. All other flow duration curves showing changes in CN2 can be found in Appendix III.

In the more urban drainage areas (CP1, CP2, and CP7), changes to CN2 values do not change peak and high flow values, but changes in CN2 do change mid- and low-range flow values (Figure 14). For these mid- and low flow values, decreasing CN2 resulted in the highest flow values, and increasing CN2 resulted in the lowest flow values. In other words, decreasing CN2 increased the probability of low flows and increasing CN2 decreased the probability of low flows. All of these model runs still resulted in flows that were lower than the measurements taken at the stream gauge stations, but the model run with CN2 decreased by 10 was the closest match, and the model run with CN2 increased by 10 was the worst match for CP1, CP2, and CP7.

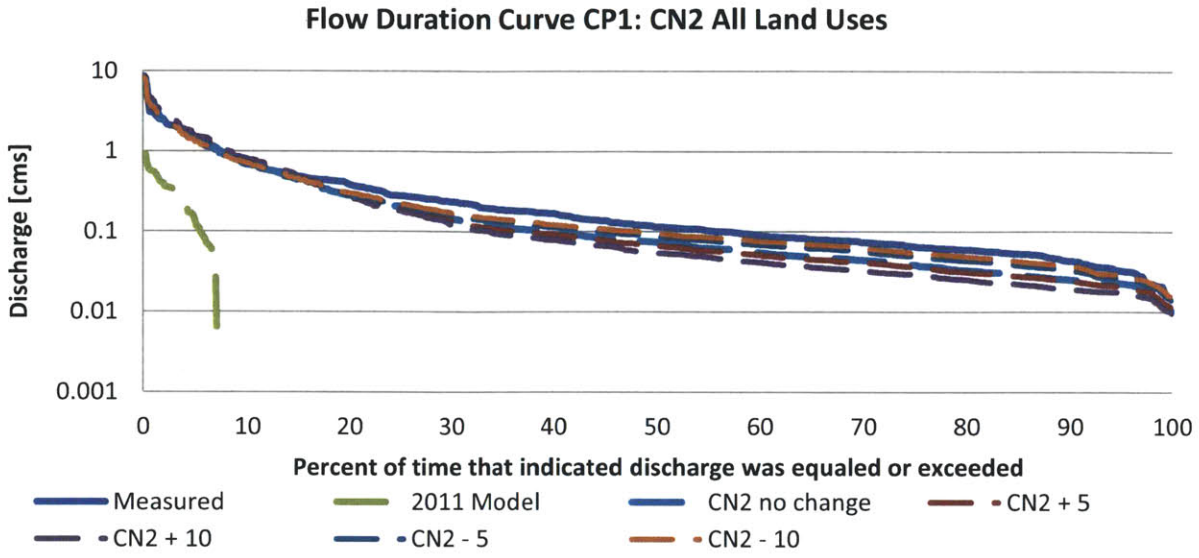

Figure 14 - Flow duration curves comparing changes in CN2 to measured values at CP1.

In the non-urban drainage areas (CP4 and CP6), changes to CN2 values do not change peak and high flow values, but changes in CN2 do change mid and low range flow values (Figure 15). The general trends of the changes made to CN2 are the same as in CP1, CP2, and CP7. For the mid- and low flow values, decreasing the CN2 resulted in increased flow values, while increasing CN2 resulted in decreased flow values However, since in CP4 and CP6, the SWAT model is overpredicting flows at both subbasin outlets, the model run with CN2 increased by 10 was the closest match, and the model run with CN2 decreased by 10 was the worst match (Figure 15).

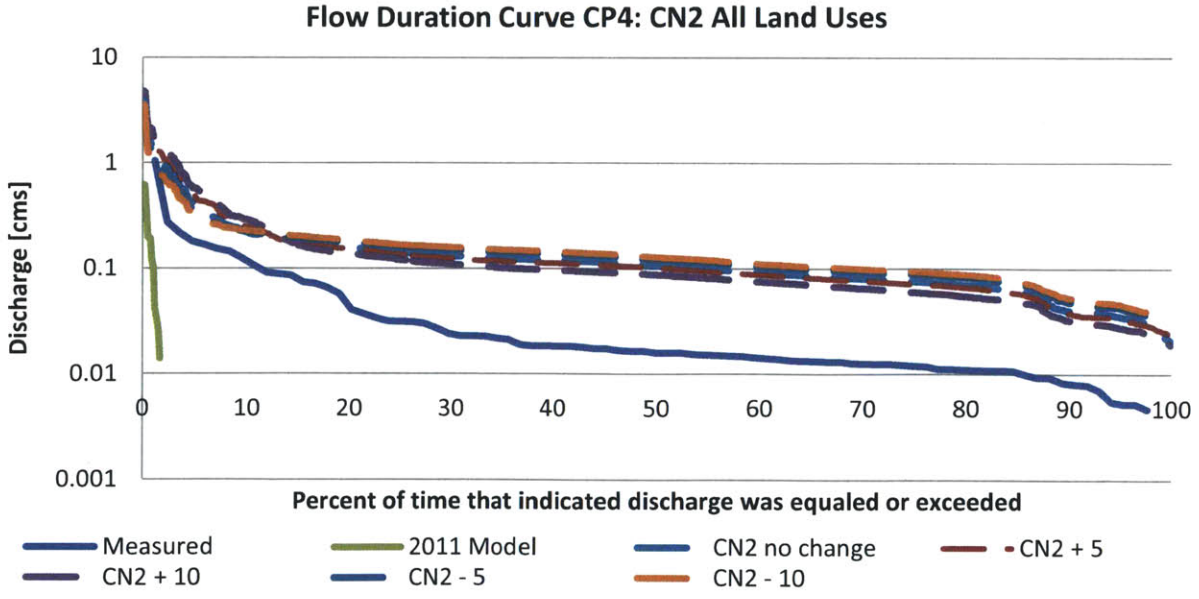

Figure 15 - Flow duration curves comparing changes in CN2 to measured values at CP4.

5.2.3. Parameter: GWQMN

Changing the parameter GWQMN has a strong effect on model outputs, and in general, changing GWQMN worsens the model's ability to match measured flow. GWQMN is the threshold depth [mm] of water in the shallow aquifer above which return flow will occur (Neitsch et al. 2004). If the depth of water in the shallow aquifer is less than GWQMN, there will be no groundwater flow into the stream reaches of the model. GWQMN can range from -500 mm to 500 mm, and the original value of GWQMN in the 2011 model was 0 mm.

Four iterations of changes to values of GWQMN were made to the SWAT model. The SWAT model was run with GWQMN equal to $\pm$ 100 mm and $\pm$ 500 mm. The subbasin outflow response to changes in GWQMN were slightly different at each of the drainage areas CP1, CP2, CP4, CP6, and CP7, but all changes made the model either did not change the outflows or resulted in outflows that were a worse match to measurements at all five stream gauge stations. A representative flow duration curve can be seen below in Figure 16. The flow duration curves for all other stream gauge stations can be found in Appendix III.

Figure 16 demonstrates the impact of GWQMN on subbasin outflows at CP2. Increasing GWQMN by 100 mm and 500 mm results in a steep tail with low flow values that are well below detection in a real stream. Decreasing GWQMN by 100 mm and 500 mm does not have a large impact on the outflows of the model at subbasin at CP2. Modeled outputs for these two runs are nearly identical to the model run with no change to GWQMN.

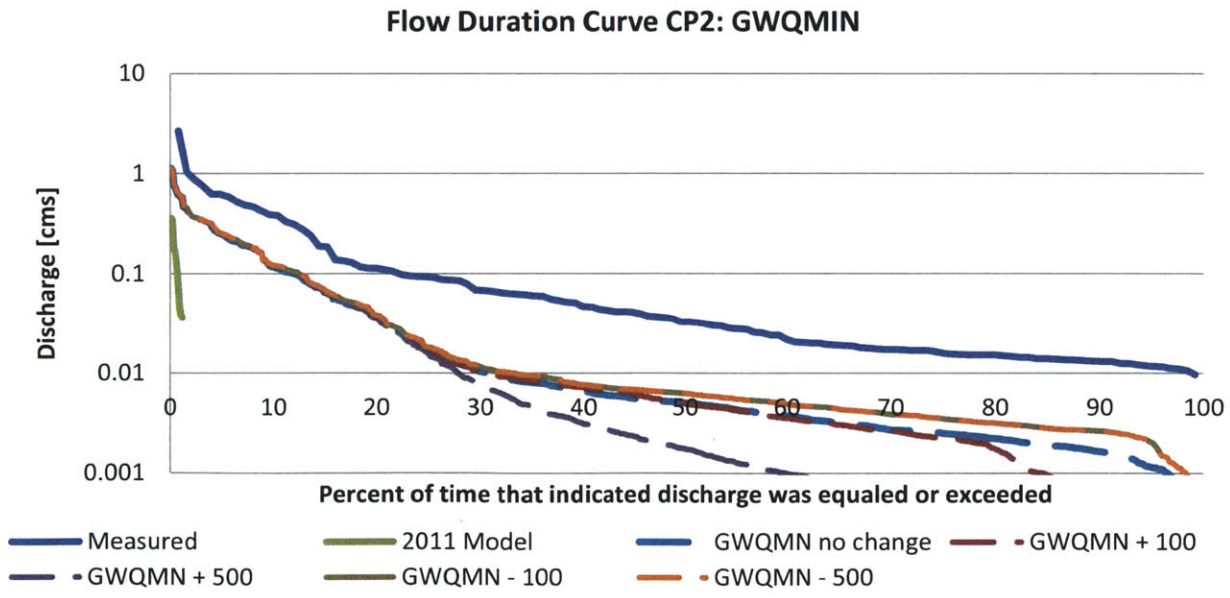

Figure 16 - Flow duration curves comparing changes in GWQMN to measured values at CP2.

5.2.4. Parameter: alpha_bf

Setting the parameter alpha_bf equal to zero had a large impact on subbasin outflows, but any other change to alpha_bf had no effect. Alpha_bf is the baseflow alpha factor, or the SWAT baseflow recession constant, and is an index of an area's groundwater response to changes in recharge (Neitsch et al. 2004). Alpha_bf can be any value between 0.0 and 1.0, but typical values include 0.1-0.3 for a slow response and

0.9-1.0 for a quick response. The original value of alpha_bf from the 2011 model was 0.048, indicating an extremely slow groundwater response to changes in recharge.

All examined subbasins had a similar response in surface outflows to changes in alpha_bf. A representative plot of the flow duration of many changes to alpha_bf and the change in flows in subbasin 324 and CP1 can be seen in Figure 17. The remaining plots for subbasins 281 (CP2), 352 (CP4), 124 (CP6), and 164 (CP7) can be found in Appendix III.

Values of alpha_bf were set equal to 0.00, 0.005, 0.01, 0.025, 0.048, 0.2, 0.5, and 1.0 and were run in separate simulations of SWAT with precipitation equal to the rain gauge data from CP1. All subbasins responded to these eight iterations of changes to alpha_bf very similarly. Subbasin outflows from model runs with alpha_bf equal to 0.025, 0.048, 0.2, 0.5, and 1.0 all look identical and are the closest match to measured outflows (Figure 17). The subbasin outflows from the model run with alpha_bf equal to 0.00 result in very low flow values and often have a steep tail in the flow duration curve for low flow values. Running a model with alpha_bf equal to 0.00 is the worst match to measured values at all stream gauge stations. Model runs with alpha_bf equal to 0.005 and 0.01 have similar high and mid-range flow values to other model runs, but have lower low flow values. These two model runs do not match the shape of the measured flow duration curve as well as the other model runs.

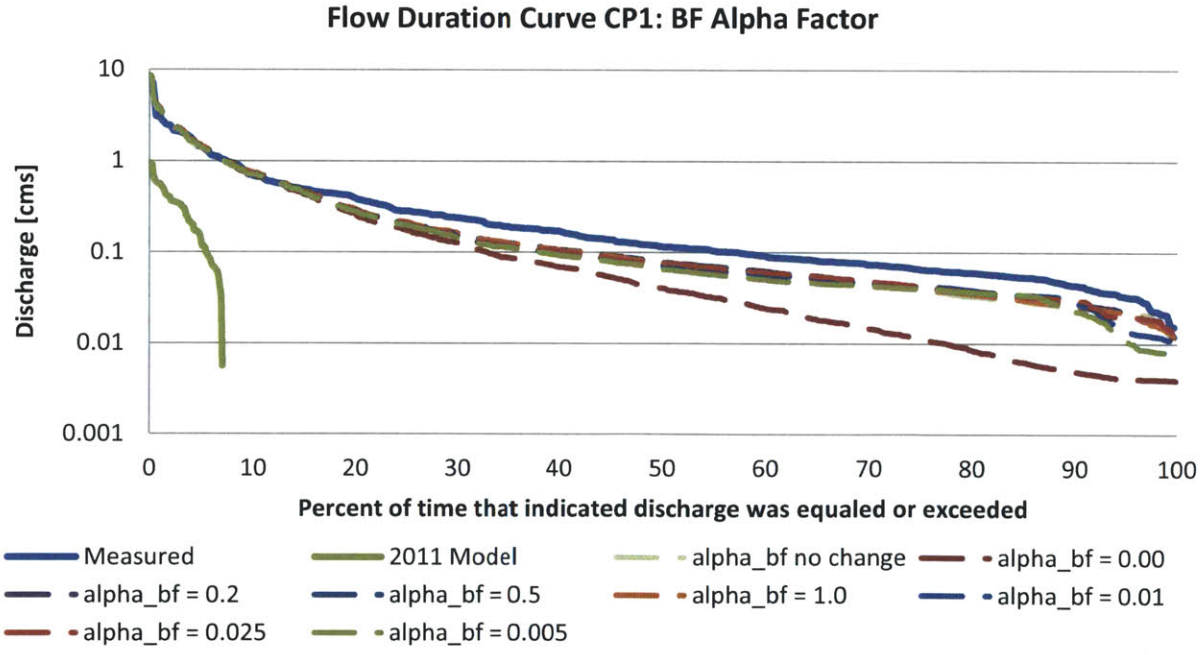

Figure 17 - Flow duration curves comparing changes in alpha_bf to measured values at CP1.

5.2.5. Parameter: sol_z

Changing the parameter sol_z did not have a large impact on subbasin outflows throughout the model. Sol_z can be any value between -25 and 25 and represents the depth [mm] between the soil surface and the bottom of the top soil layer. Values of sol_z in the 2011 SWAT model varied from HRU to HRU (Neitsch et al. 2004).

The outflow in each subbasin reacted similarly to changes in sol_z. A representative flow duration curve of model runs with changes to sol_z and precipitation set to rain gauge data from CP1 can be found in Figure 18. The remaining flow duration curves of changes made to sol_z at the other stream gauge stations can be found in Appendix III.

Sol_z was adjusted ± 5 mm and ± 10 mm in the SWAT model. The model was rerun with each adjustment made to sol_z and the impact on subbasin outflow can be seen in Figure 18. The outflow at subbasin 324 was found to be insensitive to sol_z, and the same is true for all other subbasins examined (Appendix III).

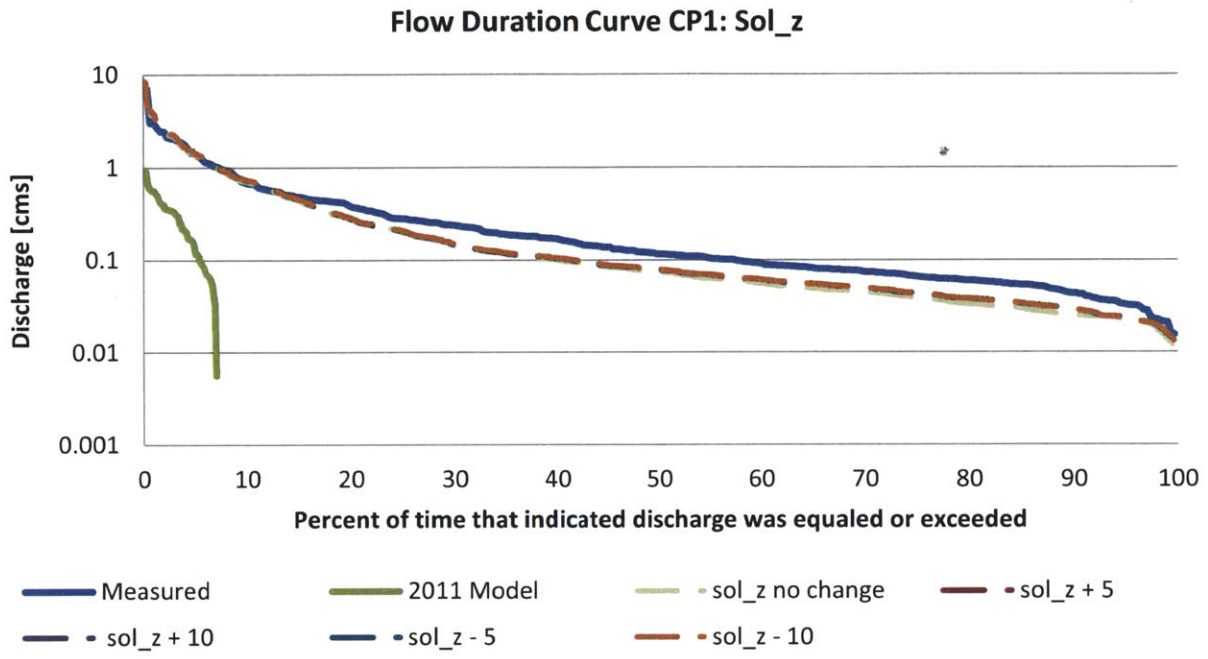

Figure 18 - Flow duration curve comparing changes to sol_z with measured values at CP1.

5.2.6. Parameter: sol_awc

Changes to the parameter sol_awc affected mid-range and low flow values in all subbasins. Sol_awc is the available water content in the soil available for plant uptake. It can be calculated by subtracting the permanent wilting point from the water content at field capacity (Neitsch et al. 2004). Sol_awc can be any value between -25 and 25 mm H_2O/mm soil, and original values for sol_awc varied with soil type in the 2011 model and ranged from 0 to 1 mm H_2O/mm soil.

Four iterations of changes were made to sol_awc, and a similar trend resulted in subbasin outflows. Since values of sol_awc vary with soil type, sol_awc was adjusted by adding and subtracting 10 mm H_2O/mm soil and 20 mm H_2O/mm soil. A representative flow duration curve for these changes can be seen in Figure 19. All other flow duration curves for the remaining stream gauge stations can be found in Appendix III.

All changes made to sol_awc did not have an effect on peak and high flow values, but the changes increased all mid-range and low flow values (Figure 19). In all five drainage areas, adding 10 and 20 mm H_2O/mm soil resulted in the same outflow values, and subtracting 10 and 20 mm H_2O/mm soil resulted in the same outflow values. Adding 10 and 20 mm H_2O/mm soil resulted in a slight increase in mid-range

and low flow values. Subtracting 10 and 20 mm H_2O/mm soil resulted in about a half an order of magnitude increase in mid-range and low flow values.

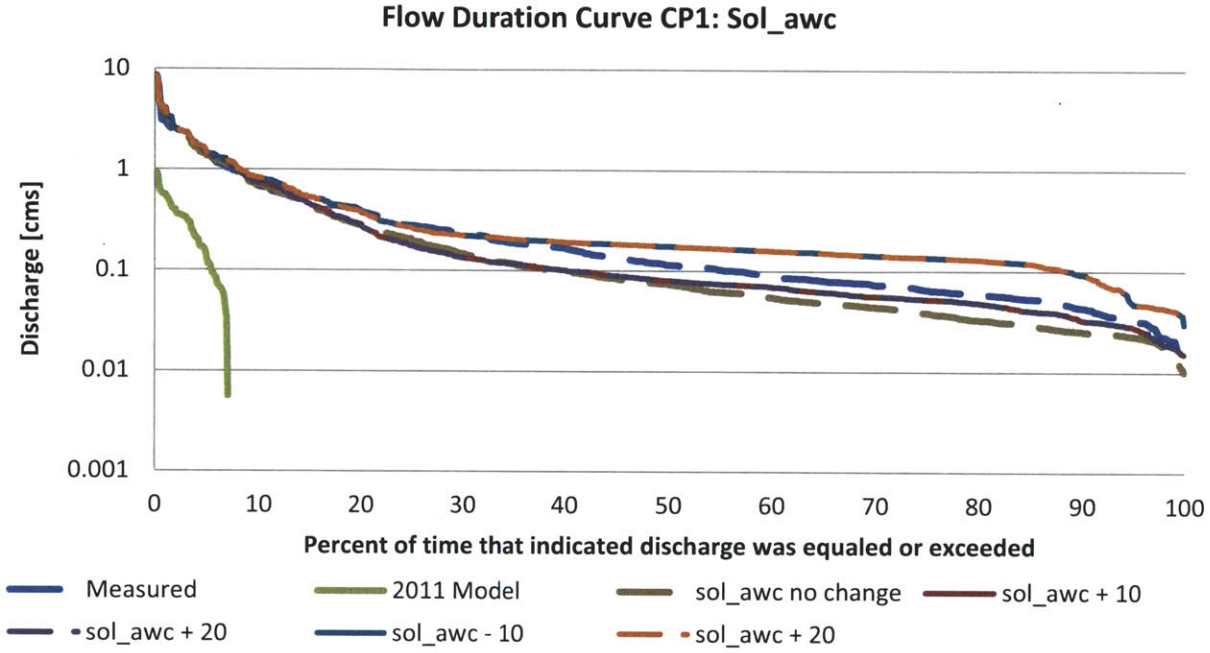

Figure 19 - Flow duration curves comparing changes in sol_awc to measured values at CP1.

The best match to measured values for changes in sol_awc varied with subbasin. At CP1, the model runs with sol_awc +10 and +20 mm H_2O/mm soil resulted in the closest match to field measurements. At CP2 and CP7, the model runs with sol_awc –10 and –20 mm H_2O/mm soil were the closest match. At CP4 and CP6, the model run with no change to sol_awc was the closest match.

6. Discussion

6.1. Precipitation

Of the three iterations of precipitation change made to the SWAT model, using measured rain gauge data from CP1 best matches modeled outflows to measurements taken at the stream gauge stations. The model run with this actual rainfall record most closely matches measurements taken at CP1, CP2, CP6, and CP7. While the high SWAT-simulated rainfall matches CP4 the best, the model run with rain gauge data from CP1 also matches fairly well. This precipitation is known to be a representative dataset of Kranji Catchment because it actually is a rainfall dataset measured within the boundaries of Kranji Catchment.

The other iterations of precipitation were simulated by SWAT using rainfall statistics. In addition to the monthly mean rainfall, standard deviation and number of wet days described in Section 4.2, the rainfall statistics also consist of skewness factors, probability of a wet day following a dry day, probability of a wet day following a wet day, and maximum rainfall in a half-hour period. These parameters were estimated for Kranji by Granger (2010) and do not produce a representative set of daily precipitation for Singapore. Rain events in Singapore are generally frequent, generally with fewer than several dry days between rain events. The inter-storm periods for the SWAT simulated rainfall are lower than the inter-storm periods for the rainfall record at CP1 (Figure 20). A longer inter-storm period allows for longer durations of evaporation without rainfall and explains the lower flow values that occur in the SWAT simulated rainfall runs, even when the yearly total rainfall is higher than the rainfall record at CP1.

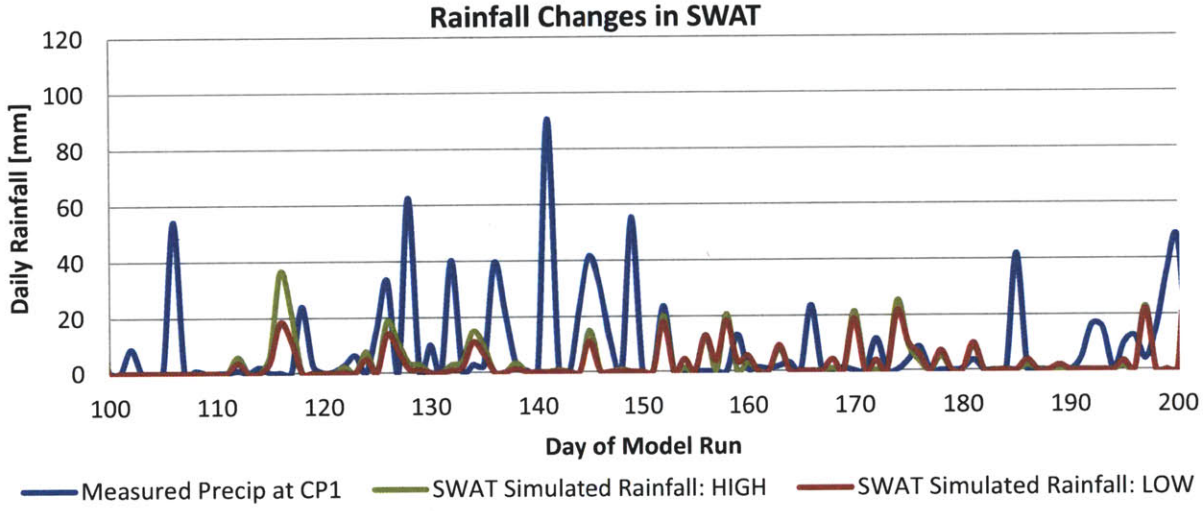

Figure 20 - Daily rainfall for all precipitation changes made to SWAT.

6.2. Final Parameter Adjustments

Of the six calibration parameters evaluated in Section 5.2, only ESCO and CN2 were adjusted in the final model calibration. In the final, calibrated model, ESCO was set equal to 1.0 and CN2 was decreased by 5 for urban land-use areas only. These two changes made the modeled outflows match measured values more closely at CP1, CP2, and CP7 and had no impact on outflows when compared to measured values at CP4 and CP6 (Section 6.3). All other parameter changes, or combinations thereof, had conflicting results between subbasins—improving the match at some stations but simultaneously worsening it others.

The four parameters described in Section 5.2 that were not changed in the final SWAT model are alpha_bf, GWQMN, sol_z, and sol_awc. Alpha_bf was not adjusted in the final calibration because increasing alpha_bf did not have an impact on subbasin outflows and decreasing alpha_bf created steep tails in low flow values that did not match flow duration curves for measured values. GWQMN was not adjusted in the final calibration for similar reasons—decreasing GWQMN did not have an impact on subbasin outflows, but increasing GWQMN also resulted in a steep tail in low flow values in the flow duration curve that did not match the shape of measured values. sol_z was not adjusted in the final calibration because no changes made to sol_z had an impact on subbasin outflows. sol_awc was not adjusted in the final calibration because changes in sol_awc had conflicting results between subbasins.

Since monitoring locations within Kranji Catchment were limited for this calibration, any parameter changes needed to make universal improvements, not just improvements in one subbasin or area of the model. There are not enough measurements to indicate that one area of the catchment behaves differently or has very different parameter values than any other area of the catchment. For this reason, only parameter changes that improved, or at least did not worsen, modeled outflows at each stream gauge station were considered for this calibration. Of the iterations of changes made to parameters in the SWAT model, the only changes that met this standard were increasing ESCO to 1.0 and subtracting 5 from CN2 values for urban land uses.

The increase in ESCO was applied to the entire catchment area, but the decrease in CN2 values was applied to urban land uses only. ESCO is a catchment-wide parameter and cannot be adjusted by land use or soil type. CN2 is a function of both land use and soil type. As described in Section 5.2.2, increasing CN2 made an improvement in modeled outflows for non-urban drainage areas, while decreasing CN2 made an improvement in modeled outflows for urban drainage areas. Changes in CN2 were made to both urban land uses only and non-urban land uses only, and the full results can be found in Appendix IV: Modifications to CN2 by Land-Use Type. Decreasing CN2 for urban land uses only made improvements to the modeled outflows when compared to measurements taken at CP1, CP2, and CP7, but did not have an impact on modeled outflows at CP4 or CP6 because both of those drainage areas have very little urban land. Increasing CN2 for non-urban land uses only made improvements to the modeled outflows at CP4 and CP6, but at a detriment to the model results at CP1, CP2, and CP7. For this reason, no change was made to CN2 values for non-urban areas, but CN2 was decreased by 5 for urban areas only.

6.3. Evaluation of Calibration Criteria

Since the manual hydrologic calibration of this SWAT model was conducted under strict time constraints, the main calibration criterion was to make the hydrology of the model match measured values as closely as possible. Without a time constraint however, a model can be iteratively improved for an indefinite amount of time. Generally, a strict criterion is applied to the model in order to help the modeler decide "How good is good enough?" This section compares the results of the 2012 hydrologic calibration of the SWAT to general criteria of $\pm$ 10 percent of the variation in outflows at each stream gauge station. Each subsection of this section shows a flow duration curve at a different stream gauge station comparing the final model calibration, including changes to precipitation and the parameters ESCO and CN2, as well as the model results of only changing precipitation in the model to these calibration criteria.

6.3.1. Calibration Criteria at CP1

The calibrated model meets calibration criteria at CP1 (Figure 21). The flow duration curves of the model run with changes to precipitation and with changes to precipitation and the parameters ESCO and CN2 both fall between the upper and lower bounds of the calibration criteria for the entire flow duration. Each

of the two runs of the model have similar flow duration curves, but the model run with changes in precipitation and parameter changes is a slightly better match to measured results at CP1.

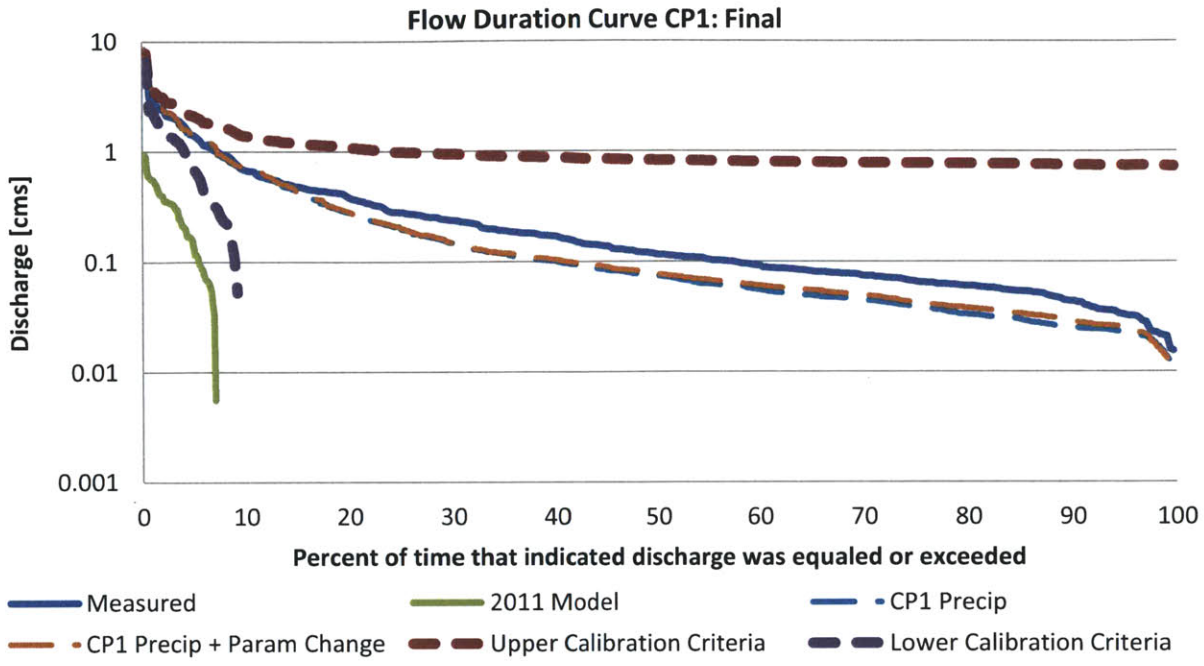

Figure 21 - Flow duration curves showing final, calibrated SWAT model run versus calibration criteria at CP1.

6.3.2. Calibration Criteria at CP2

The modeled flow outputs almost meet the calibration criteria at CP2 (Figure 22). Modeled outflows are slightly lower than the lower bound of the calibration criteria for the highest 10 percent of flows, but modeled outflows fall between the upper and lower bounds of the criteria for the remaining 90 percent of flow values. This is true for both model runs with changes to precipitation only and with changes made to precipitation and calibration parameters. The model run with changes made to precipitation and calibration parameters matches the flow duration curve of measured flows at CP2 better than the model run that contained changes to precipitation alone.

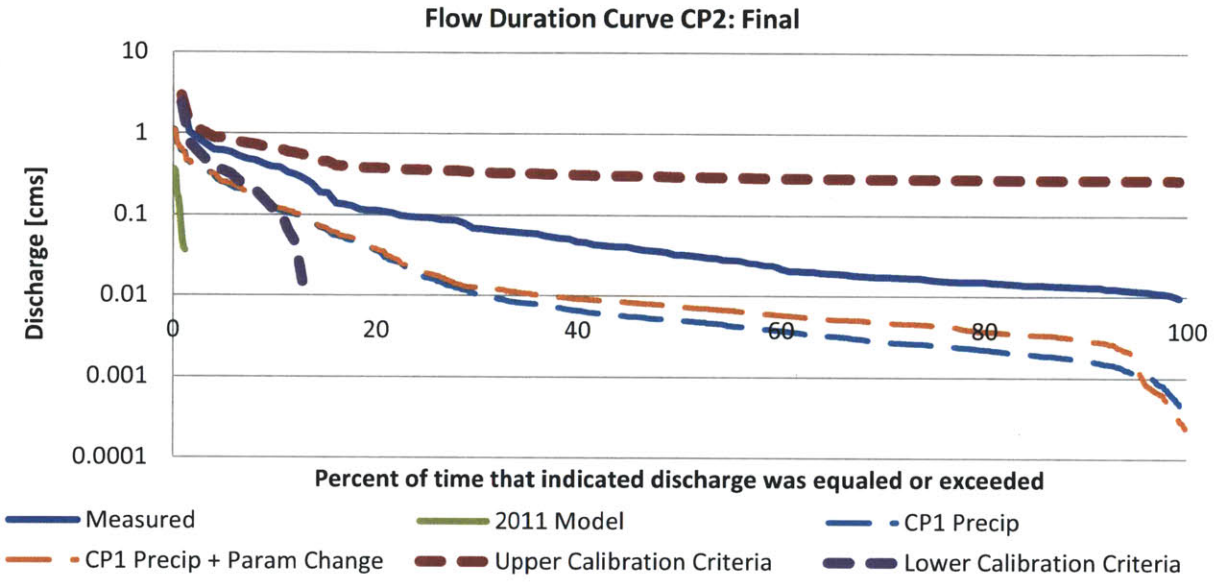

Figure 22 - Flow duration curves showing final, calibrated SWAT model run versus calibration criteria at CP2.

6.3.3. Calibration Criteria at CP4

The modeled flow outputs almost meet the calibration criteria at CP4 (Figure 23). Modeled outflows are slightly higher than the upper bound of the calibration criteria for the highest 10 percent of flows, but modeled outflows fall between the upper and lower bounds of the criteria for the remaining 90 percent of flow values. This is true for both model runs with changes to precipitation only and with changes made to precipitation and calibration parameters. These two model runs have exactly the same outflow values, indicating that the parameter changes have no impact on outflows at CP4.

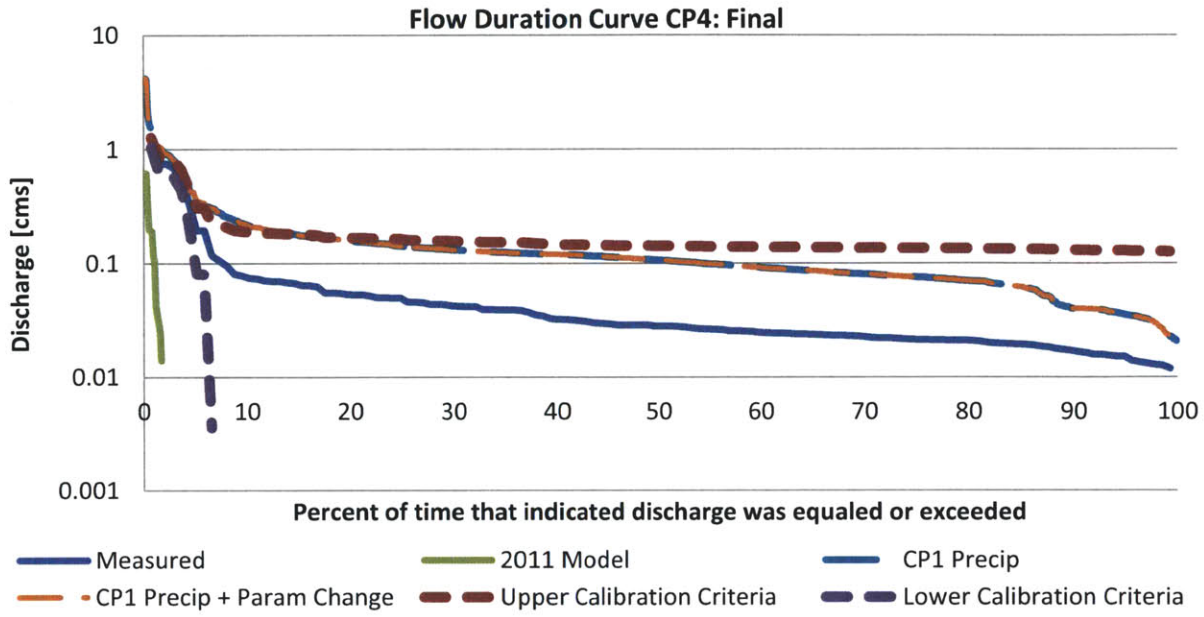

Figure 23 - Flow duration curves showing final, calibrated SWAT model run versus calibration criteria at CP4.

6.3.4. Calibration Criteria at CP6

The modeled flow outputs almost meet the calibration criteria at CP6 (Figure 24). Modeled outflows are slightly higher than the upper bound of the calibration criteria for the highest 5 percent of flows, but modeled outflows fall between the upper and lower bounds of the criteria for the remaining 95 percent of flow values. This is true for both model runs with changes to precipitation only and with changes made to precipitation and calibration parameters. These two model runs have exactly the same outflow values, indicating that the parameter changes have no impact on outflows at CP6.

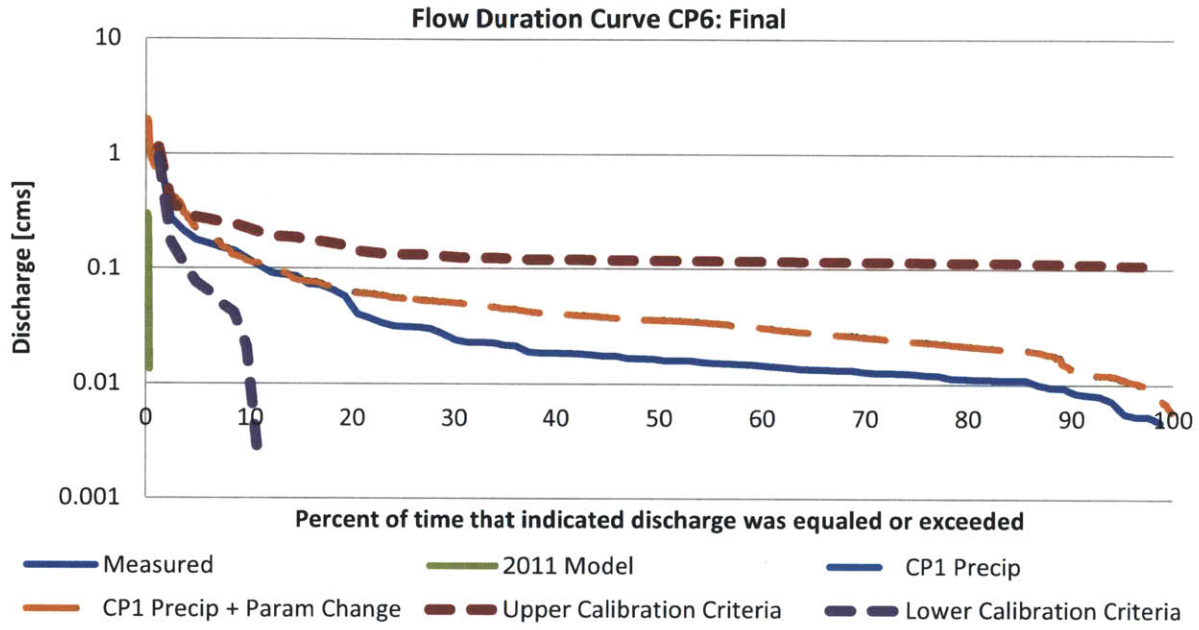

Figure 24 - Flow duration curves showing final, calibrated SWAT model run versus calibration criteria at CP6.

6.3.5. Calibration Criteria at CP7

The modeled flow outputs almost meet the calibration criteria at CP7 (Figure 25). Modeled outflows are slightly higher than the upper bound of the calibration criteria for the highest 2 percent of flows, but modeled outflows fall between the upper and lower bounds of the criteria for the remaining 98 percent of flow values. This is true for both model runs with changes to precipitation only and with changes made to precipitation and calibration parameters. The model run with changes made to precipitation and calibration parameters matches the flow duration curve of measured flows at CP7 better than the model run that contained changes to precipitation alone.

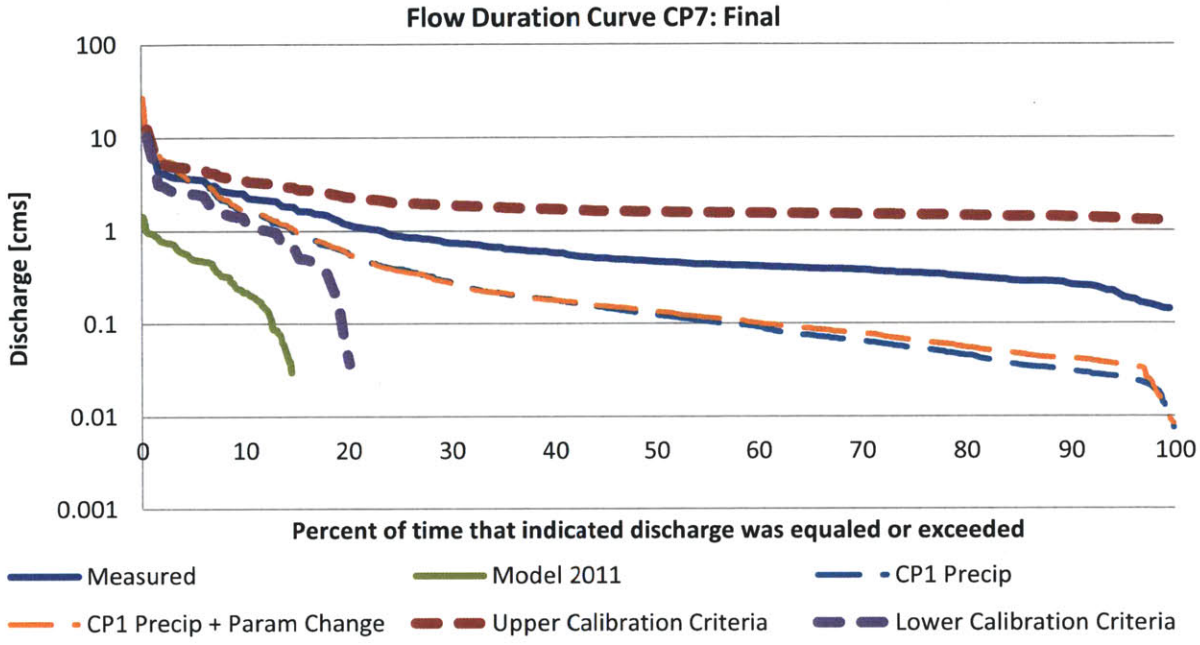

Figure 25 - Flow duration curves showing final, calibrated SWAT model run versus calibration criteria at CP7.

6.4. Daily Flow Comparison

Daily subbasin outflows were compared to daily stream gauge measurements as a secondary check of the model's accuracy. Daily measurements during the year 2005 are compared to model-predicted outflows at subbasin 324 (Figure 26). While there are gaps in the dataset of measurements, flow peaks in the model and in the field generally occur at the same times and reach similar magnitudes.

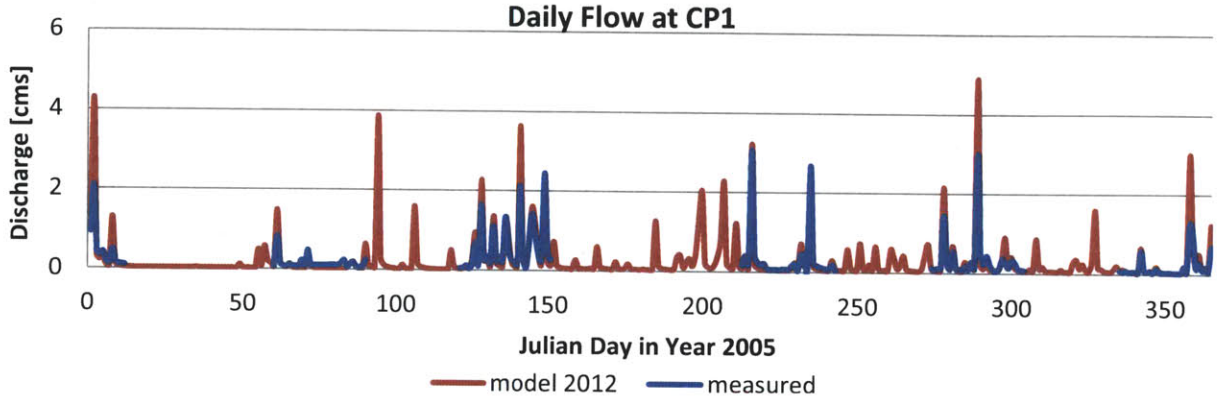

Figure 26 - Daily flow at CP1 during 2005.

Figure 27displays the same daily flow at CP1 according to measurements and predictions made by SWAT during 2005, but zooms in on the time period between days 121 and 151. This represents a time period of roughly one month. For this month, the model's predictions line up very nicely with measurements at CP1. Flow peaks occur on the same days in the model and the field, and the magnitudes of both flows are very similar. This indicates the model is accurately calculating surface flows.

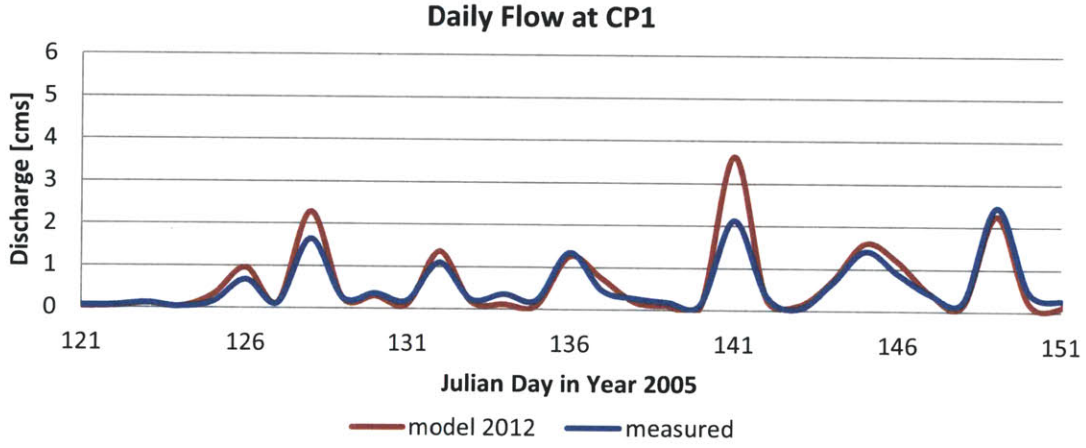

Figure 27 - Daily flow at CP1 during days 121 - 151 of 2005.

7. Conclusions and Recommendations

Three key changes to the 2011 version of the SWAT model of the Kranji Catchment made a vast improvement in the calculation of surface runoff by the model. The first and most drastic improvement came from changing the precipitation. The SWAT model now uses a rain gauge data set from CP1 as the precipitation in model simulations. The other changes were to calibration parameters ESCO and CN2. The value for ESCO, or the soil evaporation compensation factor, was increased from 0.95 to 1.0 throughout the entire model. Values for CN2, or the curve number for moisture condition II, were decreased by 5 in land areas with an urban land use.

These three changes greatly improved the model's calculation of surface outflows and brought modeled values very close to measurements taken at stream gauges in Kranji Catchment. The SWAT-modeled hydrology meets a calibration criterion of $\pm$10 percent of the natural variation in surface flows for all mid-range and low flow values. The peak surface flows at all five stream gauge stations are close to the 10 percent calibration criterion, but only peak outflows at CP1 meet the criteria.

The primary motivation for building a SWAT model of Kranji Catchment was to accurately predict surface concentrations of total coliform and *E. coli* throughout the catchment. The SWAT model was built by Granger in 2010 and improved by Bossis in 2011, but even after improvements, the SWAT model was underestimating bacteria concentrations by 2 to 3 orders of magnitude. The motivation of the calibration effort reported in this thesis was to bring bacteria concentrations predicted by the model closer to actual measurements. In the following paragraphs, the recalibrated model is referred to simply as the "2012 model." Before bacteria concentrations could be calibrated in the SWAT model of Kranji Catchment, the hydrology needed to be calibrated. Discrepancies between modeled and measured bacteria loading in Kranji Catchment could be due either to errors in the way the hydrology is modeled or in the way the bacterial is modeled, or both. This project has addressed the need to calibrate the hydrology of the model and now work can be continued to calibrate the bacteria loading rates predicted by the model to field measured data.

While the hydrology of the SWAT model in Kranji Catchment has been greatly improved, the bacteria loading still requires calibration. The cumulative density of bacteria concentrations throughout Kranji Catchment do not better match measured values after calibrating the hydrology. *E. coli* loading predicted by both the Bossis (2011) and the hydrology-calibrated 2012 models can be seen in Figure 28. A comparison of total coliform loading in the 2011 and 2012 models to measurements can be seen in Figure 29. In both of these figures, modeled bacteria counts are compared to measurements taken at 35 different subbasins within Kranji Catchment. In both of these cumulative density plots, it is evident that there is no significant change to bacterial loading rates between the 2011 and 2012 models. This leads to the counter-intuitive conclusion that the hydrologic calibration had little to no impact on bacterial loading within the SWAT model.

In order to improve bacteria loading predictions in the SWAT model, a full calibration of the bacteria loading should be conducted. Some parameters of interest for a bacterial calibration include bacteria growth factors, bacteria die-off factors, export coefficients, partitioning coefficients, and amounts of bacteria in fertilizers. One area of concern with bacteria loading predictions in SWAT is that in the 35 subbasin analysis for the 2011 model, 60 percent of daily reported bacteria concentrations were above 0 cfu/100mL, but 98 percent of daily reported flows were 0 cms. Of the days SWAT predicted a non-zero concentration of bacteria, 61 percent were on a day with no flow reported. This may indicate that a SWAT surface flow output of 0 cms is not truly 0, but very low (i.e., less than 10^{-5} cms), or that bacteria concentrations are calculated independently of flow. This issue must be addressed first in a future calibration of the SWAT model for Kranji Catchment. The SWAT theory must be closely examined to

determine exactly how bacteria concentrations are calculated by the model, what the SWAT outputs for bacteria represent, and why major changes to the hydrology have little effect on bacteria concentrations.

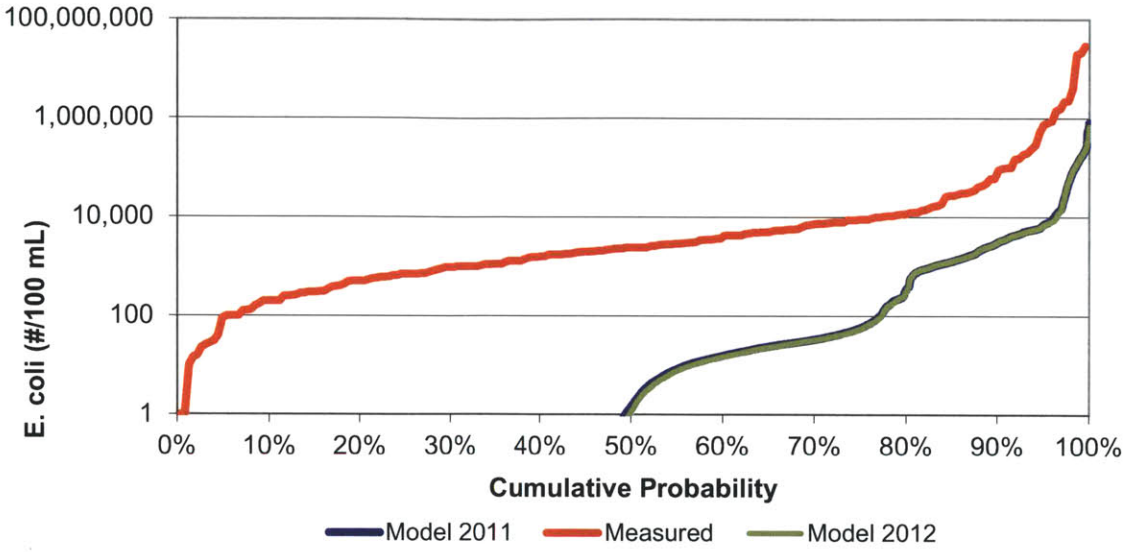

Figure 28 - Cumulative density plot comparing E. coli loading at 35 subbasins to 2011 and 2012 SWAT model.

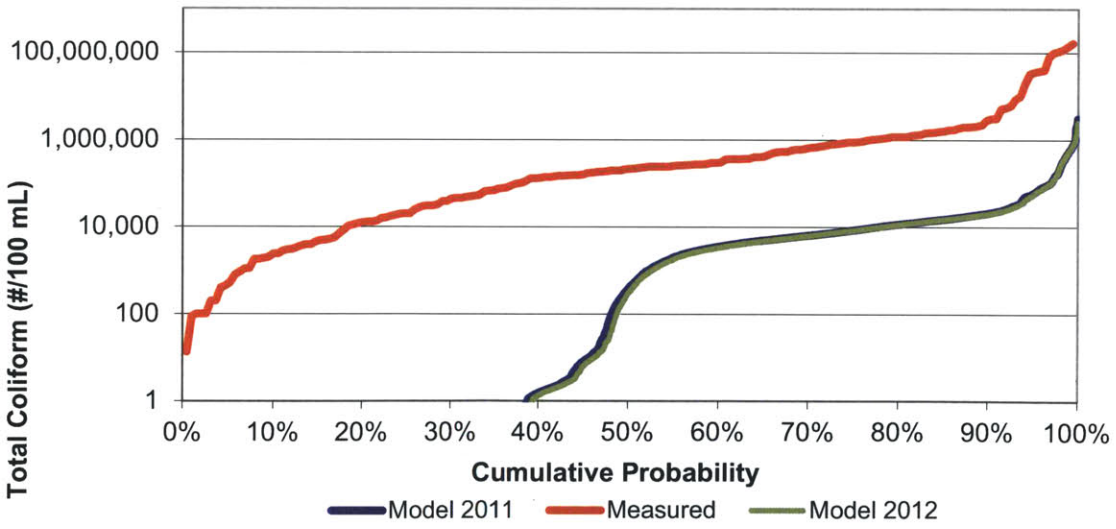

Figure 29 - Cumulative density plot comparing total coliform loading at 35 subbasins to 2011 and 2012 SWAT model.

References

Bossis, R. C. (2011). *Application of the SWAT Model to Bacterial Loading in Kranji Cachtment, Singapore.* (Master in Engineering), Massachusetts Institute of Technology, Cambridge, MA.

Chew, V. (2009). Singapore-Malaysia Water Agreements: National Library Board Singapore. Retrieved from http://infopedia.nl.sg/articles/SIP_1533_2009-06-23.html

Chui, P. (1997). Characteristics of stormwater quality from two urban watersheds in Singapore. *Environmental monitoring and assessment, 44*(1), 173-181.

CIA. (2011). The World Factbook: Singapore. Central Intelligence Agency. Retrieved December 1, 2011, from https://www.cia.gov/library/publications/the-world-factbook/geos/sn.html

Evans, G. (2008). Singapore's Self Sufficiency: Net Resources International. Retrieved from http://www.water-technology.net/features/feature2026/

Granger, E. C. (2010). *Water Quality Monitoring in Kranji Catchment.* (Master in Engineering), Massachusetts Institute of Technology, Cambridge, MA.

Hurst, C. J., & Crawford, R. L. (2007). *Manual of environmental microbiology* (3rd ed.). Washington, D.C.: ASM Press.

Ives, D. W. (1977). Soils of the Republic of Singapore. New Zealand Soil Bureau.

MDEQ. (2011). *Model Calibration.* Michigan Department of Environmental Quality. Retrieved from http://www.michigan.gov/deq/0,4561,7-135-3313_21698-55863--,00.html.

Ministry of the Environment and Water Resources. (2008). *PUB awards tender for the fifth and largest NEWater plant at Changi to Sembcorp.* Retrieved December 1, 2011, from http://app.mewr.gov.sg/web/Contents/Contents.aspx?Yr=2008&ContId=992

Moe, C. L. (2007). Waterborne Transmission of Infectious Agents. *Manual of environmental microbiology* (3rd ed.). Washington, D.C.: ASM Press. 3, 222-248.

National Research Council. (2004). Committee on Indicators for Waterborne Pathogens. Indicators for waterborne pathogens. Washington, DC: National Academies Press.

NEA. (2010). *Annual Weather Report 2010.* Singapore: National Environment Agency. Retrieved from http://app2.nea.gov.sg/data/cmsresource/20110524444301448687.pdf.

Neitsch, S. L., Arnold J. G., Kiniry, J. R., and Williams J. R. (2005). *Soil and Water Assessment Tool Theoretical Documentation: Version 2005.* Temple, Texas: United States Department of Agriculture-Agricultural Research Service. Retrieved from http://swatmodel.tamu.edu/media/1292/swat2005theory.pdf

Neitsch, S. L., Arnold, J. G., Kiniry, J. R., Srinivasan, R., & Williams, J. R. (2002). *Soil and water Assessment Tool User's Manual: Version 2000.* Temple, Texas: United States Department of Agriculture-Agricultural Research Service. Retrieved from http://swatmodel.tamu.edu/media/1294/swatuserman.pdf

Neitsch, S. L., Arnold, J. G., Kiniry, J. R., Srinivasan, R., & Williams, J. R. (2004). *Soil and water Assessment Tool User's Manual: Input/Output File Documentation: Version 2005.* Temple, Texas: United States Department of Agriculture-Agricultural Research Service. Retrieved from http://swatmodel.tamu.edu/media/1291/swat2005io.pdf

Nie, H. Y. (2011). Water Industry Investments Doubled in Singapore.*Channel NewsAsia.* Retrieved fromhttp://www.channelnewsasia.com/stories/singaporelocalnews/view/1131311/1/.html

NTU. (2008). *Water quality monitoring, modelling and management for Kranji Catchment/Reservoir system - Phases I and 2*. Edited by Division of Environmental and Water Resources Engineering - School of Civil and Environmental Engineering - Nanyang Technological University.

Pitts, J. (1985). A Review of Geology and Engineering in Singapore. [Discussion]. *Quarterly Journal of Engineering Geology, 18*(3), 291-293. doi: 10.1144/gsl.qjeg.1985.018.03.11

PUB Singapore. (2011a). *Active, Beautiful and Clean Waters: Design Guidelines*. Singapore: Public Utilities Board. Retrieved from http://www.pub.gov.sg/abcwaters/abcwatersdesignguidelines/Documents/ABCWatersDesignGuidelines_2011.pdf.

PUB Singapore. (2011b). *Annual Report 2011*. Singapore: Public Utilities Board. Retrieved from http://www.pub.gov.sg/mpublications/Pages/AnnualReport.aspx.

Rahman, A. (1993). Hydrological Problems and Solutions of a Small Island State in a Warm Humid Regions – Case of Singapore.In: Gladwell, JS. (ed.) *Hydrology of Warm Humid, Regions, Proceedings of an international symposium held at Yokohama Japan, 13-15 July 1993* (216). International Association of Hydrological Sciences. 343-351.

Rahman, A., Chia, L. S., and Tay, D. B. H. (1991). *The Biophysical Environment of Singapore*. Kent Ridge, Singapore: Singapore University Press.

Sharma, J. S., Chu, J., & Zhao, J. (1999). Geological and geotechnical features of Singapore: an overview. *Tunnelling and Underground Space Technology, 14*(4), 419-431. doi: 10.1016/s0886-7798(00)00005-5

Singapore Department of Statistics. (2011). Population (Themes) Statistics: Singapore Government. Retrieved from http://www.singstat.gov.sg/index.html

Soon, T. Y., Jean, L. T., & Tan, K. (2009). *Clean, Green and Blue: Singapore's Journey Towards Environmental and Water Sustainability* (1 ed.). Pasir Panjang, Singapore: ISEAS Publishing.

Thomas, G. S. P. (1991). Geology and Geomorphology. In C. Sien, A. Rahman & D. T. B.H (Eds.), *The Biophysical Environment of Singapore* (pp. 50-88). Kent Ridge, Singapore: Singapore University Press.

Toranzos, G. A., McFetters, G. A., Borrego, J. J. & Savill, M.(2007). Detection of Microorganisms in Environmental Freshwaters and Drinking Waters. *Manual of environmental microbiology* (3rd ed.). Washington, D.C.: ASM Press. 3, 250-264.

Tortajada, C. (2006). Water management in Singapore. [Article]. *International Journal of Water Resources Development, 22*(2), 227-240. doi: DOI 10.1080/07900620600691944

UC Davis. (2008). SWAT: Soil and Water Assessment Tool Retrieved Nov. 1, 2011, from http://cwam.ucdavis.edu/pdfs/SWAT.pdf

Veith, T. L., & Ghebremichael, L. T. (2009). How to: Applying and Interpreting the SWAT Auto-Calibration Tools. *International SWAT Conference Proceedings, TR356*. Retrieved from http://twri.tamu.edu/reports/2009/tr356.pdf

Winchell, M., Srinivasan, R., Di Luzio, M., & Arnold, J. (2007). ArcSWAT Interface for SWAT2005: User's gGuide. 431. Temple, Texas: United States Department of Agriculture-Agricultural Research Service. Retrieved from http://www.geology.wmich.edu/sultan/5350/Labs/ArcSWAT_Documentation.pdf

Appendix I: Sensitivity Analysis Results

The following tables contain the full results of the sensitivity analyses run for subbasins 30 and 420. Both analyses were set to run with five intervals within Latin Hypercube, a 0.1 parameter change for OAT, and a random seed number of 2003. For an explanation of how SWAT runs the sensitivity analysis, see Section 3.4.4: Auto-Calibration and Uncertainty Analysis. Table 6 contains a full list of parameters included in the analysis for subbasin outflow, along with their bounds. Table 7 contains the full results of the sensitivity analysis for subbasin 30. Table 8 contains the full results of the sensitivity analysis for subbasin 420. Both tables contain all parameters ranked by sensitivity and the mean percentage change in subbasin outflow.

Table 6 - Full list of parameters assessed in sensitivity analysis.

Parameter	Lower Bound	Upper Bound	Definition
alpha_bf	0	1	Baseflow alpha factor
biomix	0	1	Biological mixing efficiency
blai	0	1	Maximum potential leaf area index for land cover/plant
canmx	0	10	Maximum canopy storage(mm H2O)
ch_k2	0	150	Effective hydraulic conductivity in main channel alluvium (mm/hr)
ch_n2	0	1	Manning's 'n' value for main channel
cn2	30	98	Initial SCS runoff curve number for moisture condition II
epco	0	1	Plant uptake compensation factor
esco	0	1	Soil evaporation compensation factor
gw_delay	-10	10	Groundwater delay (days)
gw_revap	-0.036	0.36	Groundwater "revap" coefficient
gwqmin	-1000	1000	Threshold depth of water in the shallow aquifer for return flow to occur (mm H2O)
revapmn	-100	100	Threshold depth of water in the shallow aquifer for "revap" to occur (mm H2O)
sftmp	0	5	Snowfall temperature
slope	-25	25	Mean slope within HRU
slsubbsn	-25	25	Average slope length (m)
smfmn	0	10	Minimum melt rate for snow during year (mm H2O/degC/day)
smfmx	0	10	Maximum melt rate for snow during year (mm H2O degC/day)
smtmp	-25	25	Snow melt base temp (degC)
sol_alb	-25	25	Moist soil albedo
sol_awc	-25	25	Available water capacity of soil layer (mm/mm)
sol_k	-25	25	Saturated hydraulic conductivity of second soil layer (mm/hr)
sol_z	-25	25	Depth to bottom of soil later (mm)
surlag	0	10	Surface runoff lag time (days)
timp	0	1	Snow pack temperature lag factor
tlaps	0	50	Temperature laps rate (degC/km)

Table 7 - Results of sensitivity analysis for subbasin 30.

Parameter	Rank	Mean Change (percent)	Definition
cn2	1	0.748	Initial SCS runoff curve number for moisture condition II
sol_awc	2	0.733	Available water capacity of soil layer (mm/mm)
gwqmin	3	0.470	Threshold depth of water in the shallow aquifer for return flow to occur (mm H2O)
esco	4	0.435	Soil evaporation compensation factor
sol_z	5	0.140	Depth to bottom of soil later (mm)
alpha_bf	6	0.104	Baseflow alpha factor
sol_k	7	0.0537	Saturated hydraulic conductivity of second soil layer (mm/hr)
slope	8	0.0526	Mean slope within HRU
gw_revap	9	0.0338	Groundwater "revap" coefficient
revapmn	10	0.0330	Threshold depth of water in the shallow aquifer for "revap" to occur (mm H2O)
blai	11	0.0267	Maximum potential leaf area index for land cover/plant
canmx	12	0.0220	Maximum canopy storage(mm H2O)
gw_delay	13	0.0154	Groundwater delay (days)
ch_k2	14	0.00390	Effective hydraulic conductivity in main channel alluvium (mm/hr)
epco	15	0.00247	Plant uptake compensation factor
surlag	16	0.00175	Surface runoff lag time (days)
ch_n2	17	0.000995	Manning's 'n' value for main channel
slsubbsn	18	0.000910	Average slope length (m)
sol_alb	19	0.000704	Moist soil albedo
biomix	20	0.000696	Biological mixing efficiency
sftmp	27	0.000	Snowfall temperature
smfmn	27	0.000	Minimum melt rate for snow during year (mm H2O/degC/day)
smfmx	27	0.000	Maximum melt rate for snow during year (mm H2O degC/day)
smtmp	27	0.000	Snow melt base temp (degC)
timp	27	0.000	Snow pack temperature lag factor
tlaps	27	0.000	Temperature laps rate (degC/km)

Table 8 - Results of sensitivity analysis for subbasin 420.

Parameter	Rank	Mean Change (percent)	Definition
esco	1	0.840	Soil evaporation compensation factor
gwqmin	2	0.840	Threshold depth of water in the shallow aquifer for return flow to occur (mm H2O)
cn2	3	0.542	Initial SCS runoff curve number for moisture condition II
sol_awc	4	0.354	Available water capacity of soil layer (mm/mm)
alpha_bf	5	0.150	Baseflow alpha factor
sol_z	6	0.109	Depth to bottom of soil later (mm)
slope	7	0.0522	Mean slope within HRU
ch_k2	8	0.0515	Effective hydraulic conductivity in main channel alluvium (mm/hr)
gw_revap	9	0.0471	Groundwater "revap" coefficient
sol_k	10	0.0388	Saturated hydraulic conductivity of second soil layer (mm/hr)
gw_delay	11	0.0359	Groundwater delay (days)
blai	12	0.0265	Maximum potential leaf area index for land cover/plant
revapmn	13	0.0140	Threshold depth of water in the shallow aquifer for "revap" to occur (mm H2O)
ch_n2	14	0.0120	Manning's 'n' value for main channel
canmx	15	0.0103	Maximum canopy storage(mm H2O)
slsubbsn	16	0.00119	Average slope length (m)
epco	17	0.000375	Plant uptake compensation factor
biomix	21	0.000	Biological mixing efficiency
sol_alb	21	0.000	Moist soil albedo
tlaps	21	0.000	Temperature laps rate (degC/km)

Appendix II: Names of SWAT Simulations

Table 9 - Name of and parameters changed in each SWAT simulation.

Simulation Name	Parameters Changed in Model run
escoeq1	ESCO + 0.05; ESCO = 1.0
escoeq9	ESCO – 0.05; ESCO = 0.90
escoeq50	ESCO – 0.45; ESCO = 0.50
urbanCN2plus5	CN2 + 5 (urban land-uses only)
urbanCN2plus10	CN2 + 10 (urban land-uses only)
urbanCN2minus5	CN2 – 5 (urban land-uses only)
urbanCN2minus10	CN2 – 10 (urban land-uses only)
agrCN2plus5	CN2 – 5 (non-urban land-uses only)
agrCN2plus10	CN2 – 10 (non-urban land-uses only)
agrCN2minus5	CN2 – 5 (non-urban land-uses only)
agrCN2minus10	CN2 – 10 (non-urban land-uses only)
allCN2plus5	CN2 + 5 (all land-uses)
allCN2plus10	CN2 + 10 (all land-uses)
allCN2minus5	CN2 – 5 (all land-uses)
allCN2minus10	CN2 – 10 (all land-uses)
GWQMINplus100	GWQMN + 100
GWQMINplus500	GWQMN + 500
GWQMINminus100	GWQMN – 100
GWQMINminus500	GWQMN – 500
BFalphaEQ0	Alpha_bf = 0.0
BFalphaEQ025	Alpha_bf = 0.025
BFalphaEQ01	Alpha_bf = 0.01
BFalphaEQ005	Alpha_bf = 0.005
BFalphaEQ2	Alpha_bf = 0.2
BFalphaEQ5	Alpha_bf = 0.5
BFalphaEQ10	Alpha_bf = 1.0
SolZplus5	Sol_z + 5
SolZplus10	Sol_z + 10
SolZminus5	Sol_z – 5
SolZminus10	Sol_z – 10
SolAWCplus10	Sol_awc – 10
SolAWCplus20	Sol_awc + 20
SolAWCminus10	Sol_awc – 10
SolAWCminus20	Sol_awc – 20
Combo1	• ESCO = 1.0 • CN2 – 5 (Urban only) • GWQMN + 100 (Non-Urban only)
Combo2	• ESCO = 1.0 • CN2 – 5 (Urban only) • GWQMN + 100 (Non-Urban only) • Sol_awc – 10 (Urban only)
Combo3	• ESCO = 1.0 • CN2 – 5 (Urban only) • Sol_awc – 10 (Urban only)
Combo4	• ESCO = 1.0 • CN2 – 5 (Urban only)

Appendix III: Parameter Change Flow Duration Curves

This appendix contains the set of flow duration curves for parameter changes made to SWAT for each stream gauge station not shown in Section 5.2. These plots were omitted from Section 5.2 because they shared a general trend that could be explained by a single representative plot, which was included in Section 4.2.

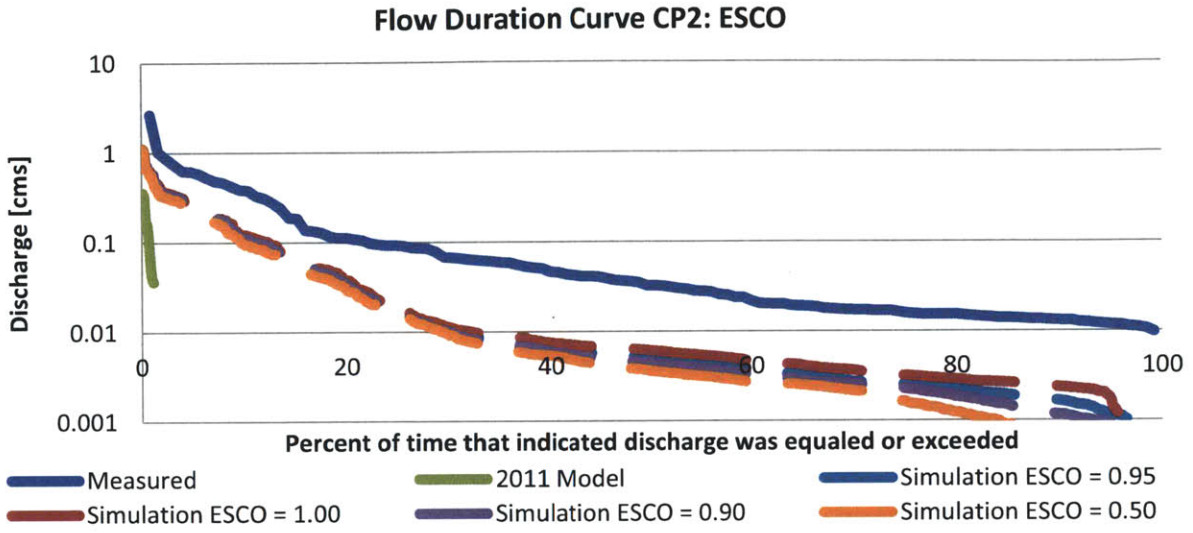

Figure 30 - Flow duration curve comparing changes to ESCO to measured values at CP2.

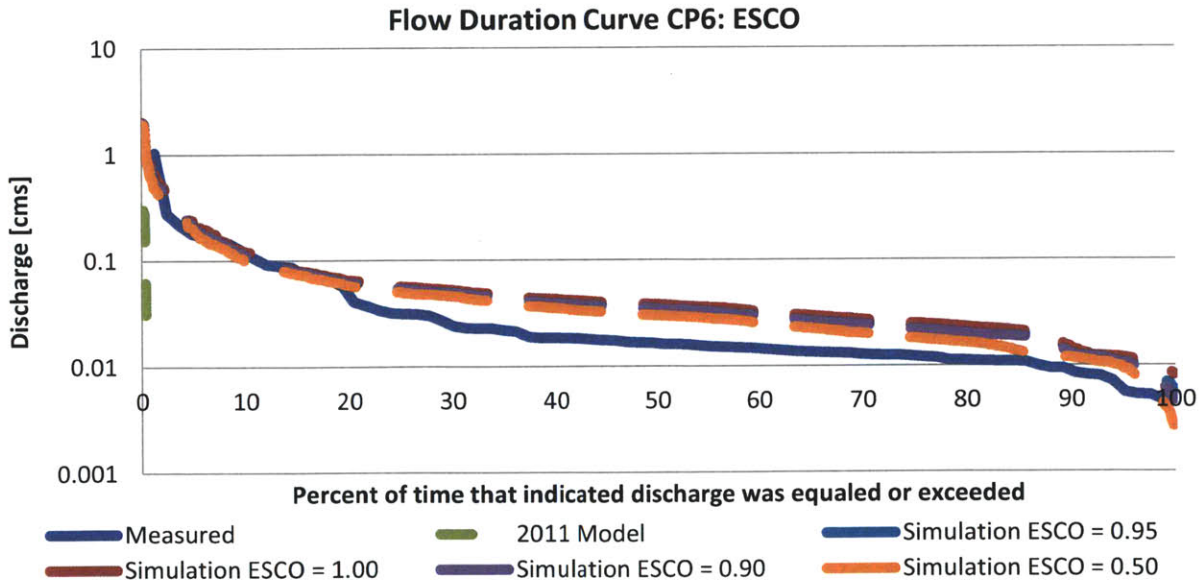

Figure 31 - Flow duration curve comparing changes to ESCO to measured values at CP6.

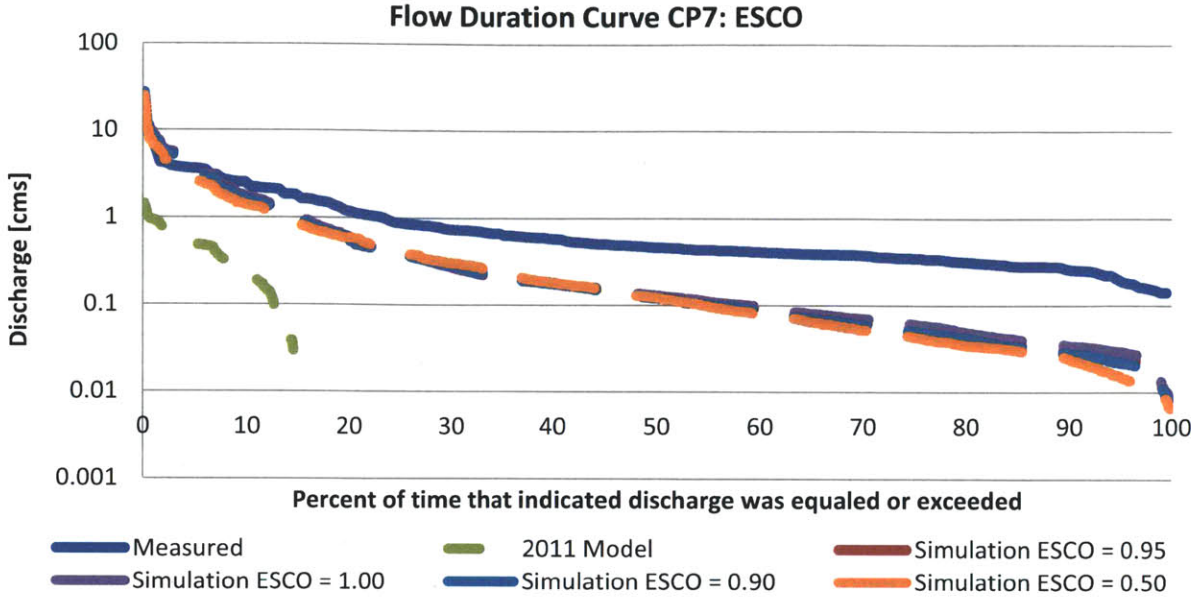

Figure 32 - Flow duration curve comparing changes in ESCO to measured values at CP7.

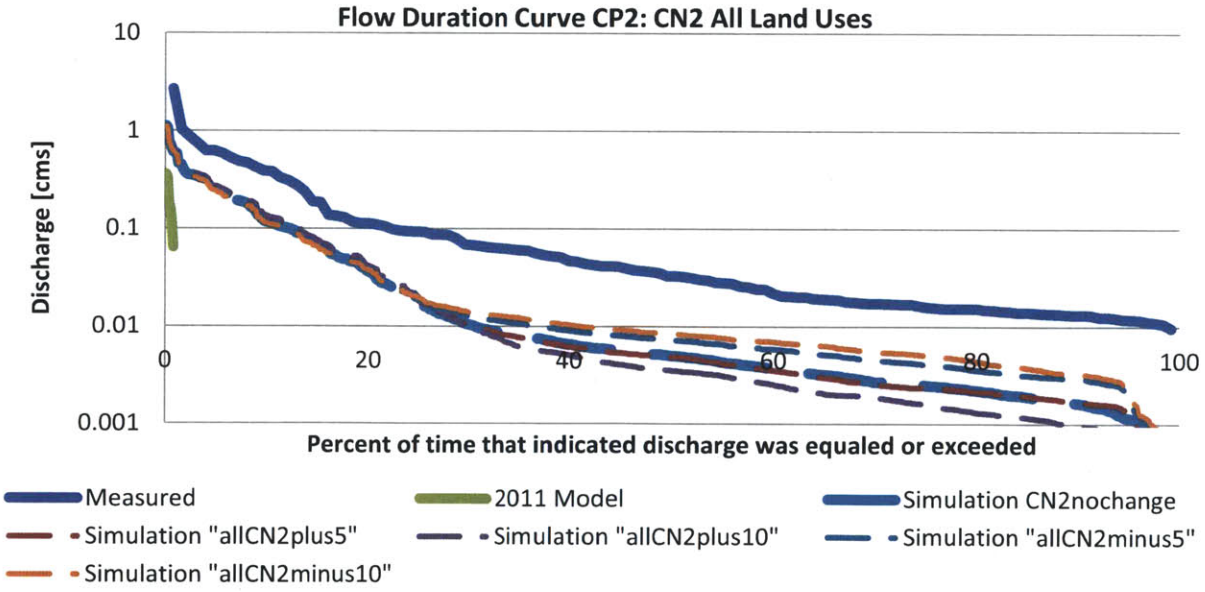

Figure 33 - Flow duration curves comparing changes in CN2 to measured values at CP2.

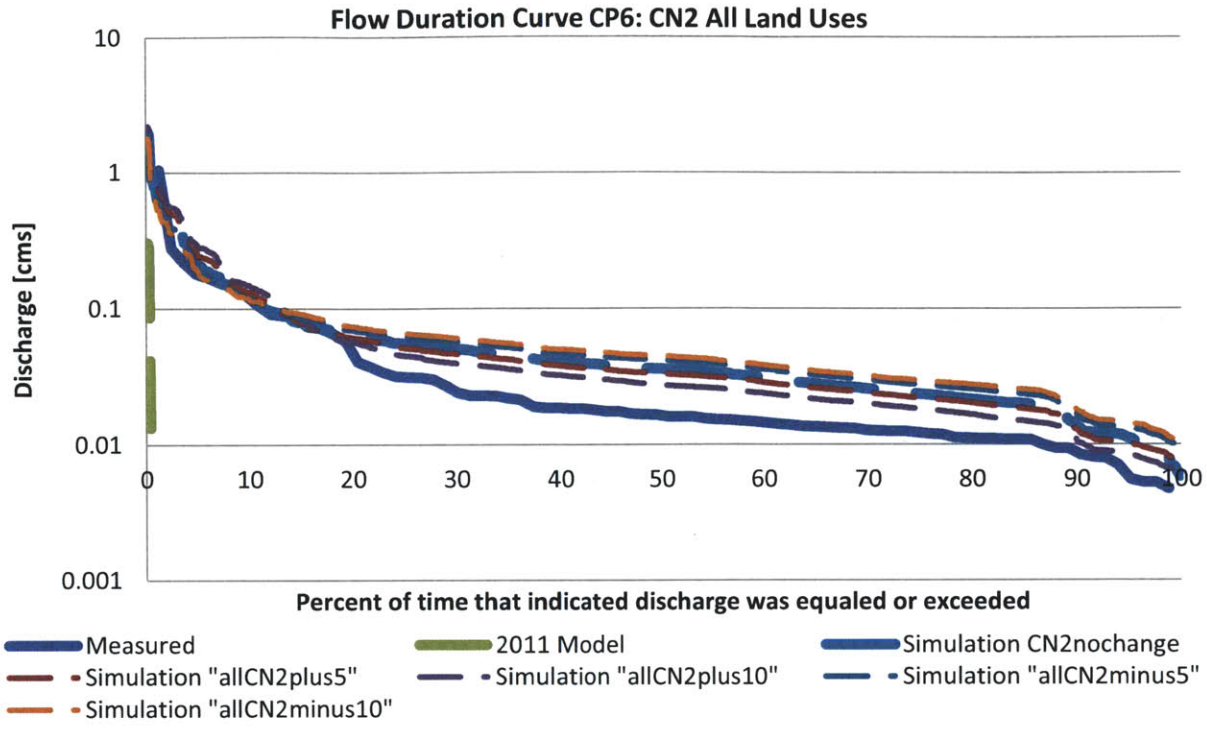

Figure 34 - Flow duration curves comparing changes in CN2 to measured values at CP6.

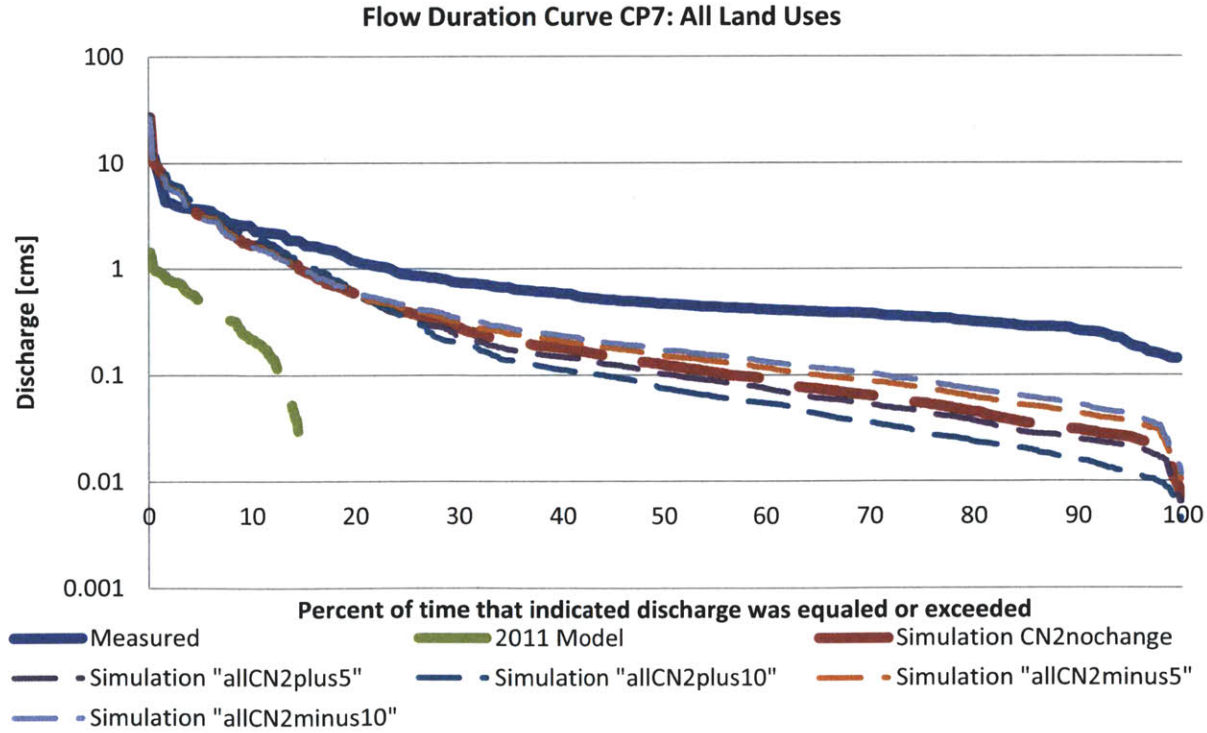

Figure 35 - Flow duration curves comparing changes in CN2 to measured values at CP7.

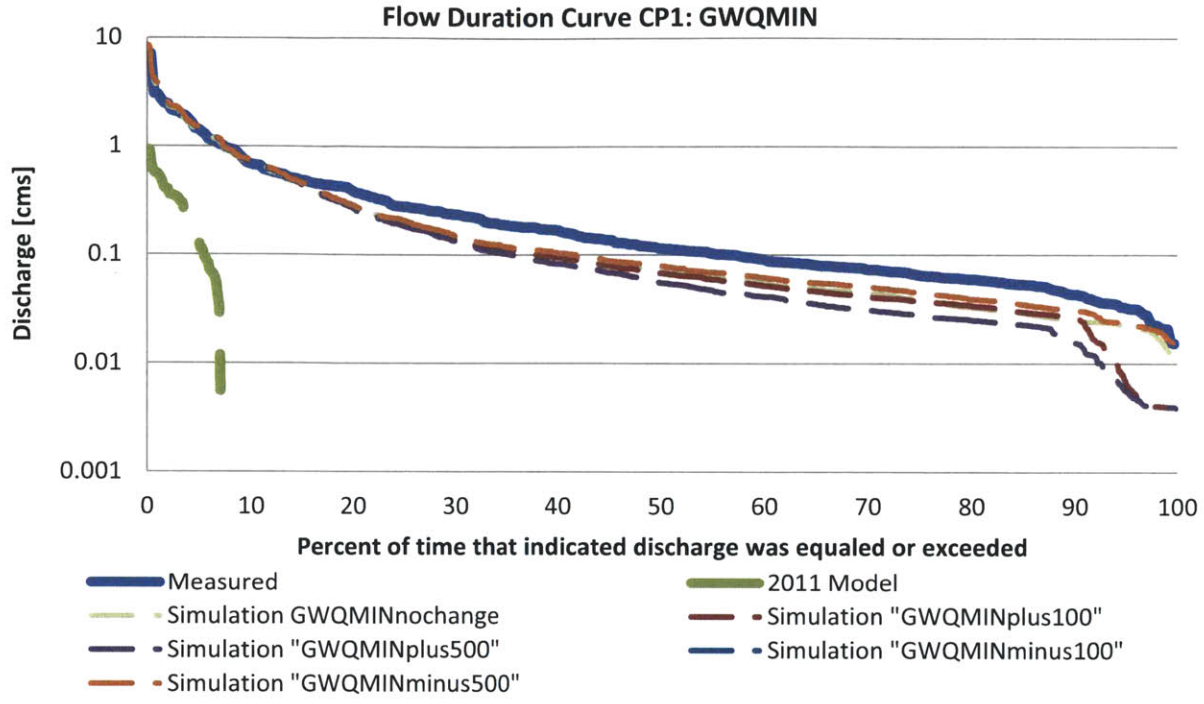

Figure 36 - Flow duration curves comparing changes in GWQMN to measured values at CP1.

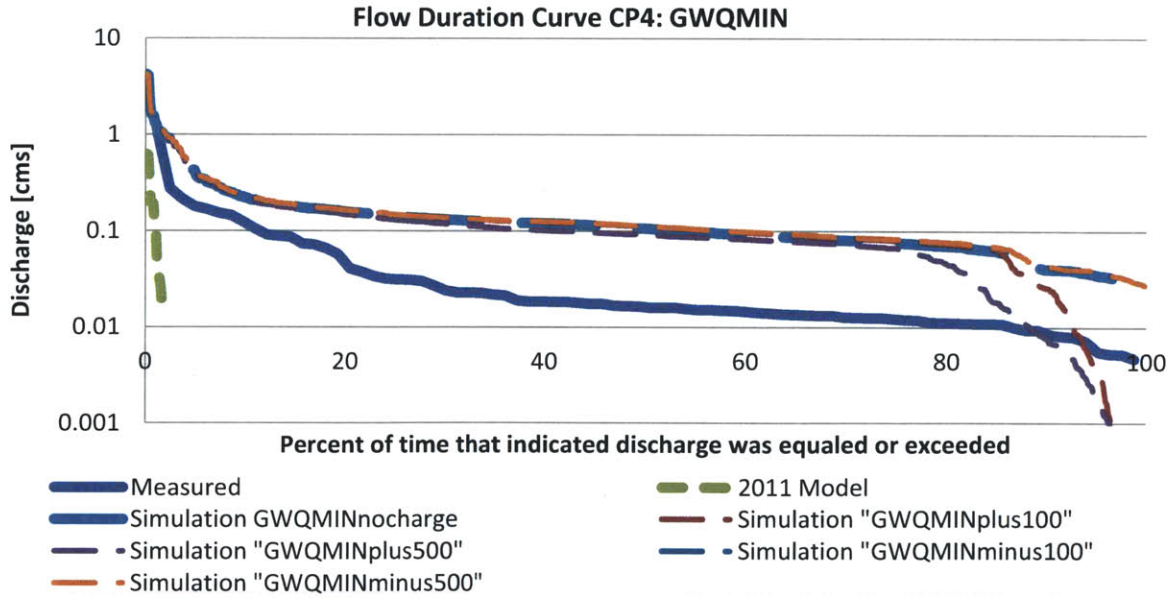

Figure 37 - Flow duration curves comparing changes in GWQMN to measured values at CP4.

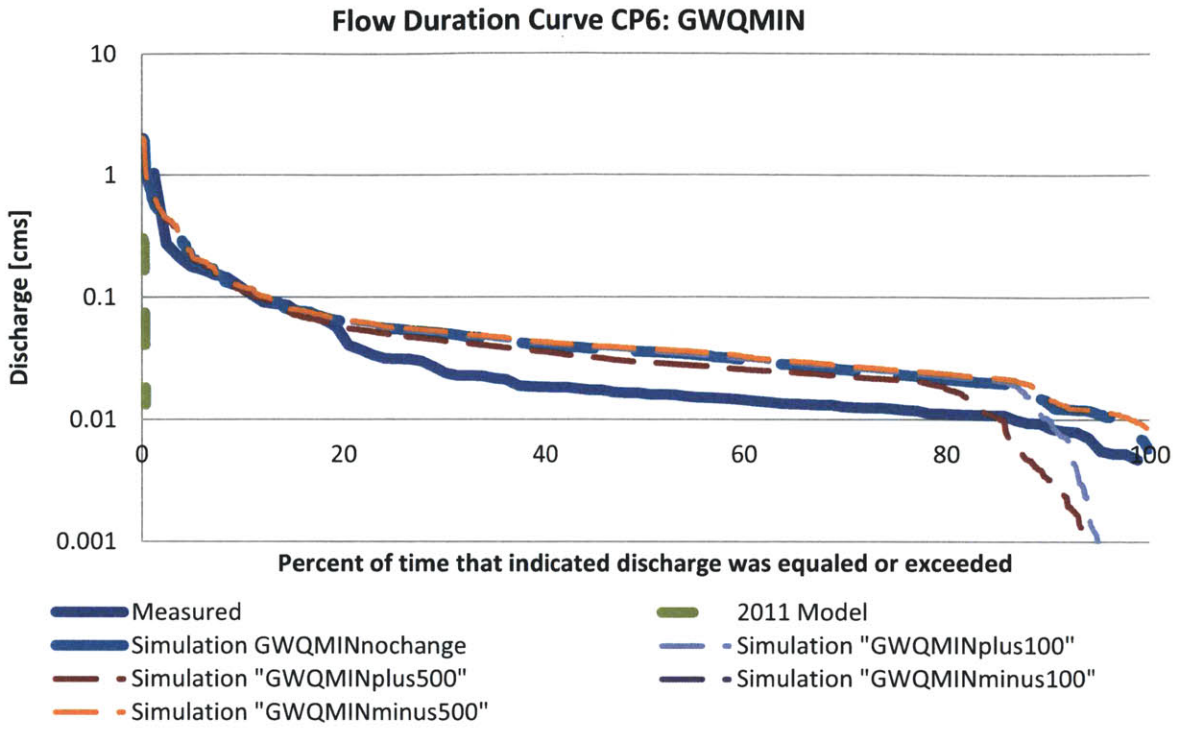

Figure 38 - Flow duration curves comparing changes in GWQMN to measured values at CP6.

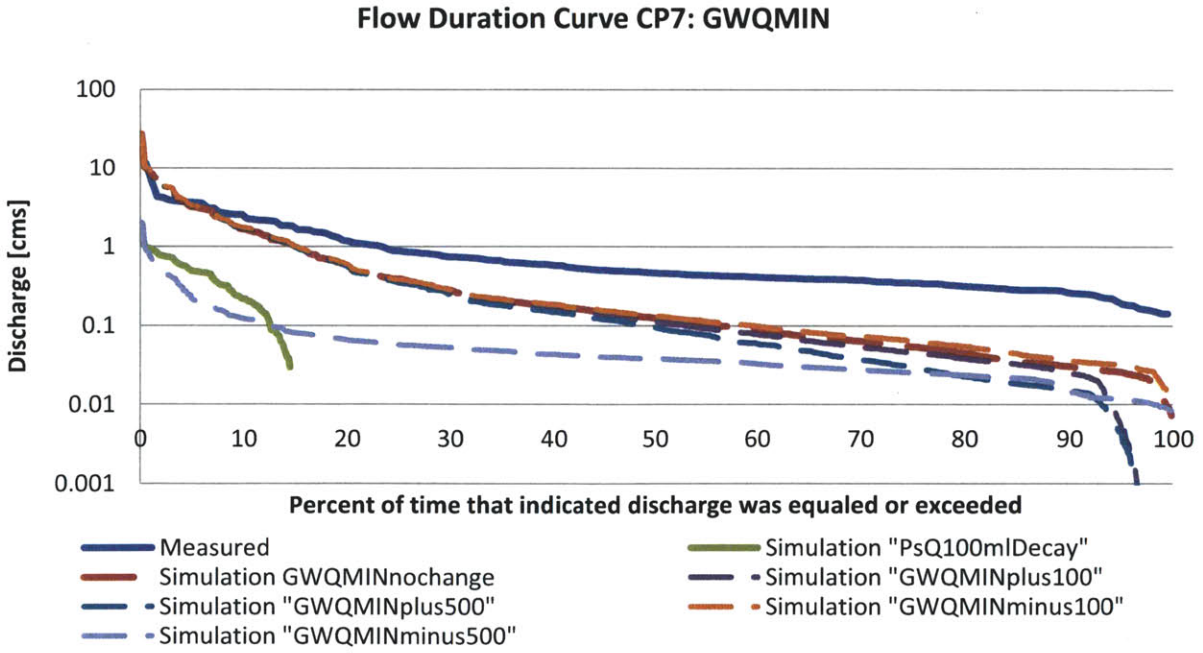

Figure 39 - Flow duration curves comparing changes in GWQMN to measured values at CP7.

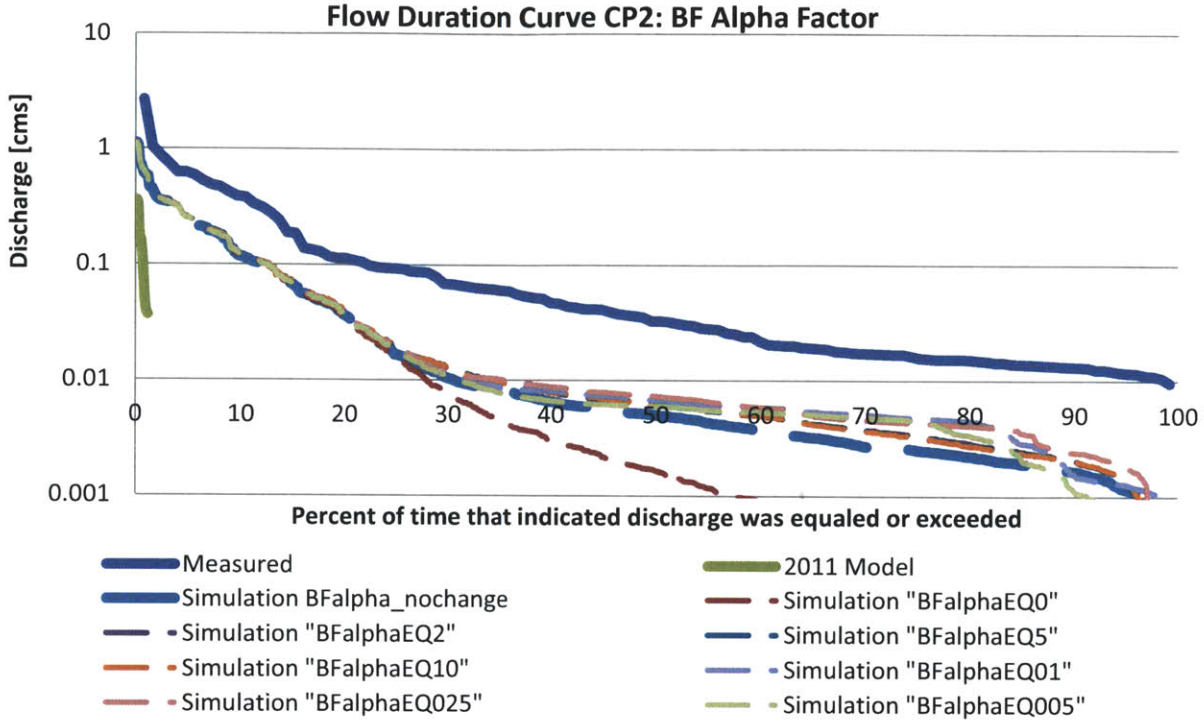

Figure 40 - Flow duration curves comparing changes to alpha_bf to measured values at CP2.

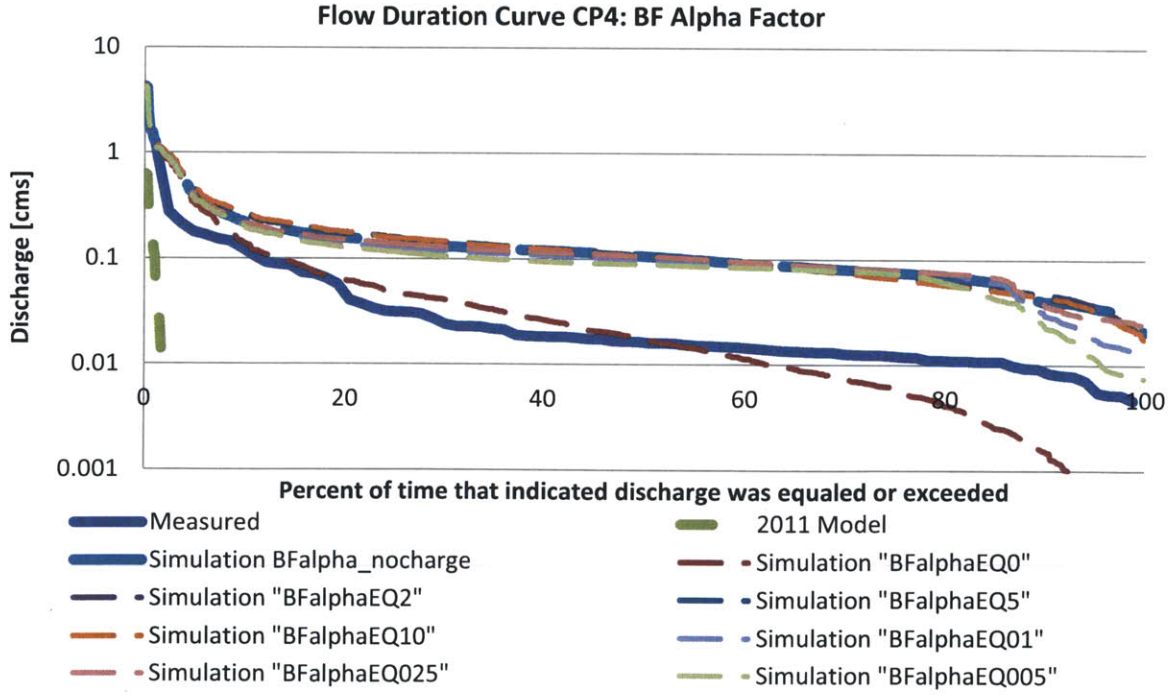

Figure 41 - Flow duration curves comparing changes in alpha_bf to measurements at CP4.

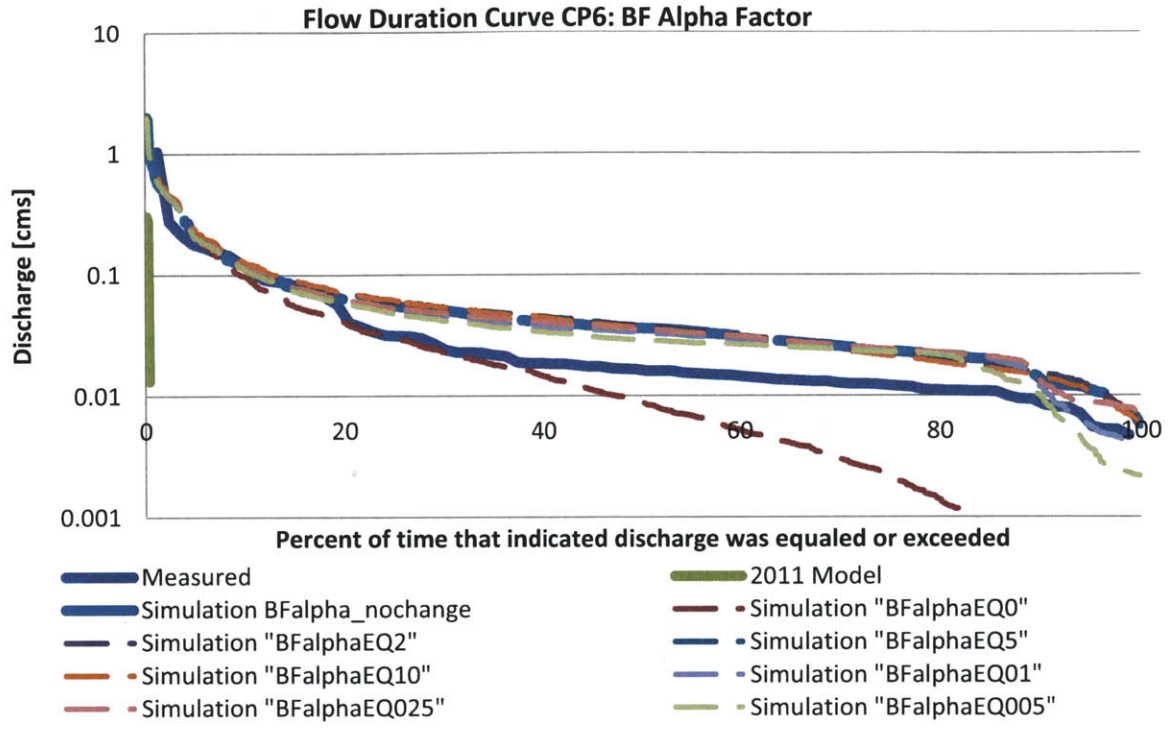

Figure 42 - Flow duration curves comparing changes in alpha_bf to measured values at CP6.

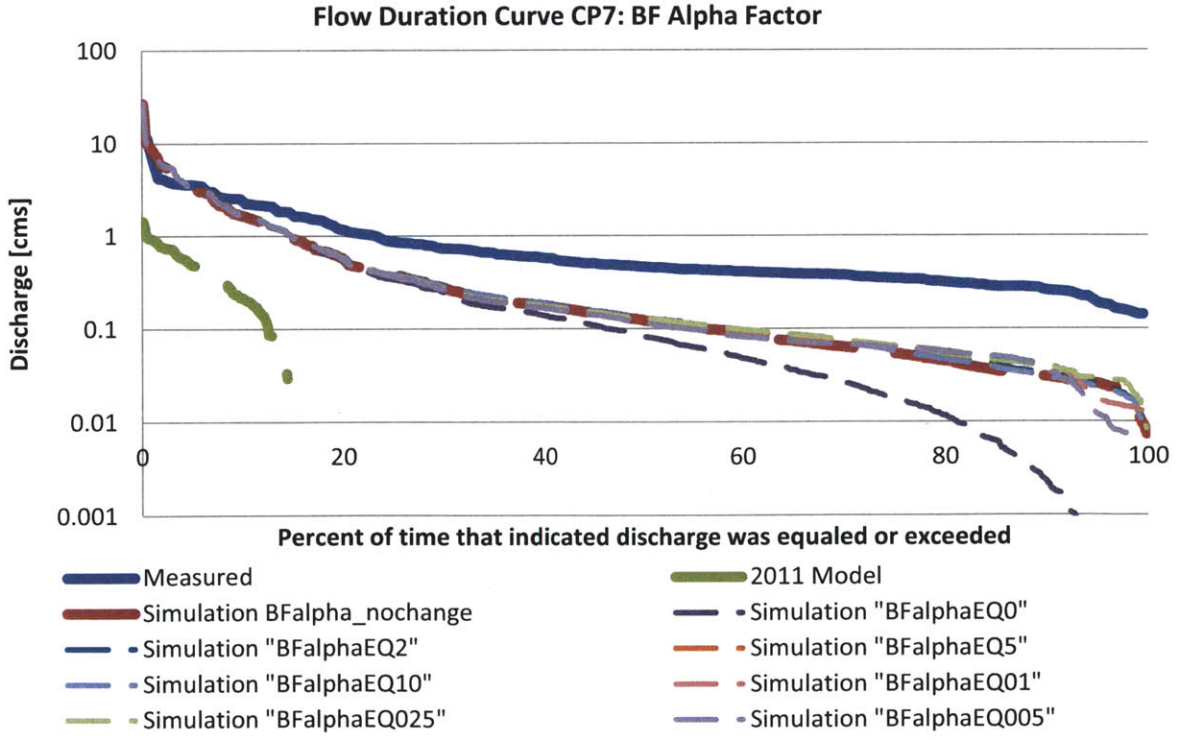

Figure 43 - Flow duration curves comparing changes to alpha_bf to measured values at CP7.

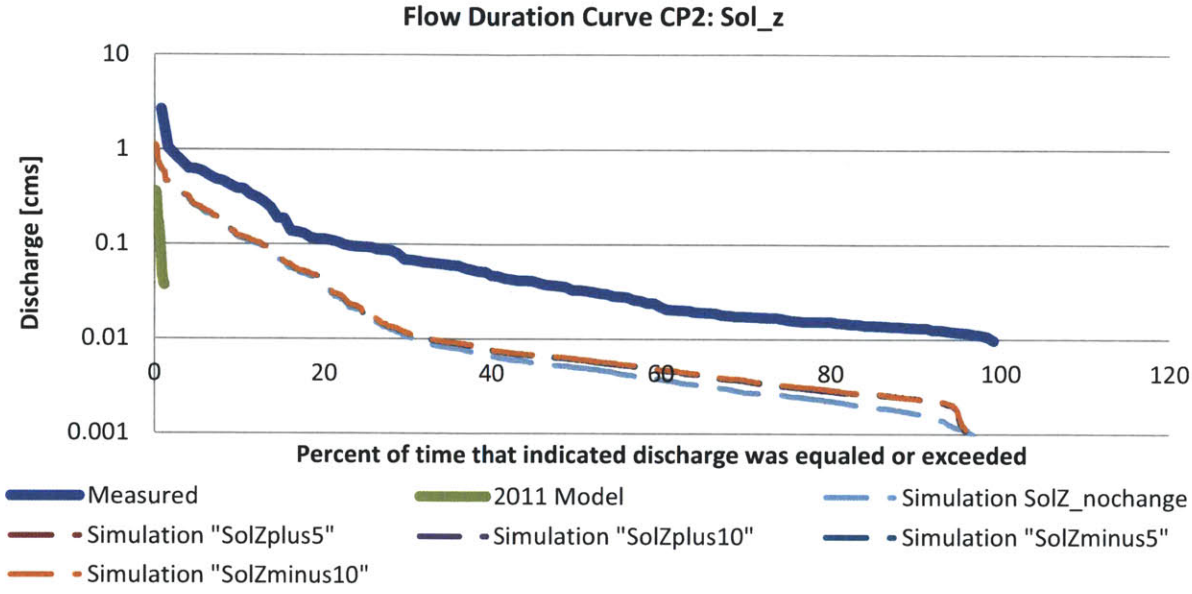

Figure 44 - Flow duration curve comparing changes to sol_z to measured values at CP2.

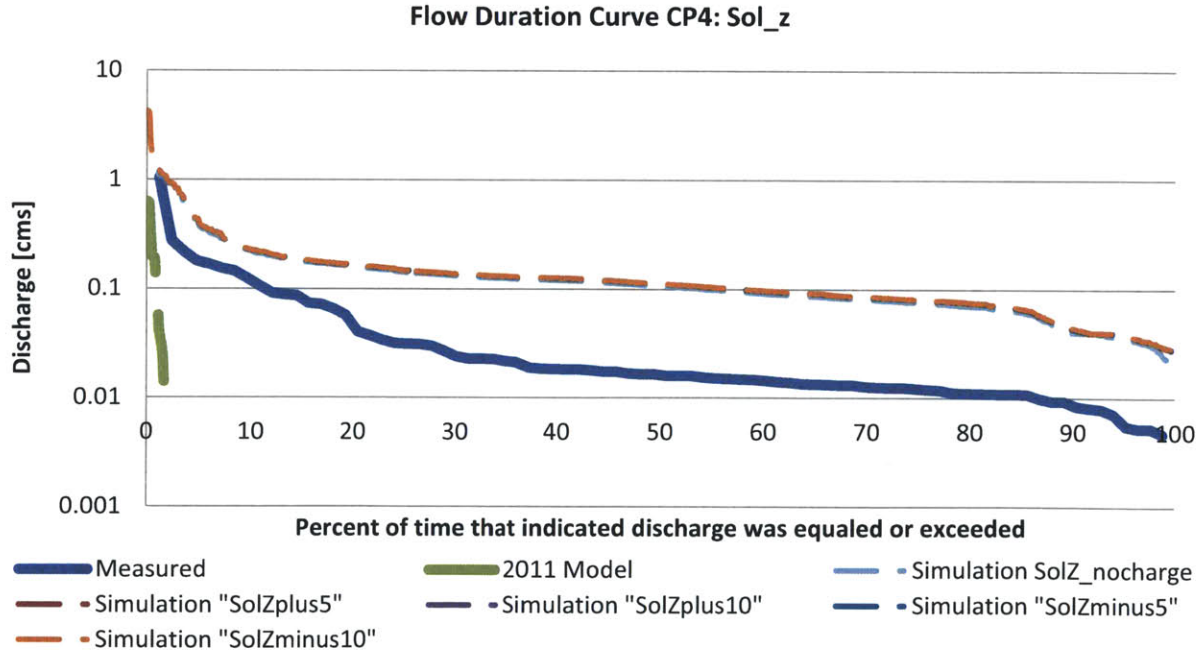

Figure 45 - Flow duration curve comparing changes in sol_z to measured values at CP4.

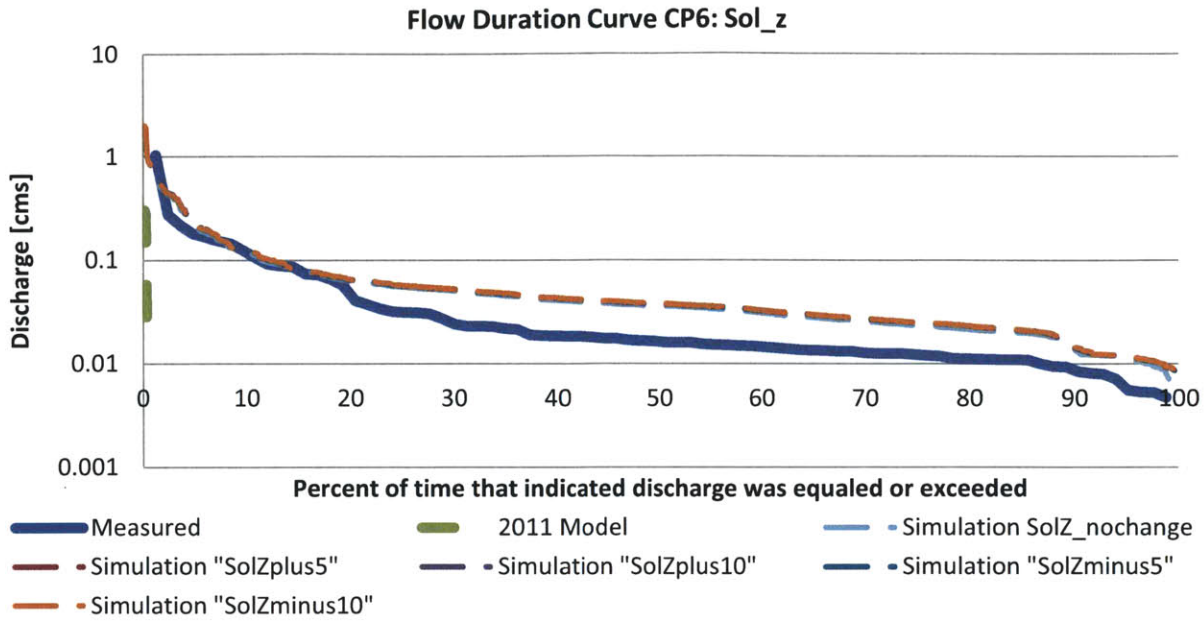

Figure 46 - Flow duration curve comparing changes in sol_z to measured values at CP6.

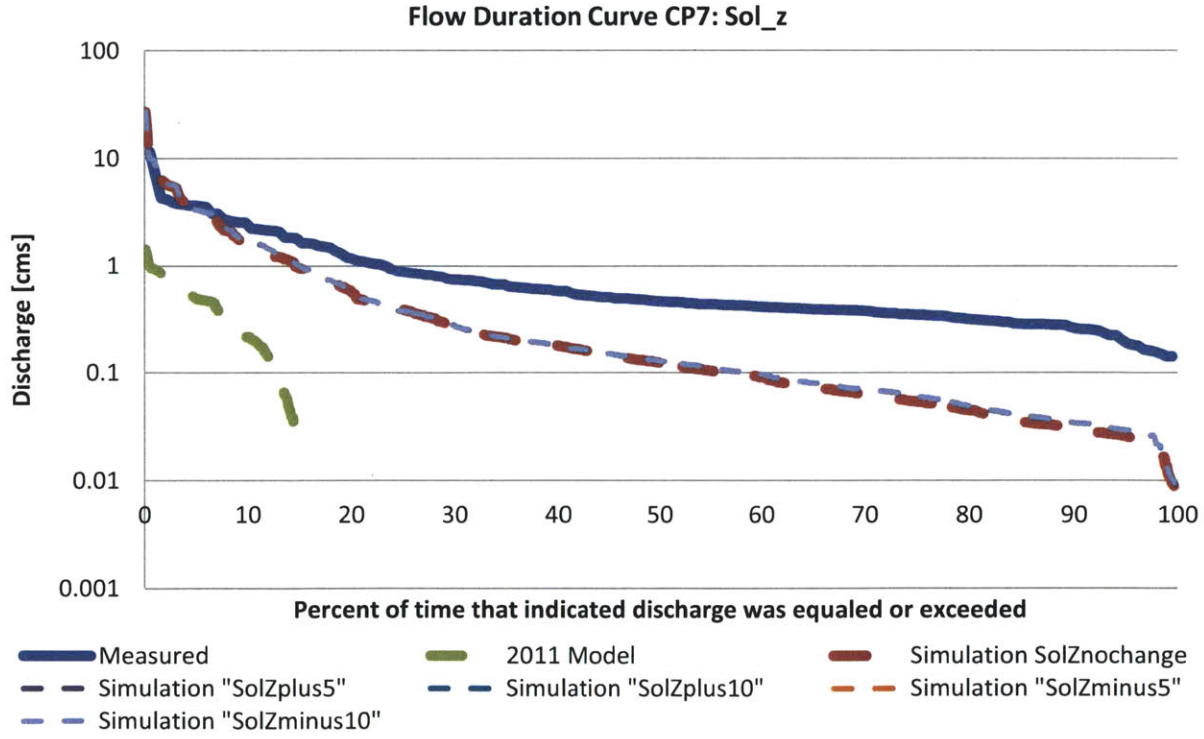

Figure 47 - Flow duration curve comparing changes in sol_z to measured values at CP7.

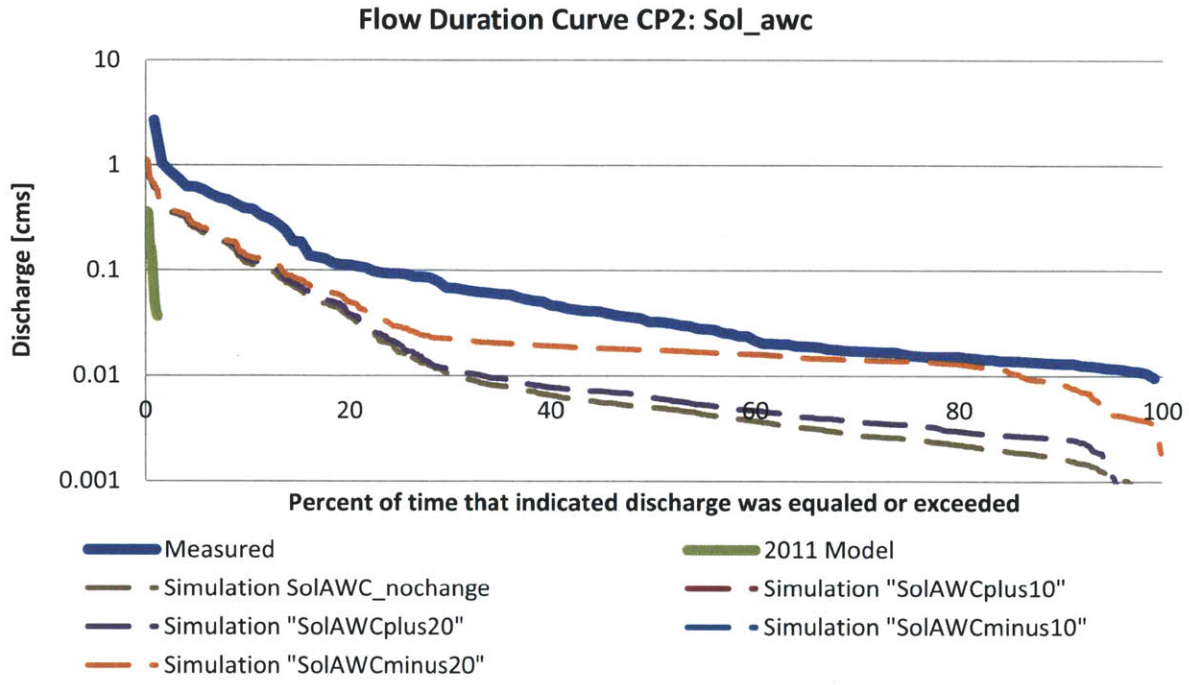

Figure 48 - Flow duration curves comparing changes in sol_awc to measured values at CP2.

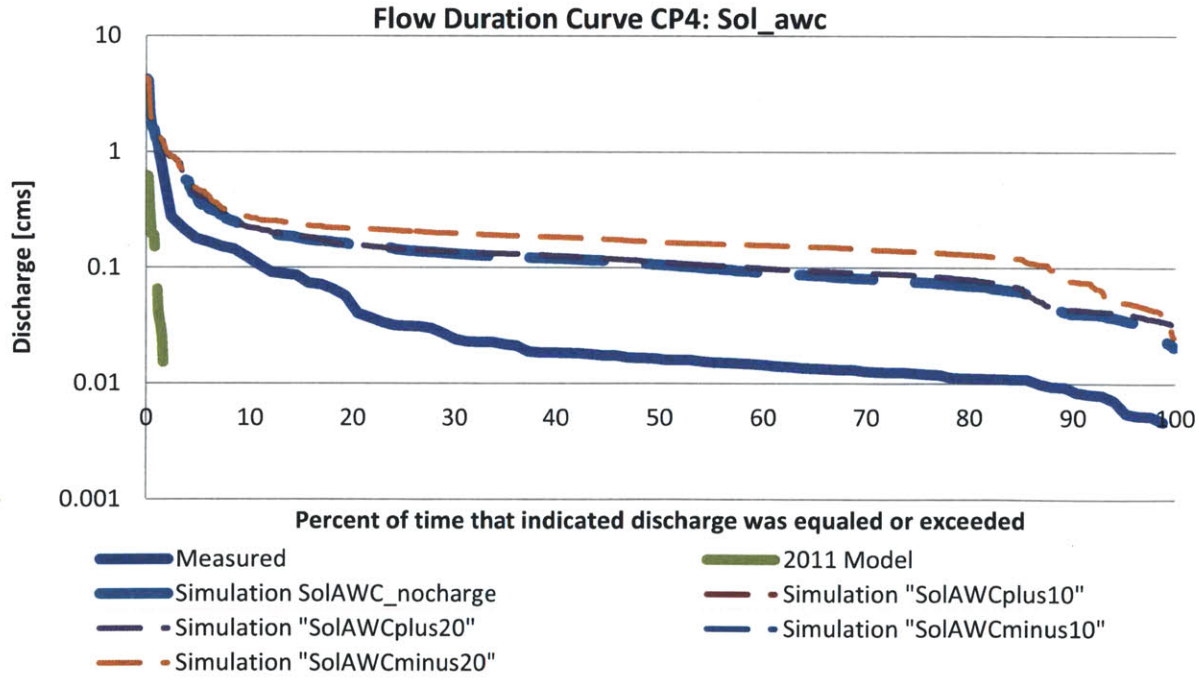

Figure 49 - Flow duration curves comparing changes in sol_awc to measured values at CP4.

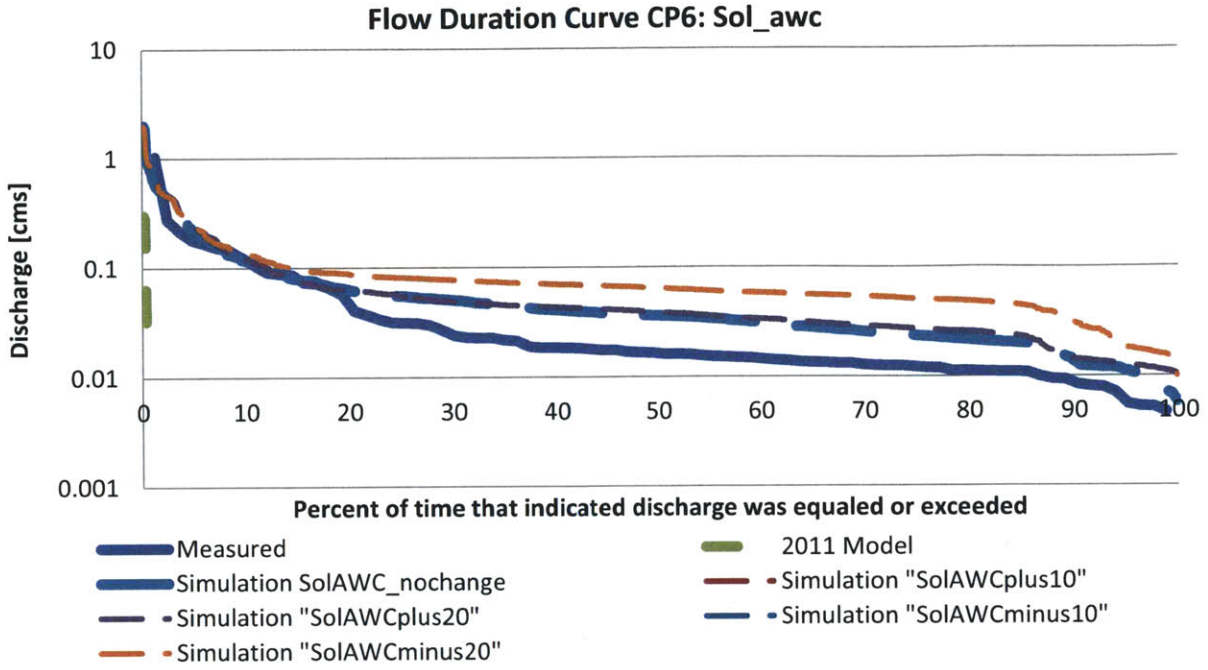

Figure 50 - Flow duration curves comparing changes in sol_awc to measured values at CP6.

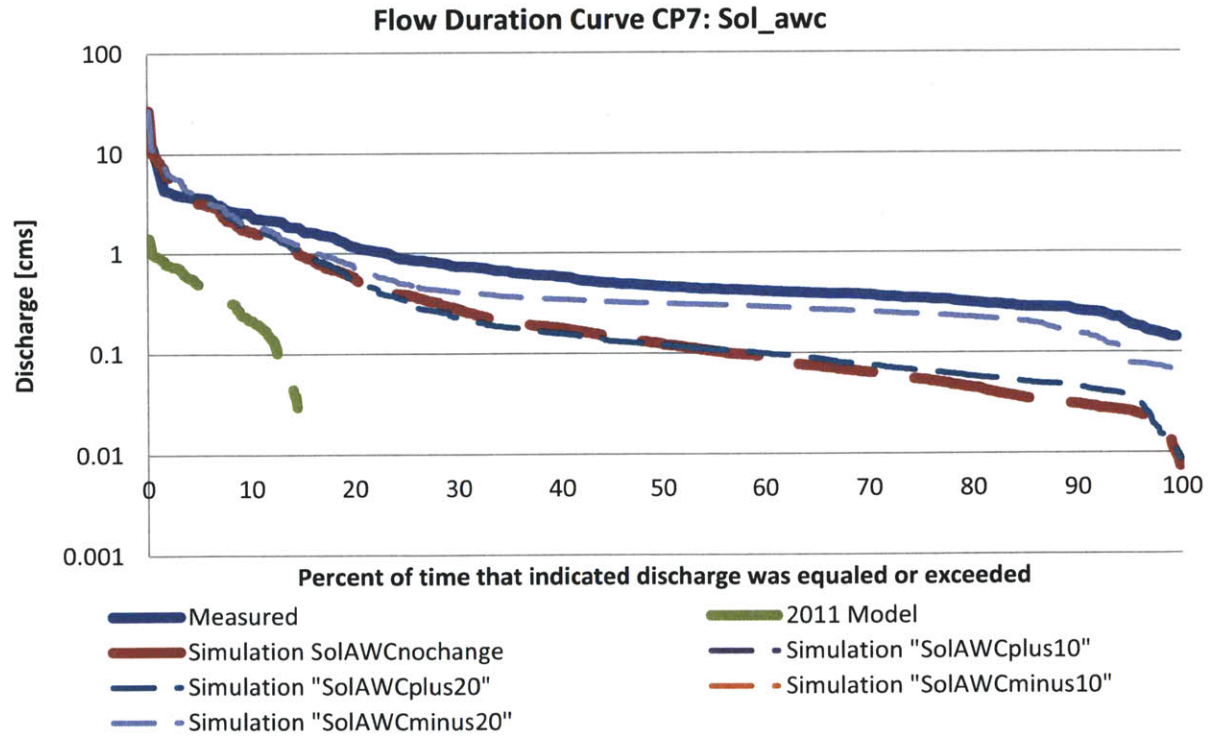

Figure 51 - Flow duration curves comparing changes in sol_awc to measured values at CP7.

Appendix IV: Modifications to CN2 by Land-Use Type

CN2 was examined according to land-use. This appendix contains the results of varying CN2 in only urban land areas and also in only non-urban areas.

i. Changes to CN2 for Urban Land-Uses

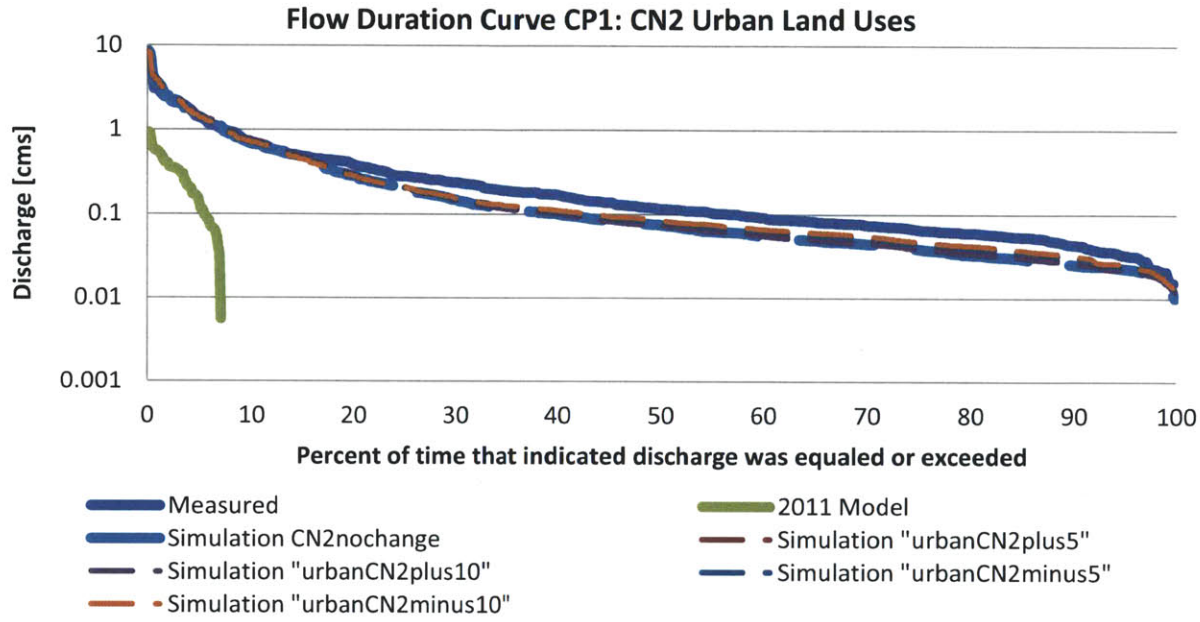

Figure 52 - Flow duration curves comparing changes in urban CN2 to measured values at CP1.

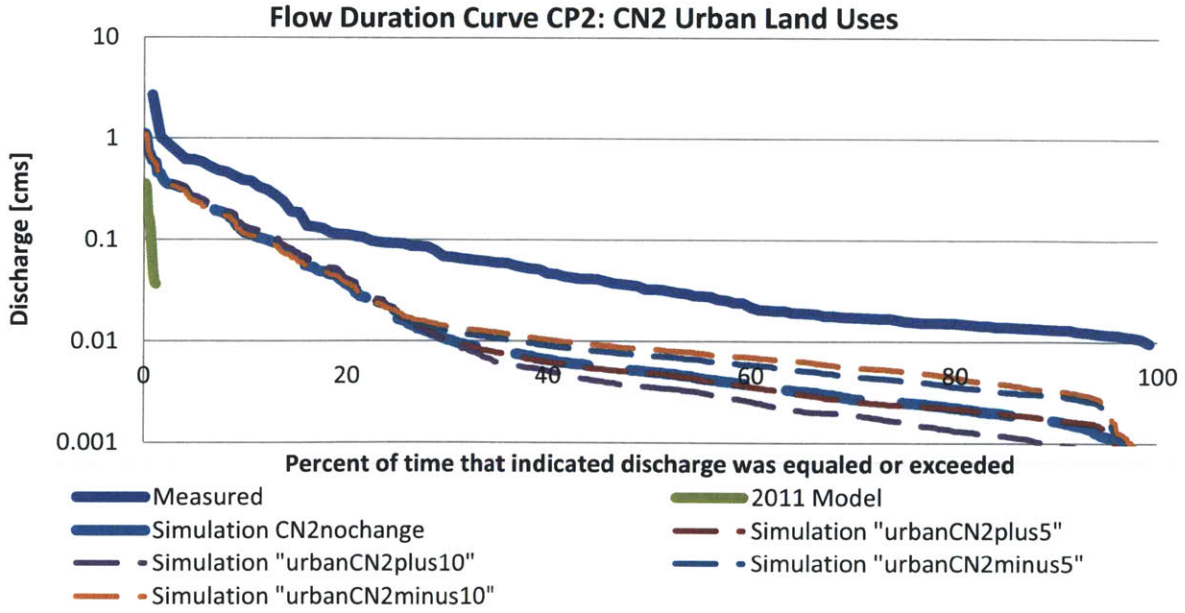

Figure 53 - Flow duration curves comparing changes in urban CN2 to measured values at CP2.

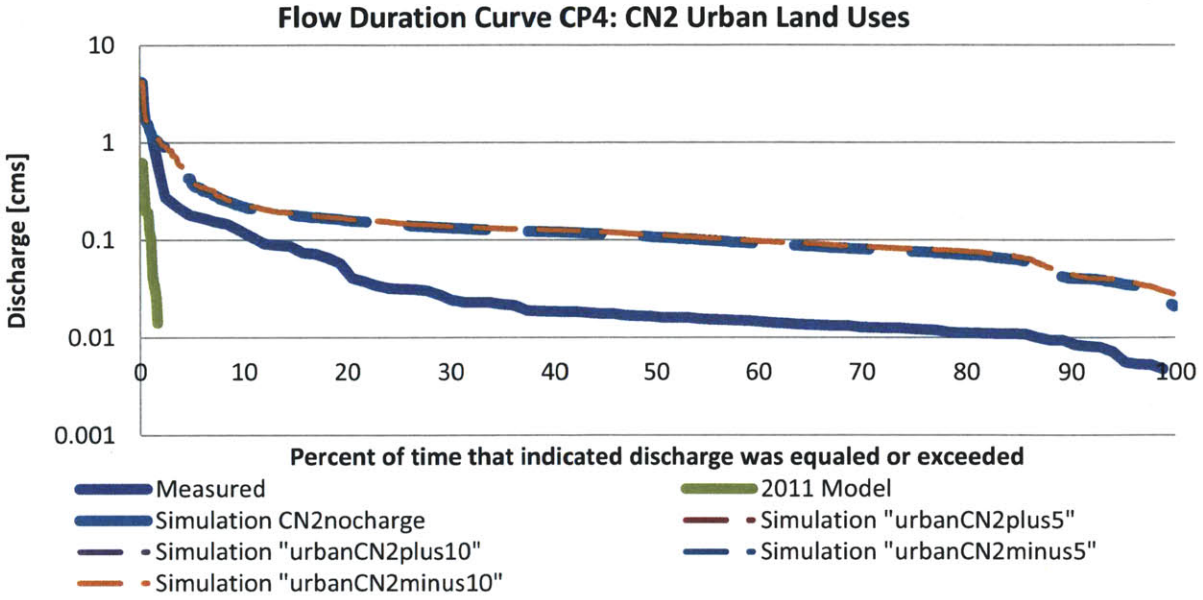

Figure 54 - Flow duration curves comparing changes in urban CN2 to measured values at CP4.

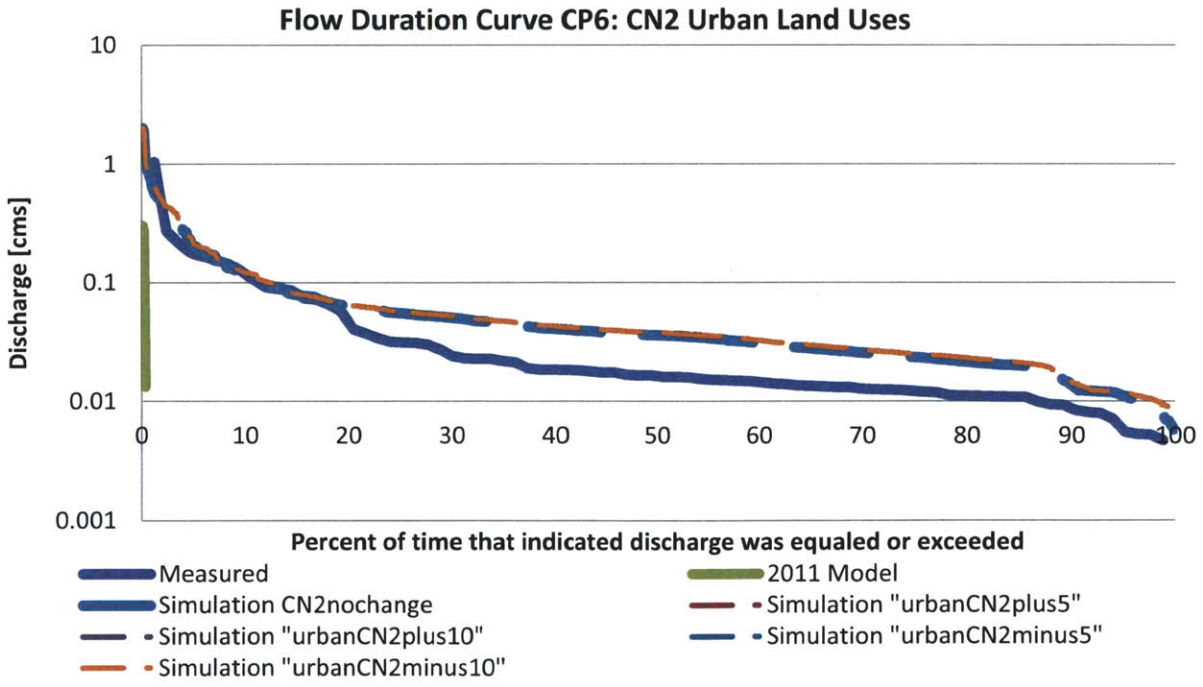

Figure 55 - Flow duration curves comparing changes in urban CN2 to measured values at CP6.

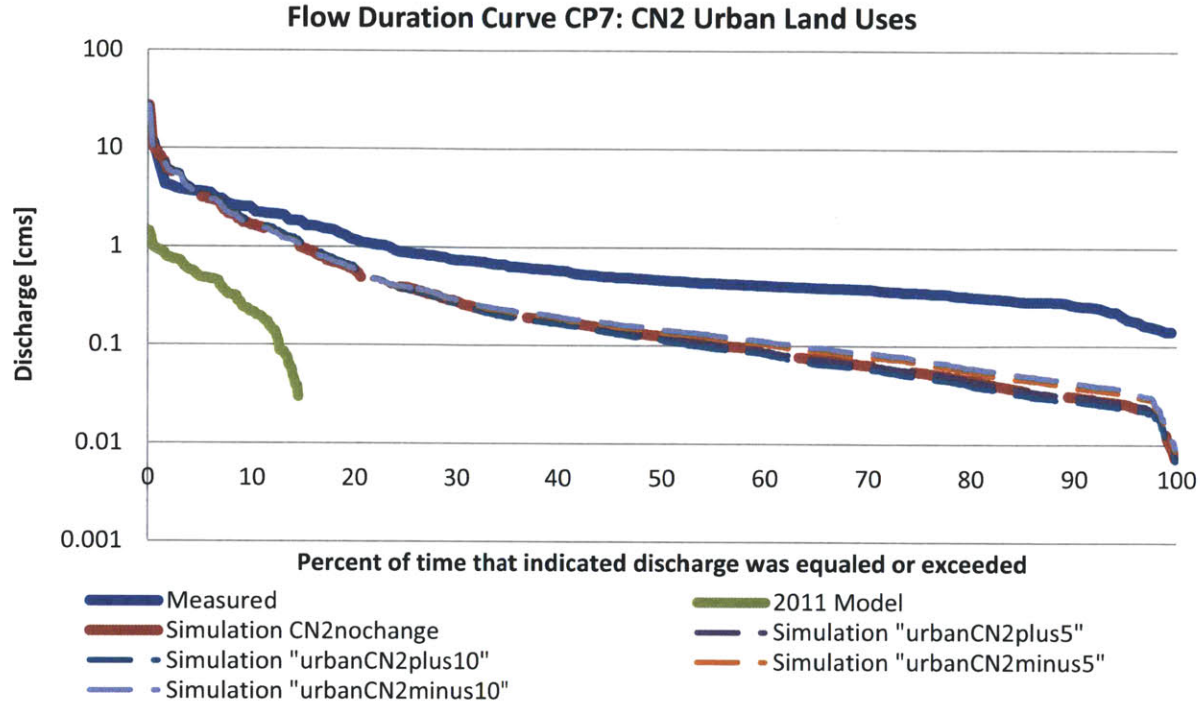

Figure 56 - Flow duration curves comparing changes in urban CN2 to measured values at CP7.

ii. Changes to CN2 for Non-Urban Land-Uses

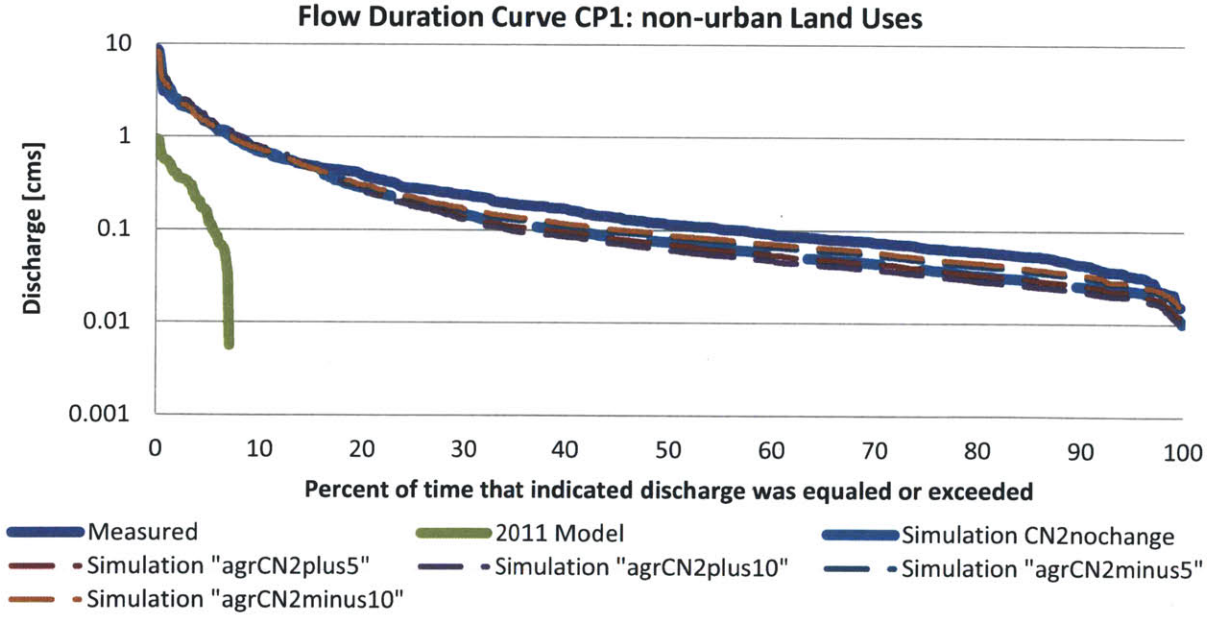

Figure 57 - Flow duration curves comparing changes in non-urban CN2 to measurements at CP1.

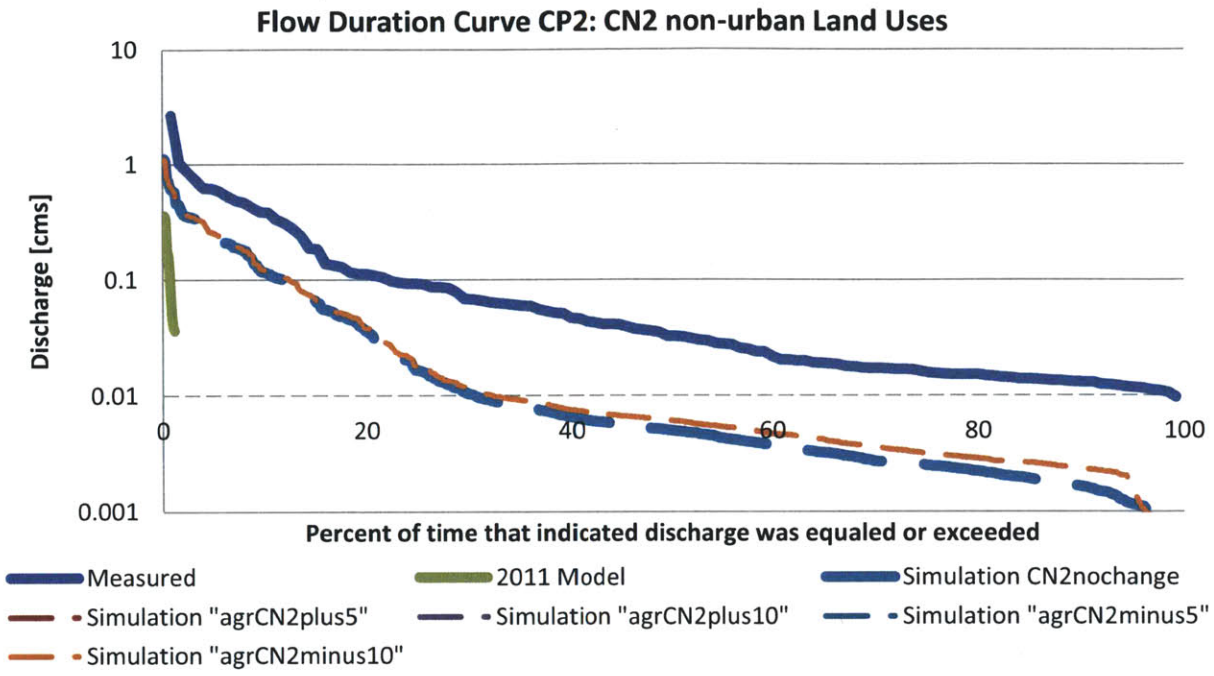

Figure 58 - Flow duration curves comparing changes in non-urban CN2 to measured values at CP2.

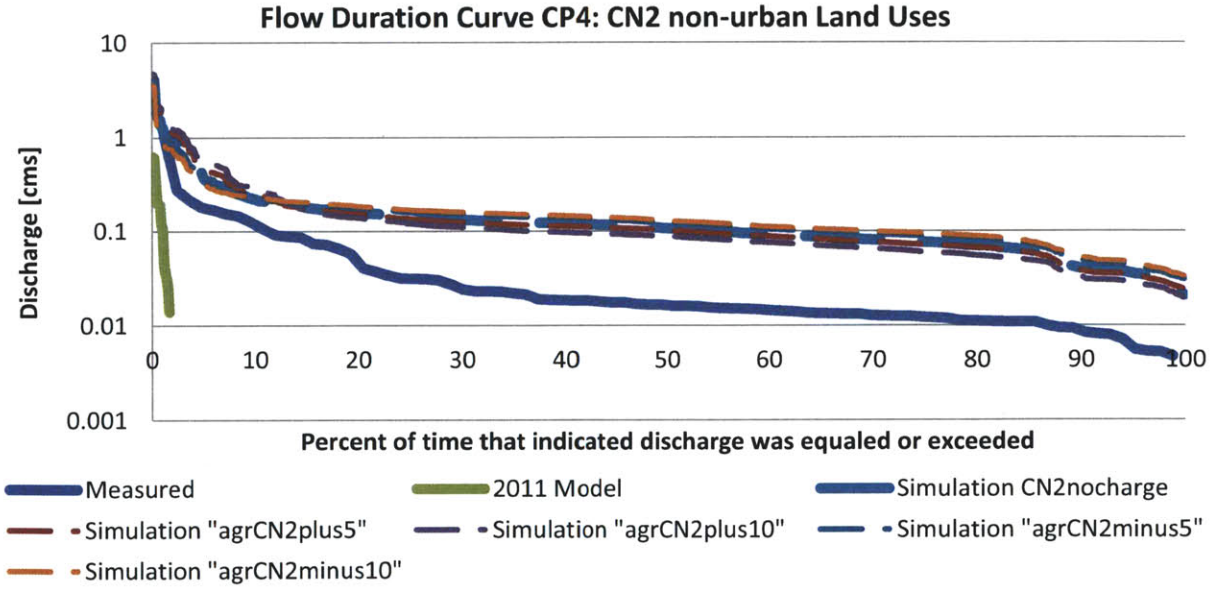

Figure 59 - Flow duration curves comparing changes in non-urban CN2 to measured values at CP4.

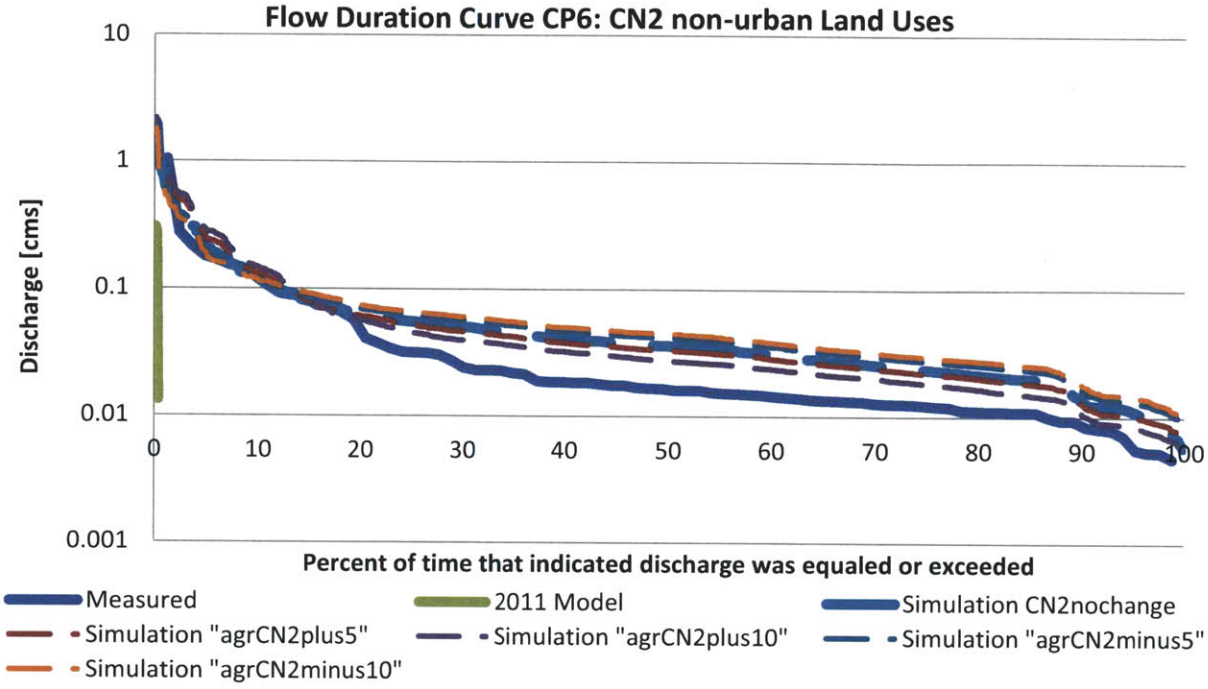

Figure 60 - Flow duration curves comparing changes in non-urban CN2 to measurements at CP6.

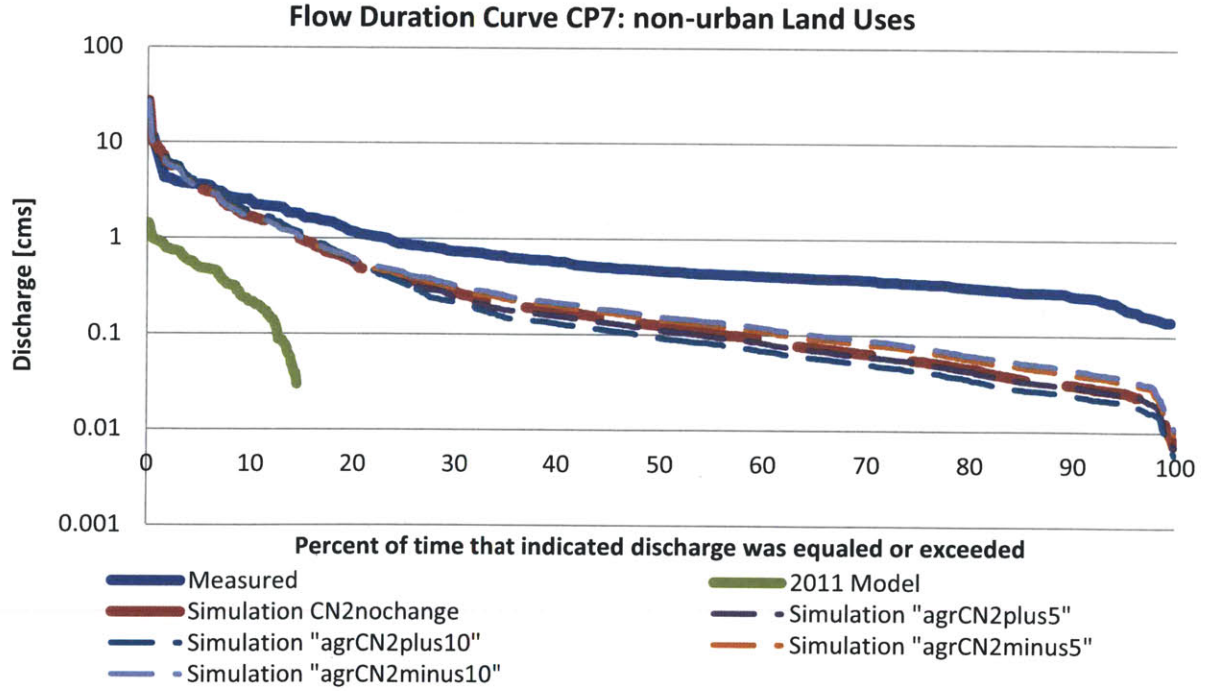

Figure 61 - Flow duration curves comparing changes in non-urban CN2 to measurements at CP7.